Volume - 2

Research Trends IN CHEMICAL SCIENCES

Chief Editor

Dr. Ashok Kumar Acharya
Assistant Professor PG Department of Chemistry Ranchi College,
Ranchi, Jharkhand, India

AkiNik Publications
New Delhi

Published By: *AkiNik Publications*

AkiNik Publications
169, C-11, Sector - 3,
Rohini, Delhi-110085, India
Toll Free (India) – 18001234070

Chief Editor: *Dr. Ashok Kumar Acharya*

Publication Year: *2019*

Pages: *137*

ISBN:

Price: *₹585/-*

Contents

Chapter - 1
An Overview of Tsuji-Trost Reaction

Author

Dr. Madhurjya Borah
Chemistry Department, North Lakhimpur College, Lakhimpur, Assam, India

Chapter - 1

An Overview of Tsuji-Trost Reaction

Dr. Madhurjya Borah

Abstract

Tsuji-Trost reaction is a most versatile and powerful tool in organic synthesis for carbon-carbon and carbon-heteroatom bond formation, with high chemo-, regio-, and stereo-selectivities. This palladium-catalysed reaction has been an extensively studied and fruitful area of research in synthetic organic chemistry. This chapter highlights the recent developments of palladium-catalyzed allylic substitution reaction towards the synthesis of carbocyclic as well as heterocyclic compounds and applications of the reaction for the synthesis of various natural products and bioactive compounds.

Keywords: Tsuji-Trost reaction, organic synthesis, palladium, allylation, catalysis.

1. Introduction

The Tsuji-Trost Reaction is the palladium-catalyzed allylation of activated nucleophiles such as active methylenes, enolates, amines and phenols with allylic derivatives via π-allylpalladium intermediates. Traditionally, Tsuji-Trost reactions utilize a pre-activated allylic substrate by transforming the alcohol moiety into a better leaving group such as acetate, carbonates, phosphates, carbamates or halides (Scheme 1).

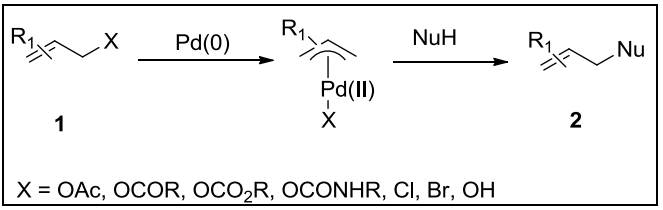

Scheme 1

This work was first demonstrated by Jiro Tsuji in 1965 [1] and subsequently modified by Trost and co-workers in 1973 [2] hence the name "Tsuji-Trost reaction". Both the chemists were awarded the Tetrahedron

prize for Creativity in Organic & Biomedical Chemistry in 2014 for this pioneer work.

Initially, Tsuji reported a palladium mediated allylic substitution as a stoichiometric reaction. Tsuji carried out the reaction of allyl palladium(II) chloride dimer 3 with the sodium salt of ethyl malonate 4 to produce ethyl allylmalonate 5 and ethyl diallylmalonate 6 respectively (Scheme 2).

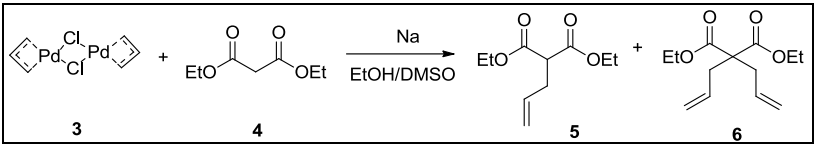

Scheme 2

Later in 1973, Barry M. Trost has further modified the reaction by starting from alkenes and using additional phosphine ligands. The reaction of the π-allyl palladium complex (generated from stoichiometric $PdCl_2$ and 1, 1-dipropylethene 7) with the anion of diethylmalonate 4 in the presence of triphenylphosphine resulted in a mixture of three allylated compounds 8, 9 and 10 respectively (Scheme 3).

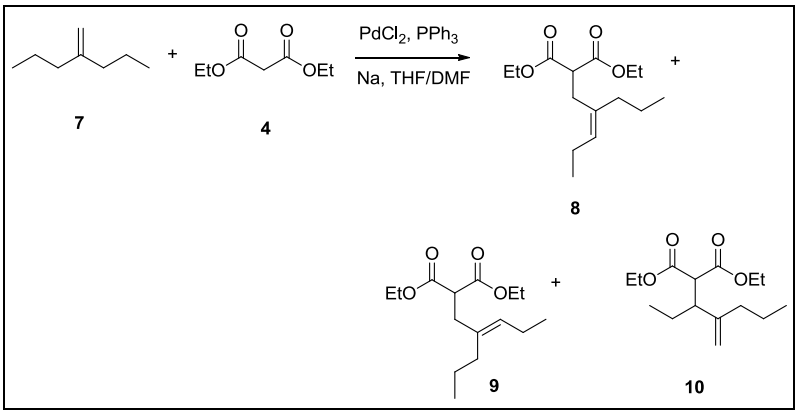

Scheme 3

These phosphine ligands can modulate the properties of palladium catalyst, such as electronic as well as the steric properties. In addition, asymmetric synthesis can be carried out by using chiral ligands, thereby imparting chirality to the final product.

2. Mechanism of the Reaction

The general mechanism of palladium-catalyzed allylic substitution is shown in Scheme 4. An allylic substrate 1, typically an acetate or a

carbonate, reacts with the catalyst, which enters the catalytic cycle at the Pd (0) oxidation level. Both Pd(0) and Pd(II) complexes can be used as precatalysts, as Pd(II) is easily reduced in situ to the active Pd(0) form by e.g., excess phosphine ligand, certain nucleophiles or other components present in the reaction mixture. Initial binding of the palladium (0) with the olefin 1 forms a η^2 π-allyl-Pd (0) complex and subsequent oxidative addition of the coordinated allylic substrate to Pd (0) affords a η^3 π-allylpalladium (II) complex with the leaving group as counterion.

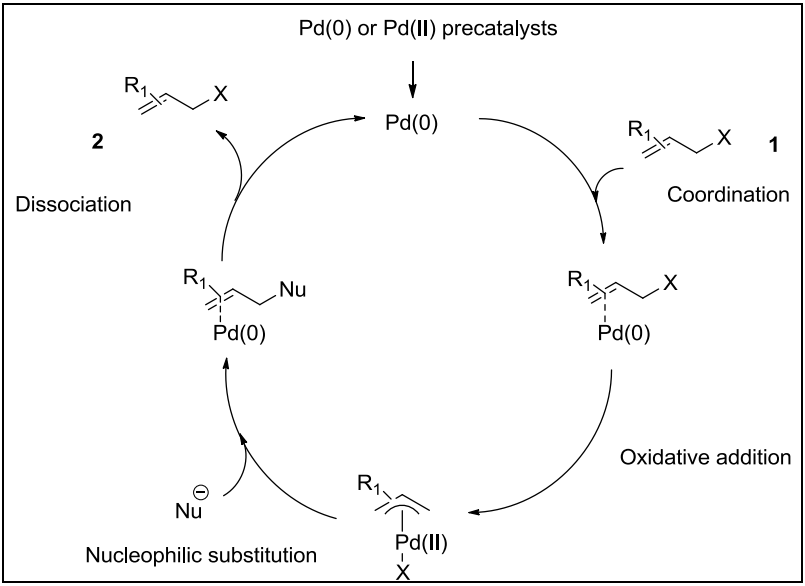

Scheme 4

The nucleophile (Nu) regioselectivity attacks at the less substituted allylic carbon of the π-allylpalladium complex from the opposite side of Pd (II) thereby regenerating the Pd (0)-allyl π complex. Finally, the Pd (0)-allyl π complex dissociates into the allylation product 2 and the active catalyst Pd (0), which again participates in the catalytic cycle.

However, the mechanistic pathway follows two different modes based on the strength of the nucleophile present in the reaction mixture. Soft nucleophiles, such as those derived from conjugate acids with a pKa < 25, normally add directly to the carbon of the allyl group. Whereas hard nucleophiles, defined as those derived from conjugate acids whose pKa > 25, normally follows a different path as depicted in Scheme 4. In this pathway, nucleophile attacks the metal center, followed by reductive elimination to give the allylation product.

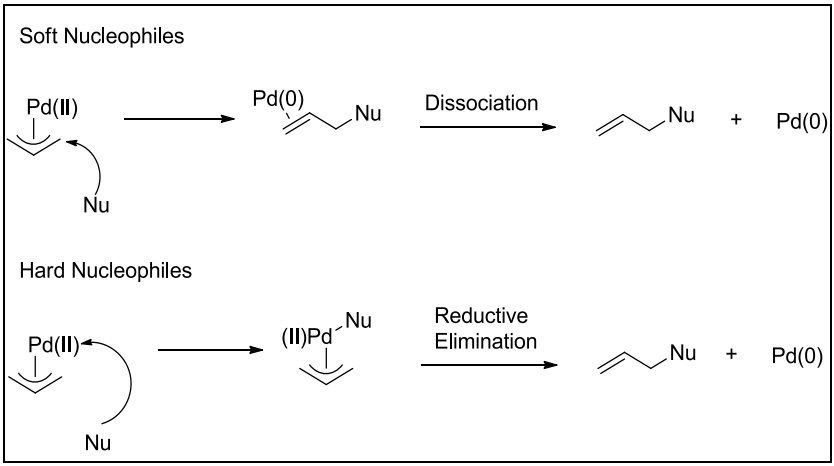

Scheme 5

These two mechanistic modes have an impact on the stereochemistry of the final product. Allylic alkylation with soft nucleophiles usually results in overall retention of stereochemistry, whereas hard nucleophiles lead to inversion of configuration.

3. Progress of Tsuji-Trost Reaction in Past 20 Years

Over the past 40 years, Tsuji-Trost reaction has been emerged as an important tool for organic chemists for the formation of variety of chemical bonds (C-C, C-O, C-N, C-S, C-P etc). Several protocols have been developed to couple the allyl substrates with carbon nucleophiles as well as heteroatom nucleophiles via π-allylpalladium intermediates with predominant/exclusive chemo-, regio-, and stereo-selectivities under appropriate conditions.

In 2003, Krische and co-workers demonstrated a methodology for the synthesis of five- and six-membered cycloallylated products 12 from mono-enone mono-allylic carbonates 11 using stoichiometric amounts of tributylphosphine and 1 mol % of $Pd(Ph_3P)_4$ in good yields [3]. This transformation unites the nucleophilic features of the Morita-Baylis-Hillman reaction with the electrophilic features of the Trost-Tsuji reaction (Scheme 6).

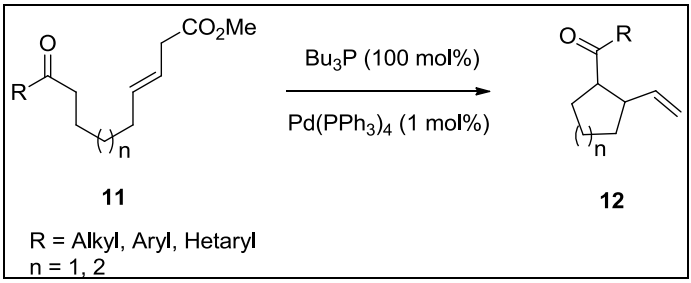

Scheme 6

During the last two decades, the use of allylic alcohols without prior derivatization for palladium-catalysed allylic substitution reactions has gained significant attention with respect to increase the environmental friendliness of the transformation. Uenishi *et al*. have described a stereospecific synthesis of 2, 6-disubstituted tetrahydropyran 14 and 3,6-dihydro[2H] pyrans 16 via Pd (II)-catalyzed cyclization of the ζ-hydroxy-δ, ε-unsaturated 13 and β-hydroxy-γ, δ-unsaturated alcohols 15 (Scheme 7) [4]. The important aspect of the method is the stereospecific transfer of chirality of the carbon center of the chiral allylic alcohol to a newly generated stereogenic center on the pyran ring *via syn*-S_N2' type process.

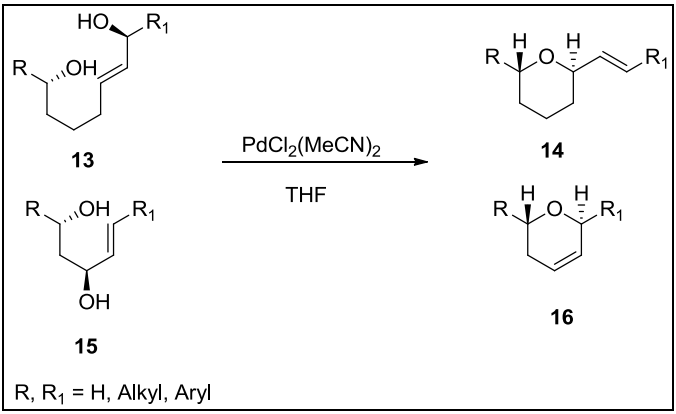

Scheme 7

Very recently, Ruijter *et al.* reported the stereoselective synthesis of γ-lactam-fused vinylcyclopropanes 18 via intramolecular Tsuji-Trost cascade cyclization reaction with high degree of diastereoselectivity and enantioselectivity [5]. The process involves double intramolecular Tsuji-Trost reaction of (homo) allylic vicinal diacetates 17 with pendant *β* ketoamide or related carbon nucleophiles (Scheme 8).

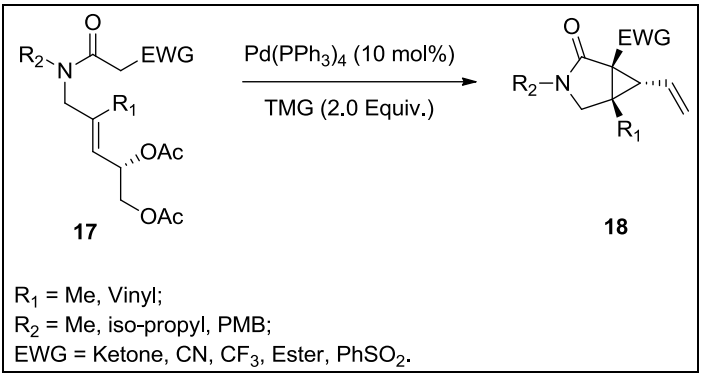

Scheme 8

Roulland and co-workers reported a novel counteranion-directed catalysis approach for the diastereoselective synthesis of 2, 5-disubstituted 3-hydroxy-tetrahydrofurans 20, 22 through the formation of a π-allyl/Pd (II) intermediate (Scheme 9) [6]. They have further utilised the methodology in the synthesis of the C8-C15 fragment of (-)-Obtusallene III and C9-C19 fragment of (+)-Oocydin A.

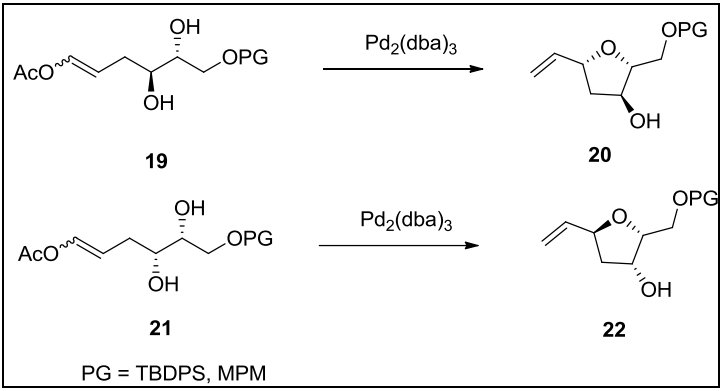

Scheme 9

An instructive example of the intramolecular Tsuji-Trost reaction of allylic alcohols can be found in the total synthesis of (-) -Cassine 25 by Hirota and co-workers [7]. (-) - Cassine is a piperidine alkaloid isolated from the leaves and twigs of *Cassia excels*, which exhibits antimicrobial activity against *Staphylococcus aureus* [8]. The key step of the synthesis is the diastereoselective Pd (II)-catalyzed cyclization of allyl alcohol 23 to give the *cis*-2, 6-piperidine derivative 24 (Scheme 10).

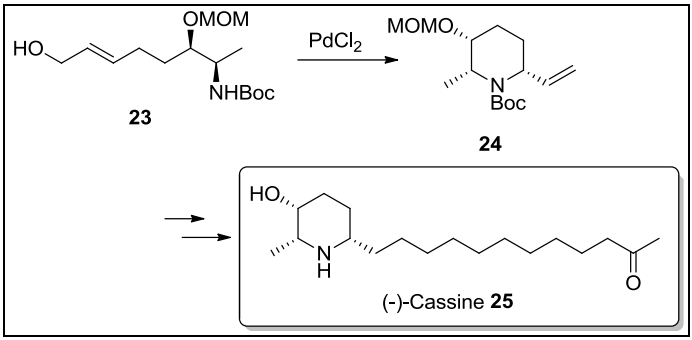

Scheme 10

In a similar manner, Yamada and co-workers utilized the π-allylpalladium intermediate chemistry as the central step to achieve the total synthesis of (+)-Biotin (Scheme 11) [9]. Palladium-catalyzed allylic amination of *cis*-allylic carbonate 26 produced the cyclic intermediate 27, which was further manipulated to give (+)-Biotin 28.

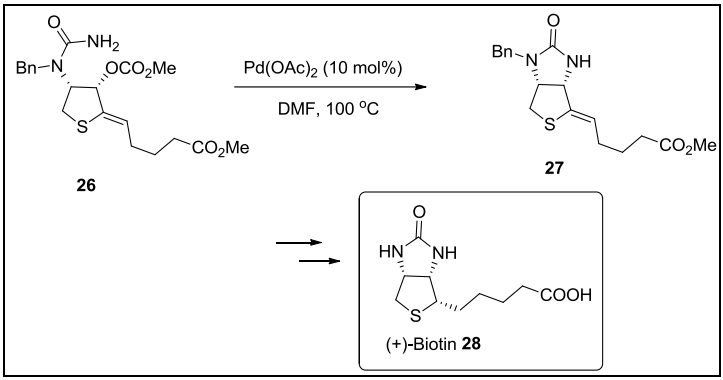

Scheme 11

(+)-Biotin is a water-soluble vitamin isolated in 1941, associated with useful biological properties for human nutrition and animal health [10].

Saisic *et al*. reported an organocatalyzed Tsuji-Trost reaction for the efficient synthesis of carbo- and heterocyclic, five- and six-membered rings from aldehydes containing a suitably positioned allylic moiety 29, in good yields and with reasonable diastereoselectivity. In the presence of chiral phosphine ligands, a catalytic asymmetric cyclization afforded vinylcyclopentane derivative with high levels of enantioselectivity (Scheme 12) [11].

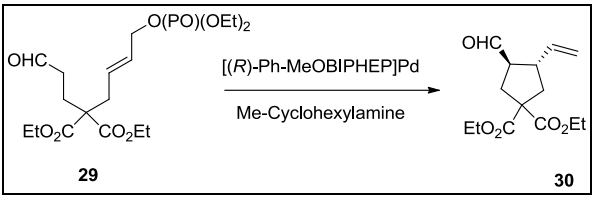

Scheme 12

A formal synthesis of Jiadifenin 33 was reported using intramolecular tandem Tsuji-Trost cyclization/lactonization reaction of allyl carbonate and *β*-keto-ester cyclization as the key step (Scheme 13) [12]. This natural product Jiadifenin 33, isolated from the methanol extract of the pericarps of *Illicium jiadifengpi*, indigenous to the southern part of China [13]. It promotes neurite outgrowth in the primary cultured rat cortical neurons at low concentrations and may have potential for use against Parkinson's and Alzheimer's disease.

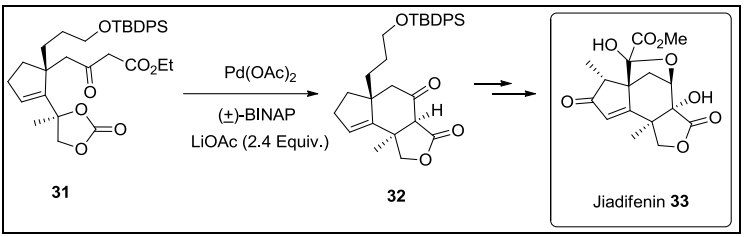

Scheme 13

In 2015, Tsukamoto and co-workers reported the synthesis of *cis*-disubstituted pyrrolidine, tetrahydrofuran, and spiro carbocycles 35 via palladium/chiral diphosphine-catalyzed umpolung cyclization of allylic acetate-aldehyde 34 using formate as a terminal reductant (Scheme 14) [14]. The most important aspect of the reaction was that the formate acts as the terminal reductant and did not reduce the allylpalladium under the catalysis. The reaction proceeds through the formation of cationic η^1-allylpalladium intermediate ligated by the diphosphine ligands 36.

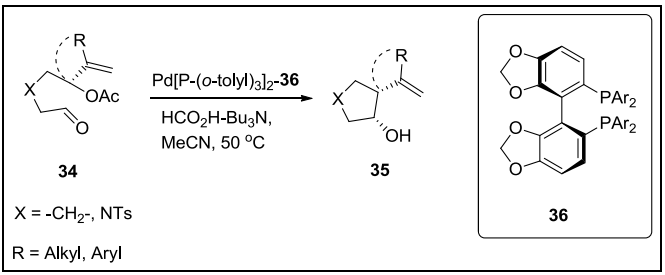

Scheme 14

Poli *et al*. developed a methodology for the synthesis of 3, 4-disubstituted pyrrolidin-2-ones 38 via intramolecular palladium-catalyzed allylic alkylation reaction using acetamide enolate anion as nucleophile (Scheme 15) [15]. The reaction was highly regio- and stereoselective leading exclusively to the Trans product via a 5-exo process. In 2010, the same group developed the asymmetric version of the methodology by using an enantiopure sulfinyl-derived substrate and an enantiopure BINAP as the ligand [16].

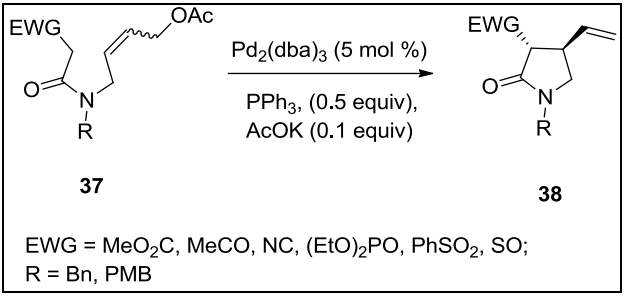

Scheme 15

Recently, Saikia and coworkers described an efficient method for the diastereoselective synthesis of 2, 6-disubstituted and 2, 5-disubstituted morpholines 40 using intramolecular C-O bond formation of *N*-tethered diols 39 consisting of alkanol and alkenol catalyzed by palladium (II) chloride [17]. This methodology was further utilized for the total synthesis of (±) - Chelonin A 41, starting from *N*-tethered diol in 5 steps with an overall 26% yields (Scheme 16).

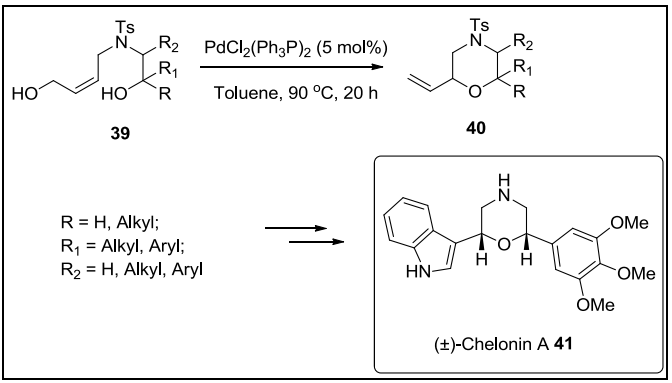

Scheme 16

In 2007, Hirai and co-workers accomplished an asymmetric synthesis of Fagomine 45 via palladium (II) catalysed aminopalladation reaction as the

key step [18]. The precursor for aminopalladation was obtained via multi step procedure from 3-(*t*-Butoxycarbonylamino) propanol 42 (Scheme 17). Fagomine is a piperidine alkaloid which was isolated from buckwheat seeds (*Fagopyrum esculentum, Polygonaceae*) and more recently from *Xanthocericis zambesiaca*, which was found in dry forests in southern Africa [19, 20]. Fagomine exhibits inhibitory activity against mammalian α-glucosidase and β-glucosidase, respectively [21].

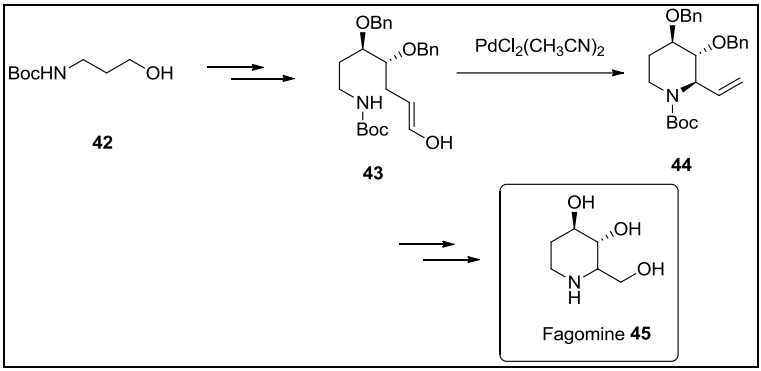

Scheme 17

In 2004, kimura *et al.* reported a Pd (0)-catalyzed amphiphilic activation of bis-allyl alcohols to furnish 3-methylenecyclopentanols using the reaction conditions shown in scheme 18. The symmetric bis-allyl alcohol, 2-hydroxymethl-2-propen-1-ol 46, undergoes electrophilic allylation at the α-position of aldehydes 47 to give hemi-acetals 48, which subsequently act as allylic nucleophiles (in the absence of base) to furnish 3-methylenecyclopentanols 49 in good yields. The reaction is also suitable for aldehydes bearing less acidic α-protons [22].

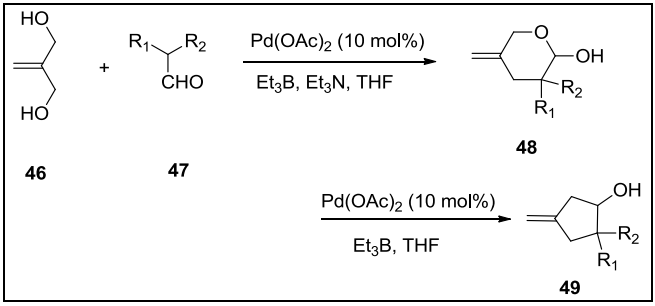

Scheme 18

In a similar manner, in 2007, Tamaru and co-workers reported a novel strategy for the synthesis of vinyl-cyclobutanols 54 from aldehydes 50 and

vinyl epoxides 51 via one pot sequential Tsuji-Trost/umpolung Tsuji-Trost reaction (Scheme 19) [23]. In the first step, aldehyde 50 undergoes α-allylation in the presence of Pd $(acac)_2$ and n-Bu_3P to produce allylic alcohol 52 and after the addition of an excess of BEt_3, nucleophilic allylation occurs to produce vinyl-cyclobutanols 54 in good yields and moderate-to-good diastereoselectivities.

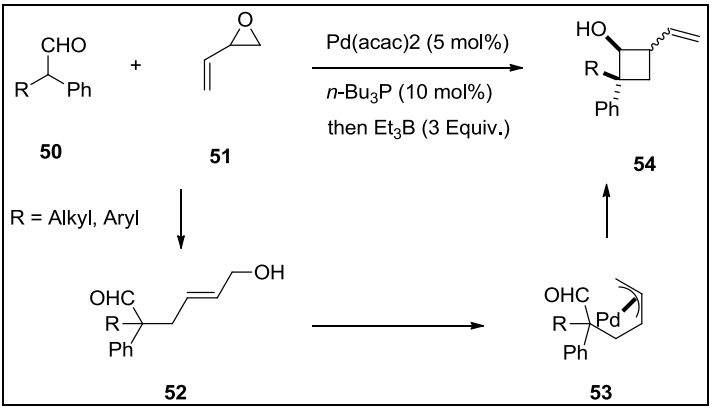

Scheme 19

Another example of asymmetric Tsuji-Trost reaction was demonstrated by Bandini and co-workers in 2006.

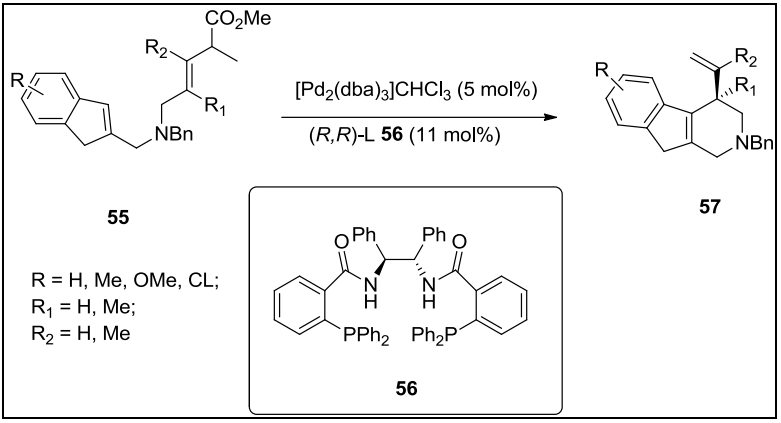

Scheme 20

The 4-vinyl-1,2,3,4-tetrahydro-β-carbolines 57 were efficiently prepared in high regio- and stereoselectivity by the palladium-catalyzed asymmetric cyclization of indolyl-substituted allyl carbonate 55 in the presence of chiral ligand (*R*,*R*)-L56 (Scheme 20) [24].

In 2011, Hiemstra and co-workers reported the total syntheses of corynanthe indole alkaloids (-)-Corynantheidine, (+) – Corynantheine 61, and (+) - dihydrocorynantheine starting from *N*-substituted tryptamine 58 and a protected α- keto ester 59, using a combination of binol phosphoric acid catalyzed enantioselective Pictet-Spengler reaction and an intramolecular Tsuji-Trost type Pd-catalyzed allylic alkylation involving an α- keto ester -derived enolate as the nucleophile (Scheme 21). These alkaloids were isolated from the stem bark of the African tree *Pseudocinchona Africana* and are associated with various pharmacological activities [25].

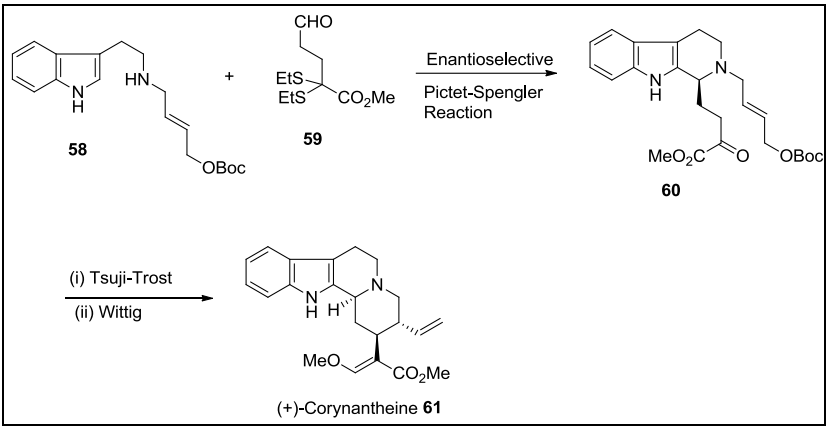

Scheme 21

4. Conclusions

Tsuji-Trost reaction has been widely exploited in synthetic organic chemistry for the diastereoselective and enantioselective transfer of allyl groups to various carbon and heteroatom nucleophiles since its discovery in 1965. The importance of this transformation is underscored by its numerous applications in the synthesis of various complex molecules. This chapter highlighted the basic Tsuji-Trost reaction along with the mechanism of the reaction and application of the reaction in synthesis of carbocyclic and heterocyclic compounds as well as synthesis of natural products and bioactive compounds in past 20 years.

5. References

1. Tsuji J, Takahashi H, Morikawa M. Organic syntheses by means of noble metal compounds XVII. Reaction of π-allylpalladium chloride with nucleophiles. Tetrahedron Letters. 1965; 6(49):4387-4388.
2. Trost BM, Fullerton TJ. New synthetic reactions. Allylic alkylation. J Am. Chem. Soc. 1973; 95:292-294.

3. Jellerich BG, Kong JR, Krische MJ. Catalytic Enone Cycloallylation via Concomitant Activation of Latent Nucleophilic and Electrophilic Partners: Merging Organic and Transition Metal Catalysis. J Am. Chem. Soc. 2003; 125(26):7758-7759.
4. Uenishi J, Ohmi M, Ueda A. Pd^{II}- Catalyzed stereospecific formation of tetrahydro- and 3, 6-dihydro [2*H*] pyran rings: 1, 3-chirality transfer by intramolecular oxypalladation reaction. Tetrahedron: Asymmetry. 2005; 16:1299-1303.
5. Braun J, Ariëns MI, Matsuo BT, Vries SD, Wordragen EDHV, Ellenbroek ED *et al.* Stereoselective Synthesis of Fused Vinyl Cyclopropanes by Intramolecular Tsuji-Trost Cascade Cyclization. Org. Lett. 2018; 20(21):6611-6615.
6. Arthuis M, Beaud R, Gandon V, Roulland E. Counteranion-Directed Catalysis in the Tsuji-Trost Reaction: Stereocontrolled Access to 2, 5-Disubstituted 3-Hydroxy-Tetrahydrofurans. Angew. Chem. Int. Ed. 2012; 51(42):10510-10514.
7. Makabe H, Kong LK, Hirota M. Total Synthesis of (-)-Cassine. Org. Lett. 2003; 5(1):27-29.
8. Peraza PS, Vallado MR, Loeza WB, Mena-Rejón GJ, Quijano, L. Cassine, an antimicrobial alkaloid from Senna racemosa. Fitoterapia. 2000; 71:690-692.
9. Seki M, Mori Y, Hatsuda M, Yamada S. A Novel Synthesis of (+)-Biotin from L-Cysteine. J Org. Chem. 2002; 67(16):5527-5536.
10. Du Vigneaud V, Hofmann K, Melvile DB, Rachele JR. The preparation of free crystalline biotin. J Biol. Chem. 1941; 140:763-766.
11. Vulovic B, Bihelovic F, Matovic R, Saicic RN. Organocatalyzed Tsuji-Trost reaction: a new method for the closure of five- and six-membered rings. Tetrahedron. 2009; 65:10485-10494.
12. Harada K, Imai A, Uto K, Carter RG, Kubo M, Hioki H *et al.* Synthesis of jiadifenin using Mizoroki-Heck and Tsuji-Trost reactions. Tetrahedron. 2015; 71(15):2199-2209.
13. Yokoyama R, Huang CM, Yang CS, Fukuyama YJ. New *seco*-Prezizaane-Type Sesquiterpenes, Jiadifenin with Neurotrophic Activity and 1, 2-Dehydroneomajucin from *Illicium jiadifengpi.* Nat. Prod. 2002; 65 (4):527-531.
14. Tsukamoto H, Kawasea A, Doi T. Asymmetric palladium-catalyzed umpolung cyclization of allylic acetate-aldehyde using formate as a reductant. Chem. Commun. 2015; 51:8027-8030.

15. Giambastiani G, Pacini B, Porcelloni M, Poli G. A New Palladium-Catalyzed Intramolecular Allylation to Pyrrolidin-2-ones. J Org. Chem. 1998; 63(3):804-807.

16. Vogel S, Bantreil X, Maitro G, Prestat, G, Madec D, Poli G. Palladium-catalyzed intramolecular allylic alkylation of α-sulfinyl carbanions: a new asymmetric route to enantiopure γ-lactams. Tetrahedron Letters. 2010; 51:1459-1461.

17. Borah M, Borthakur U, Saikia AK. Diastereoselective Synthesis of Substituted Morpholines from *N*-Tethered Alkenols: Total Synthesis of (±)-Chelonin A. J. Org. Chem. 2017; 82(3):1330-1339.

18. Yokoyama H, Ejiri H, Miyazawa M, Yamaguchi S, Hirai Y. Asymmetric synthesis of fagomine. Tetrahedron: Asymmetry. 2007; 18:852-856.

19. Koyama M, Sakamura S. The Structure of a New Piperidine Derivative from Buckwheat Seeds. Agricultural and Biological Chemistry. 1974; 38:1111-1112.

20. Kato A, Asano N, Kizu H, Matsui A, Watson AA, Nash RJ. Fagomine Isomers and Glycosides from Xanthocercis zambesiaca. Journal of Natural Products. 1997; 60:312-314.

21. Nojima H, Kimura I, Chen FJ, Sugiura Y, Haruno M, Kato A *et al*. Antihyperglycemic Effects of N-Containing Sugars from Xanthocercis zambesiaca, Morus bombycis, Aglaonema treubii, and Castanospermum australe in Streptozotocin-Diabetic Mice. Journal of Natural Products. 1998; 61:397-400.

22. Mukai R, Horino Y, Tanaka S, Tamaru Y, Kimura M. Pd(0)-Catalyzed Amphiphilic Activation of Bis-allyl Alcohol and Ether. J Am. Chem. Soc. 2004; 126(36):11138-11139.

23. Kimura M, Mukai R, Tamaki T, Horino Y, Tamaru Y. Pd (0)-Catalyzed Amphiphilic Allylation of Aldehydes with Vinyl Epoxide J Am. Chem. Soc. 2007; 129:4122-4123.

24. Bandini M, Melloni A, Piccinelli F, Sinisi R, Tommasi S, Umani-Ronchi A. Highly Enantioselective Synthesis of Tetrahydro-β-Carbolines and Tetrahydro-γ-Carbolines Via Pd-Catalyzed Intramolecular Allylic Alkylation. J Am. Chem. Soc. 2006; 128(5):1424-1425.

25. Wanner MJ, Claveau E, Maarseveen JH, Hiemstra H. Enantioselective Syntheses of Corynanthe Alkaloids by Chiral Brønsted Acid and Palladium Catalysis. Chem. Eur. J. 2011; 17:13680-13683.

Chapter - 2
Introduction and Synthesis of Conducting Polymers

Authors

R.K. Shukla
Department of Physics, University of Lucknow, Lucknow, Uttar Pradesh, India

S.K. Singh
Department of Physics, Shia P.G. College, Lucknow, Uttar Pradesh, India

K.C. Dubey
Department of Physics, H.L.Y. P.G. College, Lucknow, Uttar Pradesh, India

Chapter - 2

Introduction and Synthesis of Conducting Polymers

R.K. Shukla, S.K. Singh and K.C. Dubey

Abstract

The conducting polymer has continuous its speedy development throughout the past fifteen years since the innovation that an organic polymer, polyacetylene, could be doped to the metallic regime. A number of original conducting polymers have since been synthesized and numerous chemical, structural and physical studies have helped in elucidate the doping process and electronic and magnetic property of this material; however, an adequate considerate of many elementary phenomenon will only be attain by additional research. The first important signs of scientific applications of these polymers now appear are predictable to encourage even more basic and applied research in this field in the future.

Keyword: Conducting polymers, polypyrrole, polythiophene, polyaniline

1.1 Historical Developments

Although polymeric materials have been used by mankind since prehistoric times in the form of wood, bone, skin, and fibers, the existence of macromolecules was accepted only after Hermann Staudinger developed the concept of macro-molecules during the 1920s, which got him the Nobel Prize in Chemistry in 1953 ‘‘for his discoveries in the field of macro-molecular chemistry’’ [2]. The research field of conjugated (conducting) polymers came into spotlight with the preparation of Polyacetylene by Shirakawa and coworkers along with the subsequent discovery of enhancement in its conductivity after doping [3-6]. Some of the most important representatives in the family of conjugated polymers in non-conducting as well as conducting forms viz., Polythiophene (PTh), Polyaniline (PANI) and Polypyrrole (PPy) were already being prepared chemically or electrochemically in the nineteenth century. The existence of Polyaniline (PANI) in four oxidation states was also recognized. A reaction scheme for the electro-oxidation of aniline at a carbon electrode was suggested by Yasui in 1935 [7]. It was almost a century after Leatherby’s

observations that Mohilner and coworkers reinvestigated the mechanism of the electro-oxidation of aniline in aqueous sulphuric acid solution at a platinum electrode and characterized Polyaniline (PANI) [8]. The first real breakthrough came in 1967, when Duvet and his group established that Polyanilines are redox active electronic conductors and PANI pellets can be used as electrodes for conductivity measurements [9-10].

Polypyrrole (PPy), on the other hand, was known as pyrrole black and was formed due to the oxidation of Pyrrole in air. PPy is an inherently conducting polymer with interesting electrical properties first discovered and reported in the early 1960s [11]. It was followed by the preparation of coherent and free standing Polypyrrole films by electrochemical polymerization by Diaz and his co-workers [12].

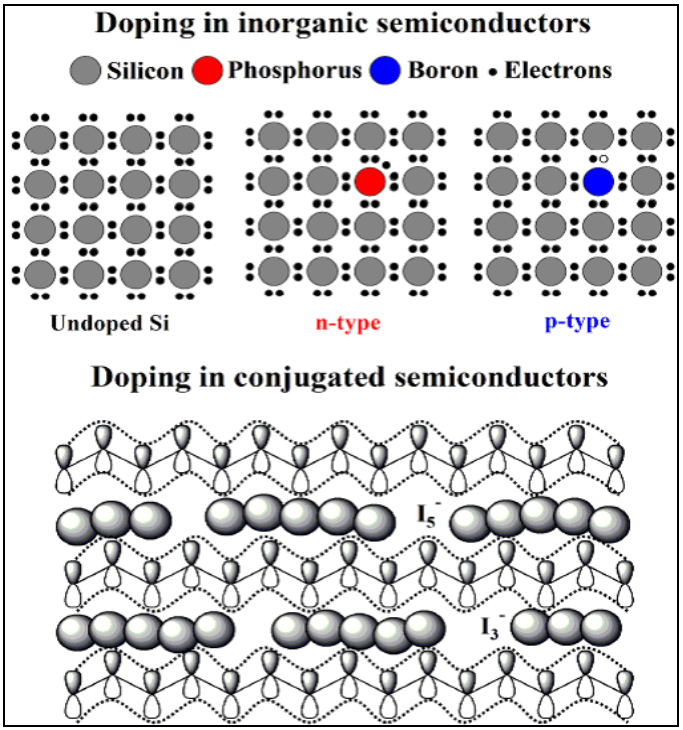

Fig 1.2: Schematic illustration indicating the difference between the doping mechanisms in inorganic semiconductors and conjugated polymers

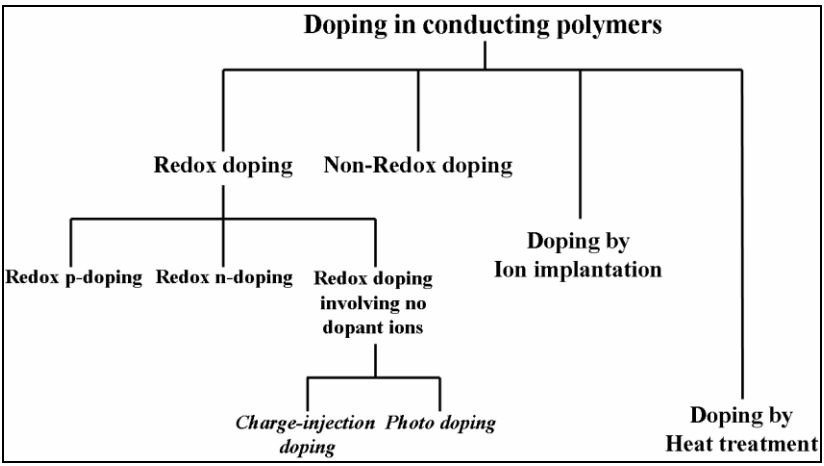

Fig 1.3: Different methods for doping in conducting polymers

Doping of conjugated polymers either by oxidation or by reduction in which the number of electrons in the polymeric backbone gets changed is generally referred to as redox doping [13]. The charge neutrality of the conducting polymer is maintained by the incorporation of the counter ions.

Redox doping can be further subdivided into three main classes: *p* type doping, *n* type doping and doping involving no dopant ions viz., photo-doping and charge injection doping [15, 16]. Both chemical and electrochemical redox doping techniques can be employed to dope conjugated polymers either by removal of electrons from the polymer back-bone chain (*p*-doping) or by the addition of electrons (*n*-doping) to the chain. In chemical doping the polymer is exposed to an oxidizing agent such as iodine vapours or a reducing agents viz., alkali metal vapours, whereas in electrochemical doping process a polymer coated, working electrode is hanging in an electrolyte solution in which the polymer is unsolvable along with separate counter and reference electrodes.

Photo-doping is a process where conducting polymers can be doped without the insertion of cations or anions simply by irradiating the polymer with photons of energy higher than the band gap of the conducting polymer. This leads to the promotion of electrons to higher energy levels in the band gap. Charge injection doping is another type of redox doping that can also be used to dope an undoped conducting polymer [14, 17, 18]. In this method, thin film of conducting polymer is deposited over a metallic sheet separated by a high dielectric strength insulator. The non-redox doping of conducting polymer is a process of doping conducting polymers in which the number of

electrons associated with the polymer chain is kept constant. In fact it is the energy level in the conducting polymer that gets rearranged in the non-redox doping process [19]. The best example of non-redox doping is the conversion of emeraldine base form of Polyaniline to protonated emeraldine base (poly-semiquinone radical cation) when treated with protic acids [10]. It has been observed that the conductivity of Polyaniline is increased by approximately 10 orders of magnitude by non-redox doping. Ion implantation and heat treatment methods have also been used to dope conducting polymers; however, it has rarely been used for doping conducting polymers.

1.2 Ionization Process in Conducting Polymers

Ionization in conducting polymer is due to doping. The introduction of charge during the doping process leads to a structural distortion of a polymeric structure in the region of the charge, giving an energetically favorable conformation. These structural distortions are intrinsic to the development of ionization states called polarons and bipolarons.

1.3 Common Structural Features of Conducting Polymers the Common Structural Features of These Polymers Include

1) Conjugated system along the polymer backbone.
2) Generally planar structure.
3) Intra-chain conductivity $\rho_{\parallel}$ is larger, to inter–chain conductivity ($\rho_{\perp}$).

The anisotropy ratio is $\rho_{\perp}/\rho_{\parallel}$ a parameter used to estimate the one-dimensionality of a particular system. Baughman *et al*. in 1982 have considered the various factors related to structure which lead to enhanced electrical conductivities in conducting polymers. It has been observed that polymers which have uniform chain structures show to be the best conductors. Heterogeneity, on the other hand, can give in carrier localization on the chain element, which provides the lowest potential for holes (or electrons in the case of donor doping). Bredas *et al*. have shown that there exists a connection between the uniform character of the polymer backbone and the width of the highest occupied π-band. The width of the π-bands can be correlated to the degree of delocalization of the π-systems along the polymer backbone and also to the mobility of the carriers in these bands. It showed that as the ionization potential deceases and the breadth of the highest occupied π band increases, the band gap decrease thus creating a better conductor. These results show why polymer research is primarily centered on π-bonded unsaturated systems since these materials have low ionization potentials and large electron affinities. The π electrons can be

easily detached or added to this system and little effect is noted on the σ-bonds which are necessary to hold the basic backbone of the polymer intact.

1.4 Bulk and Nanopolymer

Polymer nanocomposites (PNC's) consist of a polymer or copolymer having nanoparticles or nanofillers dispersed in the polymer matrix. These may be of different shape (e.g. platelets, fibres, spheroids), but at least one measurement must be in the range of 1-50 nanometer. These PNC's fit in to the class of multi-phase systems (MPS, viz. blends, composites and foams) that consume almost 95% of plastics manufacture. These systems require controlled mixing/compounding, stabilization of the achieved dispersion, orientation of the dispersedphase, and the compounding strategies for all MPS, including PNC, are similar. Polymer nano-science is the learn and use of nano-science to polymer-nano-particle matrices, where nano-particles are those with at least one dimension of less than 100 nm. The transition from micro to nano-particles is lead to change in its physical as well as chemical properties. Two of the chief factors in this are i) increase in the ratio of the surface area to volume ii) the size of the particle. The enlarge in surface area-to-volume share, which increases as the particles get lesser, leads to an increasing dominance of the behavior of atoms on the surface area of particle over that of those interior of the particle. This affects the properties of the particles when they are reacting with other particles. Because of the higher surface area of the nano-particles, the dealings with the other particles within the mixture is more and this increases the strength, heat resistance, etc. and many factors do change for the mixture. An example of a nano-polymer is silicon nano-spheres which show quite different characteristics; their size is 40-100nm and they are much harder than silicon, their hardness being between that of sapphire and diamond.

1.5 Metal-Insulator Transition in Doped Conducting Polymers

Metal-Insulator (M-I) transition is one of the most interesting physical aspects of conducting polymers. When the mean free path becomes less than the inter-atomic spacing due to increase in disorder in a metallic system, coherent metallic transport is not possible [20]. When the disorder is sufficiently large, the metal exhibits a transition from the metallic to insulating behavior. As a result of this transition which is also known as the Anderson transition all the states in a conductor become localized and it converts into a Fermi glass with a continuous density of localized states occupied according to Fermi statistics. Although there is no energy gap in a Fermi glass but due to the spatially localized energy states a Fermi glass behaves as an insulator [21]. It has been found that electrical conductivity of a

material near the critical regime of Anderson transition obeys power law temperature dependence [22]. This type of M-I transition has been observed for different conducting polymers viz., Polyacetylene, Polyaniline, Polypyrrole and Poly (p-phenylene vinylene) etc. and is particularly interesting because the critical behavior has been observed over a relatively wide temperature range. In conducting polymers, the critical regime is easily tunable by varying the extent of disorder by means of doping or by applying external pressure and/or magnetic fields. In the metallic regime, the zero temperature conductivity remains finite, and σ (T) remains constant as it approaches zero [23]. Although disorder is normally familiar to play a significant role in the physics of metallic polymers, the effective length scale of the disorder and the nature of the M-I transition [24-25].

In this thesis, we have taken two most popular host conducting polymers such as Polyaniline (PANI) and Polypyrrole (PPy), which are synthesized in laboratory in the form conducting polymer composites.

Polypyrrole is a kind of organic polymer produced by polymerization of Pyrrole. It is also known as conducting polymers. The Nobel Prize in Chemistry was awarded in 2000 for work on conductive polymers including Polypyrrole [6].

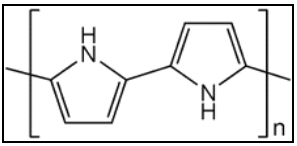

Generally PPy is prepared by oxidation of pyrrole, which can be achieved using ferric chloride in methanol:

$$N\ C_4H_4NH + 2\ FeCl_3 \rightarrow (C_4H_2NH)_n + 2\ FeCl_2 + 2\ HCl$$

Polymerization is thought to take place via the creation of the pi-radical cation $C_4H_4NH^+$. This electrophile attacks the C-2 carbon of an un-oxidized molecule of pyrrole to give a dimeric cation $(C_4H_4NH)_2]^{++}$. The process repeats itself many times. PPy are prepared by oxidation of the polymer in Conductive forms:

$$(C_4H_2NH)_n + x\ FeCl_3 \rightarrow (C_4H_2NH)_n\ Cl_x + x\ FeCl_2$$

The polymerization and p-doping could be affected electrochemically. The resulting conductive polymers are peeled off of the anode. Polypyrrole is also being investigated in low temperature fuel cell technology to increase the catalyst dispersion in the carbon support layers [7-10] and to sensitize cathode electro-catalysts, as it has been inferred that the metal electro-

catalysts (Pt, Co etc.) when coordinated with the nitrogen in the Pyrrole monomers show enhanced oxygen reduction activity.

Polypyrrole (together with other conjugated polymers such as Polyaniline, Poly (ethylene dioxythiophene) etc. has been keenly study as a material for artificial muscles, a technology that would offer numerous advantages over traditional motor actuating elements [11]. Polypyrrole was used to coat silica and reverse phase silica to yield a material capable of anion exchange and exhibiting hydrophobic connections. Polypyrrole was used in the microwave fabrication of multi-walled carbon nanotubes (CNTs), a new method that allows obtaining CNTs in a matter of seconds [12]. Chemical and Engineering News reported in June 2013 that Chinese research has produced a water-resistant polyurethane sponge coated with a thin layer of Polypyrrole that absorbs 20 times its weight in oil and is reusable.

A conducting polymer like Polyaniline is of the semi-flexible rod polymer family. This interest is due to the research of large electrical conductivity. Both the family of conducting polymers and organic semiconductors, Polyaniline has many attractive processing properties. Because of its rich chemistry, Polyaniline is one of the most studied conducting polymers of the past 50 years [13].

Polymerized from the not expensive aniline monomer, Polyaniline can be originating in one of three idealized oxidation states:

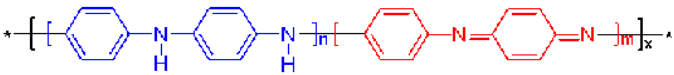

Polyaniline (PANI)

Above Figure shows that *x* is half the degree of polymerization. With n=1, m=0 is the fully reduced state of Leucoemeraldine. Pernigraniline is the fully oxidized state (n=0, m=1) with imine links instead of amine links [14]. Studies shows that mainly form of Polyaniline are one of the three states or physical mixtures of these components. The emeraldine (n=m=0.5) form of polyaniline, frequently referred to as emeraldine base (EB), is neutral, if doped (protonated) it is called emeraldine salt (ES), with the imine nitrogen's protonated by an acid. Protonation helps to delocalize the otherwise intent iminoquinone-diaminobenzene state. Emeraldine base is regarded as the mainly useful form of Polyaniline due to its high constancy at room temperature and the fact that, upon doping with acid, the resulting emeraldine salt form of Polyaniline is significantly electrically conducting. Leucoemeraldine and pernigraniline are poor conductors, even when doped with an acid [15].

The colour change linked with Polyaniline in dissimilar oxidation states can be used in sensors and electrochromic devices. While colour is helpful, the best method for making a Polyaniline sensor is arguably to take advantage of the dramatic changes in electrical conductivity between the different oxidation states or doping levels [16]. Treatment of emeraldine with acids increases the electrical conductivity by ten orders of magnitude [17]. Polyaniline has a conductivity of 6.28×10^{-9} S/m, although conductivities of 4.60×10^{-5} S/m can be achieved by doping to 4% HBr. The similar material can be produced by oxidation of leucoemeraldine. Polyaniline is nobler than copper and slightly less noble than silver which is the basis for its broad use in printed circuit board manufacturing and in corrosion protection [17].

1.6 Synthesis of Polymers and Their Polymer Composites

Electrochemical polymerization (ECP) is performed in a single-compartment cell containing electrochemical bath which includes a monomer and a supporting electrolyte dissolved in appropriate solvent. It also includes three different electrode such as working electrode (cathode), reference electrode and counter electrode (anode). Film deposited on the counter electrode (anode). Usually ECP is carried out either Potentiostatic Ally (i.e. constant voltage condition) or Galvanostatically (i.e. constant current condition) by using a suitable power supply. Potentiostatic conditions are recommended to obtain thin films while galvanostatic conditions are recommended to obtain thick films [23].

Chemical polymerization is the process in which relatively small molecules, called monomers, combine chemically to produce a very large chainlike or network molecule. The monomer molecules can be similar, or they may correspond to two, three, or more different compounds. Usually at most 100 monomer molecules have to be combined to make a product that has certain unique physical properties such as elasticity, high tensile strength, or the ability to form fibers that distinguish polymers from substances composed of smaller and simpler molecules; often, many thousands of monomer units are incorporated in a single molecule of a polymer. The formation of stable covalent chemical bonds among the monomers sets polymerization apart from other processes, such as crystallization, in which large numbers of molecules aggregate under the influence of weak intermolecular forces.

References

1. Ye Mamunya P *et al*. Eur. Polym. J. 2002; 38:1887-1897.
2. Mülhaupt R. Angew. Chem. Int. Ed. 2004; 43:1054-1063.

3. Shirakawa H *et al*. J Chem. Soc. Chem. Commun. 1977; 13:578-580.
4. Chiang CK *et al*. Phys. Rev. Lett. 1977; 39:1098-1101.
5. Chiang CK *et al*. J Chem. Phys. 1978; 69:5098-5104.
6. Chiang CK *et al*. J Am. Chem. Soc. 1978; 100:1013-1015.
7. Yasui T. Bull. Chem. Soc. Japan. 1935; 10:305-311.
8. Mohilner DM *et al*. J Electrochem. Soc. 1962; 84:3618.
9. De Surville R *et al*. Electrochim Acta. 1968; 13:1451-1458.
10. Chiang JC, MacDiarmid AG. Synth. Met. 1986; 13:193-205.
11. Bolto BA *et al*. Aust. J Chem. 1963; 16:1090-1103.
12. Kanatzidis MG. Chem. Eng. News. 1990; 68:36-54.
13. Ziemelis KE *et al*. Phys. Rev. Lett. 1991; 66:2231-2234.
14. Diaz F. Chemica Scripta. 1981; 17:145-148.
15. Ahonen HJ *et al*. Macromolecules. 2000; 33:6787-6793.
16. De Leeuw DM *et al*. Synth. Met. 1997; 87:53-59.
17. Burroughes JH *et al.* Nature. 1988; 335:137-14.
18. Burroughes JH *et al*. Nature. 1990; 347:539-541.
19. MacDiarmid AG Synth. Met. 2001; 125:11-22.
20. Heeger J. Physica Scripta. 2002; 102:30-35.
21. Anderson PW. Phys. Rev. 1958; 109:1492-1505.
22. McMillan WL. Phys. Rev. B. 1981; 24:2739-2743.
23. Menon R *et al*. 2nd ed., Skotheim, Inc. New York, 1998, 27.

Chapter - 3
Corrosion Control

Authors

Olawale
Olamide & Senior Lecturer, Chemical Engineering Department, Landmark University, Omu-Aran, Kwara, Nigeria

Ogunsemi
Bamidele T & Lecturer I, Mechanical Engineering Department. Landmark University, Omu-Aran, Kwara, Nigeria

Bello
Josiah O & Professor, Chemical Engineering Department, Landmark University, Omu-Aran, Kwara, Nigeria

Olayanju
Adeniyi, Professor of Agricultural and Mechanization, Agricultural and Biosystems Engineering, Landmark University, Omu-Aran, Kwara, Nigeria

Chapter - 3

Corrosion Control

Olawale, Ogunsemi, Bello and Olayanju

Abstract

Corrosion, if not properly controlled, can result to high cost of maintenance, loss of life or in some cases shut down of industries. Corrosion control is a method of combating degradation challenges on metals in industries. The major forms of corrosion control include: Cathodic protection, Linings and Coatings, selection of materials and the use of inhibitors. Research on inhibitors has over the years been tailored to green technology via the use of plant extracts because they are cheap, readily available and also environmentally friendly. It can be concluded that inhibitors have been confirmed to be one of the most effective methods for corrosion control.

Keywords: Corrosion control, cathodic protection, material selection, inhibitors

1. Introduction

What is Corrosion?

Corrosion is the deterioration or destruction of metals and alloys in an environment by chemical or electrochemical means. In simple terminology, corrosion processes involve reaction of metals with environmental species. It can also be defined as the gradual destruction of materials (usually metals), by chemical reaction with its environment. This means electrochemical oxidation of metals in reaction with an oxidant such as oxygen.

Rusting, which is the formation of iron oxides, is a well-known example of electrochemical corrosion. This type of damage typically produces oxide(s) or salt(s) of the original metal. Corrosion can also occur in materials other than metals, such as ceramics or polymers, although in this context, the term degradation is more common. Corrosion degrades the useful properties of materials and structures including strength, appearance and permeability to liquids and gases. Many structural alloys corrode merely from exposure to moisture in air, but the process can be strongly affected by exposure to

certain substances.However, the nature and extent of any corrosion is linked to the amount of time the metal surfaces are exposed to moisture and the amount of air pollution and the corrosion has to be controlled.

1.1 Electrochemistry of Corrosion

The corrosion reactions involve the transfer of electrons and ions between the metal and the solution. The rates are equivalent to electric currents. The rates of these reactions depend on the potential difference between the metal and the solution, i.e. the potential of the metal. As the potential of the metal becomes more positive, the rates of anodic reactions increase and the rates of cathodic reactions decrease. The converse effect on the reaction rates occurs as the potential of the metal becomes more negative. From the relationships between the potential of a metal and the currents flowing (equivalent to rates of the corrosion reactions), the corrosion behaviour can be understood. The relationships between potential and current (termed polarisation curves) can be determined as shown schematically in Fig 1. The potential in the test solution of the metal under study, the working electrode, is measured against that of a reference electrode by means of a Voltmeter. The reference electrode is chosen to give a stable and reproducible potential in the solution. The reference electrode most commonly used is the saturated calomel electrode, which consists of mercury covered with a paste of mercurous chloride and mercury in a chloride solution. The potential depends on the concentration of chloride ions and a saturated solution of potassium chloride is used because this minimises the junction potential between the test solution and the solution in the reference electrode in the measuring cell.

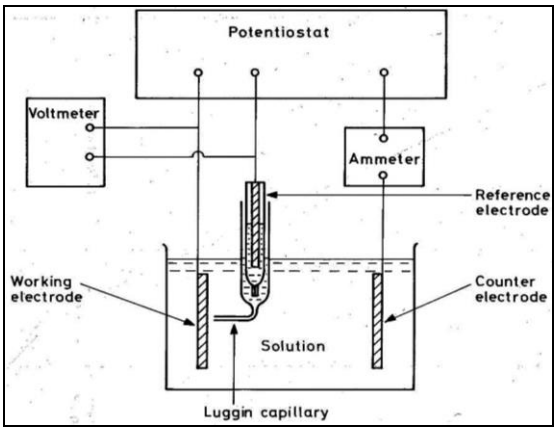

Fig 1: Schematic diagram of apparatus for the determination of polarization curves of a metal in a solution using a potentiostat

1.2 Corrosion Control

Corrosion control refers to measures that are implemented in various fields to control corrosion in: Soil, Metal, Concrete, Water, Sand and Masonry. Corrosion if not controlled can lead to the major harmful effects. Some of the effects of corrosion are the following:

1) Reduction of metal thickness leading to loss of mechanical strength and structural failure or breakdown.
2) Hazards or cause injuries to people: i.e. arising from structural failure or breakdown (e.g. bridges, cars, aircraft).
3) Loss of time in availability of profile-making industrial equipment.
4) Reduced value of goods due to deterioration of appearance.
5) Contamination of fluids in vessels and pipes (e.g. beer goes cloudy when small quantities of heavy metals are released by corrosion).
6) Perforation of vessels and pipes allowing escape of their contents and possible harm to the surroundings.
7) Loss of technically important surface properties of a metallic component.

Furthermore, corrosion control techniques can be used by industries to solve corrosion problems according to their requirements. With such measures in place, the harmful effects and negative consequences of corrosion can be reduced to the barest minimum if not completely eradicated.

1.3 Major Methods for Controlling Corrosion

The methods are: Cathodic protection (CP); Linings and coatings; Selection of Materials; and lastly use of Corrosion Inhibitors.

1.3.1 Cathodic Protection (CP)

This is a method used to control the corrosion of a metal surface by making it the cathode of an electrochemical cell. A simple method of protection connects the metal to be protected to a more easily corroded "sacrificial metal" to act as the anode. The sacrificial metal then corrodes instead of the protected metal. CP is used in long pipelines, where passive galvanic cathodic protection is not adequate, an external DC electrical power source is used to provide sufficient current.

Cathodic protection systems protect a wide range of metallic structures in various environments. Common applications are: steel water or fuel pipelines and steel storage tanks such as home water heaters; steel pier piles;

ship and boat hulls; offshore oil platforms and onshore oil well casings; offshore wind farm foundations and metal reinforcement bars in concrete buildings and structures. Another common application is in galvanized steel, in which a sacrificial coating of zinc on steel parts protects them from rust**.** In some cases, it also prevents stress corrosion cracking**.** Its advantage is that it prevents the onset of corrosion and even stops it from getting complicated.

1.3.1.1 How does Cathodic Protection Stop Corrosion?

Cathodic protection prevents corrosion by converting all of the anodic (active) sites on the metal surface to cathodic (passive) sites by supplying electrical current (or free electrons) from an alternate source. Usually, this takes the form of galvanic anodes, which are more active than steel. This practice is also referred to as a sacrificial system, since the galvanic anodes sacrifice themselves to protect the structural steel or pipeline from corrosion. However, in the case of aluminum anodes, the reaction at the aluminum surface is: (four aluminum ions plus twelve free electrons).

$4Al \Rightarrow 4AL^{+++} + 12e^-$ and at the steel surface: (oxygen gas converted to oxygen ions which combine with water to form hydroxyl ions).

$$3O_2 + 12e^- + 6H_20 \Rightarrow 12OH^-$$

As long as the current (free electrons) arrive at the cathode (steel) faster than oxygen, no corrosion will occur. Table 1 showed the comparison of cathodic and anodic protection methods.

Table 1: Comparison of cathodic and anodic protection methods

Factors	Cathodic Protection	Anodic Protection
Suitability	To all metals in general.	Only to those exhibiting active-passive behavior
Environment	Only for moderate corrosion environment.	Even aggressive chemical corrosives.
Cost benefit	Low investment, but higher operative costs.	Higher investment, but low operative costs.
Operation	Protective currents to be established through initial design and field trials	More precise electrochemical estimation of protection range possible

1.3.2 Linings and Coatings

The methods are used to combat corrosion of pipelines and to ensure a long term performance life. These typically include the application of coatings and linings as well as the additional use of a cathodic protection system. These serve as the main tools for fighting corrosion. They are

usually applied in combination with CP to achieve the highest level and most cost-effective corrosion protection. However; to control pipeline corrosion, a coating system is applied to the pipe surface to reduce or eliminate the potential between the anode and the cathode, or to provide an impermeable membrane to separate the electrolyte from the metallic surfaces. The potential current between the anode and cathode can be reduced or neutralized with the use of cement coatings, a process called "passivation." A variety of bonded dielectric coatings are available, which are designed to isolate the metallic pipeline from the surrounding environment, thus providing electrical isolation. Although coatings, by themselves, may not be the perfect answer to corrosion control in all environments, when they are however used properly in conjunction with a cathodic protection system, a nearly unlimited life can be achieved. Cathodic protection (CP) is a method which when connected to the pipeline, discharges an electrical current from a remote anode to the pipe. If enough current is discharged from the remote anode to the pipe, corrosion on the pipeline will not occur.

There are *two major categories of linings and coatings* applied to steel pipe. One is cementitious materials, which neutralize the chemical process by passivation. The second is dielectric, which provides a physical barrier separating the metallic surface from the electrolyte. Both systems can be used as either linings or coatings.

1.3.2.1 Cement Mortar Lining

Cement-mortar lining is the most commonly specified lining material in today's water transmission industry. A lean mixture of three parts sand to one part cement is centrifugally spun onto the interior surface to create a dense, smooth surface. The actual cement application is performed by pumping or pouring a high slump cement mixture onto a slowly rotating length of pipe. The rotating speed is then increased so the proper centrifugal forces level out the wet mortar to a uniform thickness. Continued spinning removes the excess water and compact the mixture to a dense and hard surface. After the spinning process, the lining is cured either by moist curing at ambient temperature or by an accelerated process using steam. Like concrete, cement-mortar lining can develop drying cracks, but these cracks will self-heal when the lining is wet. Wetting the cement lining also causes the lining to swell, which increases strength and adherence. Cement-mortar linings can add significant stiffness for resistance to deflection forces. The strength of the mortar lining may be added to the strength of the steel when calculating stiffness. Cement-mortar linings perform best when flow velocity is 20 feet per second or less.

Fig 2: Cement coating of the inner wall of water steel pipeline

1.3.2.2 Paints and Polyurethane Linings

Bonded dielectric linings have been used as protective linings for above-ground applications for many years. There are two major categories of liquid film linings used in the waterworks industry. These are: epoxies and polyurethane-based products.

Epoxies are applied per AWWA C210 and polyurethanes per AWWA C222. These linings have excellent water and chemical resistance properties and can be used as an alternative to cement mortar lining. They can be applied at various thicknesses in factories to provide an excellent dielectric lining. Bonded dielectric lining systems can be applied as either a single or a multiple coating process.

Bonded dielectric linings are tough, resilient, and extremely abrasion-resistant, making them an ideal lining choice for high internal velocities. Bonded dielectric lining systems are an excellent choice for extreme conditions such as wastewater or other industrial applications, including both gravity sewer and sanitary force mains. Epoxy and polyurethane systems do have some drawbacks that must be considered prior to applications. A critical performance factor to all film linings is the surface preparation of the metal surface. In most cases, a near-white blast surface is required for proper adhesion, and this will require good inspection. Curing times and curing temperatures must adhere to critical tolerances. With proper surface preparation, controlled applications, and strict curing procedures, thin-film materials can provide a strong, resistant, long-lived lining. Epoxies are typically solvent-based, although some 100% solids epoxies are now available. The epoxies are typically mixed and then applied by airless spray or brushed on to the pipe. The polyurethanes require heated, plural-component equipment. Epoxies typically cure in a matter of hours to days, whereas polyurethanes may be handled in a matter of minutes.

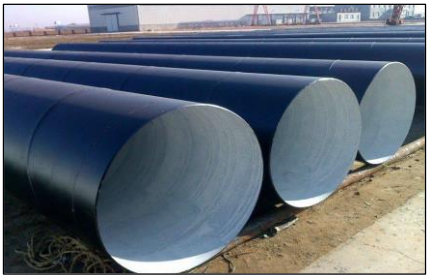

Fig 3: Coating of outside surface of pipeline with coal tar + epoxy

1.3.2.3 Enamels

Enamels are glassy layer applied to the metal by dipping it in a suspension of powdered glass, and then the metal is heated in a stove (furnace) at high temperature suitable to melt the glass powder and coat the metal.

1.3.2.4 Modern Tape Coatings

These are the most universally specified dielectric coatings in the water industry. The electrical resistance, mechanical strength, reasonable cost, and long performance record of tape coatings have contributed to their success in the water industry, the oil and also in gas industry. The tape system consists of cleaning and blasting the pipe surface, immediately applying a primer-adhesive, and then simultaneously applying the inner dielectric tape (corrosion protection) and outer-layer tapes (mechanical protection).

1.3.2.5 Surface Preparation

The pipe surface is first cleaned and then grit-blasted to achieve a surface preparation at least equal to that specified in Surface Preparation Specification No. 6, SSPC-SP 6, Commercial Blast Cleaning.

1.3.2.6 Priming

A primer is a paint containing a pigment such as lead oxide (Pb_3O_4 red lead) or zinc chromate which oxidizes the steel surface and inhibits its corrosion. Besides, the primer film increases the strength of the bond between steel and final paint film. When the primer film dries a thick film of the required paint is applied over the primer. Immediately after blasting, the pipe receives an adhesive or primer coating. The primer coating is applied as recommended by the producer. When complete, it will be uniform and free of sags, runs, and bare spots. The state of dryness of the primer should also be in accordance with the recommendation of the manufacturer.

1.3.2.7 Tape Application

The inner corrosion protection tape layer is directly applied to the primed surface using a helically wound process. The minimum overlap shall not be less than 1 inch. The applied tape is tight, wrinkle-free, and smooth. The inner tape is then tested to ensure there are no flaws or holidays using 6000- volt detectors. Outer-layer *Tape* Simultaneous to the inner wrap, one or two layers of polymeric type mechanical-protection tape is also spirally wound over the inner tape coat. The completed multi-layer tape coating system will provide a final protective encasement of between 50 and 80 mils of strong, durable, lightweight, and reliable bonded coating.

1.3.3 Selection of Materials

Materials selection refers to the selection and use of corrosion-resistant materials such as stainless steels, plastics, and special alloys to enhance the life span of a structure. Some of the most common materials used in constructing a variety of facilities, such as steel and steel-reinforced concrete, can be severely affected by corrosion. Material selection is crucial to obtain a long service life and to avoid damage such as operation failure in terms of mechanical strength or unacceptable appearance in some cases due to corrosion products.

The Important Mechanical Properties Affecting the Selection of a Material are

i) **Tensile Strength:** This enables the material to resist the application of a tensile force. To withstand the tensile force, the internal structure of the material provides the internal resistance.

ii) **Hardness:** It is the degree of resistance to indentation or scratching, abrasion and wear. Alloying techniques and heat treatment help to achieve the same.

iii) **Ductility:** This is the property of a metal by virtue of which it can be drawn into wires or elongated before rupture takes place. It depends upon the grain size of the metal crystals.

iv) **Impact Strength:** It is the energy required per unit cross-sectional area to fracture a specimen, i.e., it is a measure of the response of a material to shock loading.

v) **Wear Resistance:** The ability of a material to resist friction wear under particular conditions, i.e. to maintain its physical dimensions when in sliding or rolling contact with a second member.

vi) **Corrosion Resistance:** Those metals and alloys which can

withstand the corrosive action of a medium, i.e. corrosion processes proceed in them at a relatively low rate are termed corrosion-resistant.

vii) **Density:** This is an important factor of a material where weight and thus the mass is critical, i.e. aircraft components.

1.3.3.1 Corrosive Medium Parameter

a) Composition of the corrosive medium. For instance, if a metal is exposed to seawater, a quantitative analysis of all constituents must be made to determine the composition.

b) The physical and external factors affecting the medium, such as pH, conductivity, temperature and velocity affect the magnitude of corrosion induced by the medium.

c) The presence of dissolved gases, such as oxygen, carbon dioxide, hydrogen sulphide in fluids promotes the corrosiveness of the medium.

d) Presence of organic matter and bacteria promote the corrosiveness of the environment. For instance, sulphide reducing bacteria, desulfovibrio and clostridium, induce corrosion by producing hydrogen sulphide, a serious steel corrodent. Algae, yeasts and molds also contribute to corrosion.

e) Physical state of the corrosive medium has a pronounced effect on the corrosiveness of the medium. For instance, a dry soil would be less aggressive to corrosion than a wet soil in which salts are dissolved. Similarly, a frozen soil with a very high resistivity exceeding 10000 ohm-cm would not corrode a pipe, whereas, a wet soil with a low resistivity, such as 500 ohm-cm would cause severe corrosion to structure buried in the soil. Liquids in intimate contact with metals, such as seawater, acids alkalis and alkalis, are serious corroders for a large variety of metals and alloys. The presence of gases leads to adsorption on the surface and the formation of an oxide, sulphide, and chlorides. Dry oxidation refers to an electron producing reaction in a dry gaseous environment. It is also known as 'hot corrosion if sulphur is involved. Accelerated oxidation (catastrophic oxidation) occurs at high temperatures and leads to accelerated failure of metals.

1.3.3.2 Design Parameters

Design parameters which affect the rate of corrosion include the following:

1) Stresses acting on the materials in service
2) Relative velocity of the medium and obstacles to flow
3) Bimetallic contacts
4) Crevices
5) Riveted joint
6) Spacing for maintenance
7) Drainage and directional orientation of loop
8) Joints to avoid entrapment
9) Sharp corners
10) Non-homogeneous surface.

1.3.3.3 Materials Parameters

The following are the material parameters which may affect corrosion resistance.

1) Impurity segregation on grain boundaries leads to weakening of grain boundaries and accelerates corrosion attack.
2) Microstructural constituents. A heterogeneous microstructure forms anodic and cathodic sites which promotes corrosion. The intermetallic precipitate serves as anodic and cathodic sites and they may be anodic or cathodic to the matrix. For instance, a C11AI2 precipitate is cathodic to the aluminum matrix and Mg_2Si is anodic to the matrix. Microstructural variation plays a leading role in metal matrix composites. For instance, Al 6013-SiC composite corrodes at the Al matrix/SiC interface because of the preponderance of intermetallic secondary phases. Also a non-homogeneous distribution of SiC contributes to accelerated corrosion.
3) Surface treatment, such as galvanizing, phosphating and painting increase the resistance of materials to corrosion. Galvanizing improves the resistance of steels to corrosion and is widely used in automobile industry. Galvanized pipes are widely used for transport of hot water in domestic plumbing systems. If the temperature, however, exceeds 65 °C, reversal of polarity (steel becomes anodic) can cause corrosion of the galvanized pipes.
4) Alloying elements and film formation. Alloying elements in steels, such as chromium, nickel or molybdenum contribute to the production of a protective oxide layer which makes steel passive.

1.3.3.4 Fabrication Parameters

The following are the fabrication parameters required for analysing material selection;

1) Weldability. Welding procedures, such as electric arc welding, friction welding, spot welding, need to be carefully selected to minimize the effect of corrosion. For instance, gas welding in the sensitive temperature range may cause intergranular cracking.
2) Machinability. Machining operations, such as drilling, milling, shearing, turning, may lead to enhancement of corrosion if they are not properly controlled. Drilling fluids are highly corrosive and need to be handled with care.
3) Surface modification procedures, such as cladding, galvanizing and metallizing (metallic coatings) increase the resistance of the materials to corrosion. The success of the coating depends on the bonding between the coating and the substrate and surface preparation before the application of coatings according to the international standards.

Surface preparation techniques include hand, power tool cleaning and abrasive blast cleaning according to the American Standards for Surface Cleaning.

1.3.4 Corrosion Inhibitors

A corrosion inhibitor is a chemical compound which when added to a liquid or gas, decreases the corrosion rate of a material, typically a metal or an alloy. The effectiveness of a corrosion inhibitor depends on fluid composition, quantity of water, and flow regime.

They are common in industry, and also found in over-the-counter products, typically in spray form in combination with a lubricant and sometimes penetrating oil. Plants extracts have become focus on corrosion inhibitor research due to its low toxicity, easy availability and economical preparation. The search for an efficient inhibitor for corrosion in different aggressive media has in recent times taken a new dimension owing to the clarion call for green technology. However, use of inhibitors is one of the most used methods for creating corrosion resistance, especially in acid descaling bathes, to prevent not only the metal dissolution but also acid consumption. Inhibition protects the metals by efficiency adsorbing on its surface and blocking the active sites for metal dissolution and on hydrogen evolution; thereby hindering overall metal corrosion metal corrosion in aggressive environments.

Green corrosion inhibitors such as extracts from many plants had been investigated and reported by several authors as being biodegradable and not containing heavy metals or other toxic compounds. Plant products are organic in nature, and contain certain photochemical including tannins, flavonoids, saponins, organic and amino acids, alkaloids, and pigments which could be extracted by simple less expensive procedures. Extracts from different parts of plant have been widely reported as effective and good metal corrosion inhibitors in various corrosive environments. A lot of research had been done on the use of plant sources / extracts as effective inhibitors. These environmentally friendly inhibitor sources are natural products which are non-toxic, cheaply processed, biodegradable and readily available in plenty and are sometimes regarded as agro-waste. In this regard, some of the extracts used are: Red Peanut skin Jatropha stem; Rice husk, Bitter Kola Stem, Pawpaw leaves, and Groundnut leaves extract among several others have recorded varied levels of success; research efforts are still ongoing to search for other green inhibitor alternatives. The nature of the corrosive inhibitor depends on (i) the material being protected, which are most commonly metal objects, and (ii) on the corrosive agent(s) to be neutralized. The corrosive agents are generally oxygen, hydrogen sulphide, and carbon dioxide. Oxygen is generally removed by reductive inhibitors such as amines and hydrazine:

$$O_2 + N_2H_4 \rightarrow 2\ H_2O + N_2$$

However, corrosion inhibitors are commonly added to coolants, fuels, hydraulic fluids, boiler water, engine oil, and many other fluids used in industry

1.3.5 Classification of Inhibitors

The corrosion inhibitors can be chemicals either synthetic or natural and could be classified by: the chemical nature as organic or inorganic; the mechanism of action as anodic, cathodic or anodic-cathodic mix and by adsorption action, or; as oxidants or not oxidants. In general, the inorganic inhibitors have cathodic actions or anodic. The organics inhibitors have both actions, cathodic and anodic and the protective by a film adsorption. The classification of corrosion is shown in Figure 6.

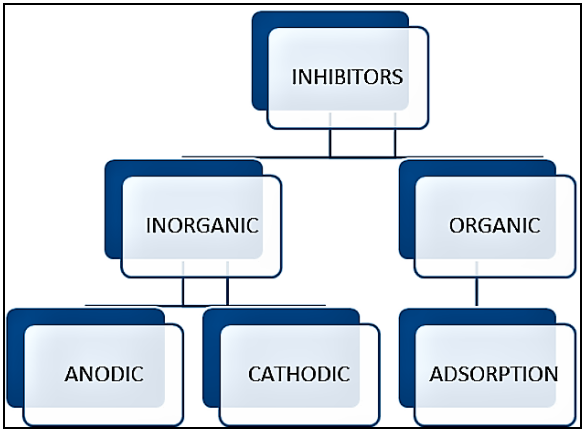

Fig 6: Classification of inhibitors

1.3.5.1 Inorganic Inhibitors

1) **Anodic Inhibitors:** Anodic inhibitors (also called passivation inhibitors) act by a reducing anodic reaction, that is, it blocks the anode reaction and supports the natural reaction of passivation metal surface, also, due to the forming a film adsorbed on the metal. In general, the inhibitors react with the corrosion product, initially formed, resulting in a cohesive and insoluble film on the metal surface. The anodic reaction is affected by the corrosion inhibitors and the corrosion potential of the metal is shifted to more positive values. The anodic inhibitors reacts with metallic ions Men+ produced on the anode, forming generally, insoluble hydroxides which are deposited on the metal surface as insoluble film and impermeable to metallic ion. When the concentrations of inhibitor becomes high enough, the cathodic current density at the primary passivation potential becomes higher than the critical anodic current density, that is, shift the potential for a noble sense, and, consequently, the metal is passivated. For the anodic inhibitors effect, it is very important that the inhibitor concentrations should be high enough in the solution. The inappropriate amount of the inhibitors affects the formation of film protection, because it will not cover the metal completely, leaving sites of the metal exposed, thus causing a localized corrosion. Concentrations below to the critical value are worse than without inhibitors at all. In general can cause pitting, due reduction at the anodic area relative to cathodic, or can accelerate corrosion, like generalized corrosion, due to full breakdown the passivity. Some examples of anodic inorganic

inhibitors are nitrates, molybdates, sodium chromates, phosphates, hydroxides and silicates.

2) **Cathodic Inhibitors:** These inhibitors have metal ions able to produce a cathodic reaction due to alkalinity, thus producing insoluble compounds that precipitate selectively on cathodic sites. Deposit over the metal a compact and adherent film, restricting the diffusion of reducible species in these areas. Thus, increasing the impedance of the surface and the diffusion restriction of the reducible species, that is, the oxygen diffusion and electrons conductive in these areas. These inhibitors cause high cathodic inhibition. The cathodic inhibitors form a barrier of insoluble precipitates over the metal, covering it. Thus, restricts the metal contact with the environment, even if it is completely immersed, preventing the occurrence of the corrosion reaction. Due to this, the cathodic inhibitor is independent of concentration, thus, they are considerably more secure than anodic inhibitor. Some examples of inorganic cathodic inhibitors are the ions of the magnesium, zinc, and nickel that react with the hydroxyl (OH-) of the water forming the insoluble hydroxides as $Mg(OH)_2$, $Zn(OH)_2$, and $Ni(OH)_2$ which are deposited on the cathodic site of the metal surface, protecting it. However; it can also be in cited polyphosphates, phosphates, tannins, lignin and calcium salts via the same reaction mechanism.

1.3.5.2 Organic Inhibitor

Organic compounds used as inhibitors, occasionally, they act as cathodic, anodic or together, as cathodic and anodic inhibitors, nevertheless, as a general rule, act through a process of surface adsorption, designated as a film-forming. Naturally the occurrence of molecules exhibiting a strong affinity for metal surfaces showing good inhibition efficiency and low environmental risk. These inhibitors build up a protective hydrophobic film adsorbed molecules on the metal surface, which provides a barrier to the dissolution of metal in the electrolyte. They must be soluble or dispersible in the medium surrounding the metal.

The efficiency of organic inhibitors depends on the following factors:

- Chemical structure, like the size of the organic molecule.
- Aromaticity and/or conjugated bonding, as the carbon chain length.
- Type and number of bonding atom or groups in the molecule (either π or σ).

- Nature and the charges of the metal surface of adsorption mode like bonding strength to metal substrate.
- Ability for a layer to become compact or cross-linked.
- Capability to form a complex with the atom as a solid within the metal lattice.
- Type of electrolyte solution like adequate solubility in the environment.

The efficiency of these organic corrosion inhibitors is related to the presence of polar functional groups with Sulphur, oxygen or Nitrogen atom in the molecule, heterocyclic compound and pi electrons; generally have hydrophilic or hydrophobic parts ionizable. The polar function is usually regarded as the reaction centre for the establishment of the adsorption process. The organic acid inhibitor that contains oxygen, nitrogen and/or Sulphur is adsorbed on the metallic surface blocking the active corrosion sites. Although the most effective and efficient organic inhibitors are compounds that have π-bonds, it present biological toxicity and environmental harmful characteristics.

1.4 Summary

Corrosion control if done successfully will reduce the premature deterioration of materials and protect both the public and the environment in the process. An important component of this process is using trained professionals equipped with the latest technologies. Another equally important aspect of controlling corrosion is recognizing that corrosion is indeed a threat and therefore taking the right steps to prevent it is vital. Implementation of effective corrosion control programs will promote a safer, cleaner environment, and a safer, healthier public.

References

1. Hubert Gräfen, Elmar-Manfred Horn, Hartmut Schlecker, Helmut Schindler "Corrosion" Ullmann's Encyclopedia of Industrial Chemistry, Wiley-VCH: Weinheim, 2002. doi:10.1002/14356007.b01_08
2. Finšgarand M, Milošev I. Inhibition of copper corrosion by 1, 2, 3-benzotriazole: A review Corrosion Science. 2010; 52:2737-2749 doi:10.1016/j.corsci.2010.05.002
3. Octel-Starreon Refinery Fuel Additives Corrosion Inhibitors for hydrocarbon fuels-corrosion inhibitor and corrosion protection to fuel distribution system

4. Corrosion Inhibition, Norman Hackerman, (August), Electrochemistry Encyclopedia, 2006.
5. Adediran *et al*. Inhibitive Potentials of Bitter Kola Stem (BKS) on Mild Steel in Acidic Media. Procee, Nig. Metallurgical Society. 2017, 137-149.
6. Nam ND, Kim JG. Effect of niobium on the corrosion behavior of low alloy steel in sulfuric acid solution. Corrosion science. 2010; 52:3377.
7. Omotioma M, Onukwuli OD. Evaluation of pawpaw leaves extract as anti-corrosion agent for aluminum in hydrochloric acid medium, Nigeria Journal of Technology. 2017; 36:496-504.
8. Olawale *et al*. Inhibitory action of rice husk extract (RHE) on the corrosion of carbon steel in acidic media. Aceh International Journal of Science and Technology. 2017, 6(2):44-51.
9. Olawale *et al*. Corrosion Inhibition of Mild Steel in Seawater using Jatropha Stem. Analele Universitatii "Eftimie Murgu" Resita. 2016; 23(1):228-238.
10. Olawale *et al*. Evaluation of Groundnut leaves extract as a corrosion inhibitor on Mild steel in 1M Sulphuric Acid using Response Surface Methodology, 2018.
11. CP-2 Cathodic Protection Technician-Maritime Student Manual NACE International, 2009, 3-11.
12. Peabody AW. Peabody's Control of Pipeline Corrosion, 2nd Ed. NACE International, 2001. ISBN 1-57590-092-0
13. Davy H, Phil. Trans. Roy. Soc. 1824, 114-151, 242-328
14. Ashworth V, Corrosion, 3rd Ed. 1994, 2. ISBN 0-7506-1077-8
15. Baeckmann, Schwenck, Prinz. Handbook of Cathodic Corrosion Protection, 3rd Edition, 1997. ISBN 0-88415-056-9
16. Corrosion Control Linings and Coatings NWP Brochure. Corporate Headquarters-5721 SE Columbia Way, Suite 200 Vancouver, Washington 98661 Telephone 360.397.6250 Toll Free 800.989.9631 Fax 360.397.6255 www.nwpipe.com.Retrieved on 4th December, by 12 noon, 2018.
17. Electrochem Corrosion inhibitor.

Chapter - 4
Application of Quantum Chemistry to Determine the Structure and Electronic Properties of Rhodium Nano Clusters

Authors

Abhijit Dutta
Research Scholar, Department of Chemistry, Assam University, Silchar, Assam, India

Dr. Paritosh Mondal
Faculty, Department of Chemistry, Assam University, Silchar, Assam, India

Chapter - 4

Application of Quantum Chemistry to Determine the Structure and Electronic Properties of Rhodium Nano Clusters

Abhijit Dutta and Dr. Paritosh Mondal

Abstract

All electron relativistic method is used for methodical exploration on the gas phase lowest energy electronic structure of Rh_n (n=21-30) clusters. All calculations are done with density functional theory (DFT) within the generalized gradient approximation. Ground state isomers of clusters are assessed with diverse spin multiplicities. Even atomic rhodium nano clusters are optimized with odd multiplicities whereas odd atomic rhodium clusters are optimized with even multiplicities. Structural and electronic parameters like bond length, bond dissociation energy, binding energy, stability function, ionization potential, electron affinity, HOMO-LUMO gap and chemical hardness, density of states, deformed electron density, dipole moment and magnetic moment are evaluated for the lowest energy structures of higher atomic rhodium clusters. Rhodium clusters prefer three dimensional arrangements. Rh_{28} cluster is found to be more stable based on the calculated structural and electronic properties. All Rh_n (n=21-30) clusters possesses non-zero magnetic moment.

Keywords: DFT, BLYP, rhodium, stability, magnetic moment

What is the Need for Cluster Study?

At present cluster study is one of the most energetic and embryonic fields of research in both physics and chemistry. This study draws awareness from both the essential scientific standpoint and also from the viewpoint of their prospective technological relevance's. These systems connect the spheres of atomic and molecular physics on one hand and condensed matter physics on the other. Their properties are directed by their outsized surface-to-volume percentage, providing an exceptional prospect for us to study the interaction between surface and volume effects. Clusters demonstrate discrete spectroscopy as of their finite dimension.

1. Introduction

Transition metal clusters have been extensively studied for both scientific and technological reasons in the current years. Nano scale [1] transition metal clusters illustrate novel and extremely size dependent electronic, chemical, optical, and magnetic properties. High surface area to volume ratio, constructs ultrafine dispersed *d*-metal clusters attractive for catalytic uses, for example in the removal of toxic pollutants such as CO, NO, and hydrocarbons [2]. Pt, Rh and Pd tiny clusters are utilized in automotive exhaust processes. Resolving the geometric arrangement of transition metal clusters is a key step in realizing catalytic and magnetic properties [3]. Adopting new magnetic materials with robust properties is one of the keystones of materials science. In earlier studies, only a few of the 3d bulk transition metals [4, 5] are rewarded with the existence of spontaneous ferromagnetism whereas none of the 4d and 5d solids are found to be magnetic in nature [5]. Some experimental evidences suggest the 4d ferromagnetism nature in two-dimensional Ru and Rh structures supported on substrates [6, 7]. It is also observed that the average magnetic moment per atom in these clusters is almost independent of the size. Theoretical calculations [8, 9] also suggested nonzero magnetic moments for other 3d TM clusters whereas their corresponding bulk phases have no moments. This type of expectation is rational as clusters possesses reduced coordination and high symmetry that characterized narrow d-band widths and suggest the prospect of large spin multiplicities in the ground states. Very few literatures on theoretical and experimental studies on 4d transition metal clusters are available. Among all 4d magnetism, rhodium has been the most studied and at the same time, the most arguable of this series. Many explorations on rhodium clusters are encouraged by the revolutionary theoretical works by Galicia [10] and Reddy *et al*. [11] along with experimental work by Cox *et al*. [12] the geometrical structure of free-standing clusters is an indefinable asset since experimental information is circuitous and not adequate to decide the structure accurately. Reddy *et al*. [11] suggested that 13-atom clusters of Pd, Rh, and Ru are magnetic in nature by using local-spin-density functional (LSD) theory. In fact, Cox *et al*. [13] experimentally found the nonzero magnetic moments in small Rh_n clusters (n = 9-34), with average moment per atom for Rh_{13} is 0.48 μ. It is also noticed that the average moment per atom of the Rh clusters depends considerably on cluster size. Rh_{15}, Rh_{16}, and Rh_{19} are found to unusually magnetic relative to their neighbours. Therefore, it is necessary to understand the atomic structures and magnetic properties properly to unravel their role in catalytic reactions.

In this study, it is examined possibly for first time the systematic aspect of electronic, structural and magnetic properties of higher rhodium clusters.

Thorough studies have been conducted to relate diverse electronic, structural and magnetic properties with size and stability of the clusters. Density of states (DOS) and spin density investigations are also performed in order to understand the electronic involvement of each atom to a cluster. Geometry optimization is done for different probable isomers of neutral Rh_n (n=21-30) clusters with different multiplicities (M) *i.e.*, M=2, 4, 6, 8, 10, 12 for odd atom clusters and M=1, 3, 5, 7, 9, 11 for even atom clusters to evaluate the stable geometry.

2. Computational Details

Double numerical plus polarization (DNP) basis set in DMol3 program is used to optimize the structural isomers of rhodium cluster [14, 15]. Generalized gradient approximation (GGA) with BLYP exchange correlation functional is used for DFT calculations [16, 17] DNP [18] basis set is employed for geometry optimization which is analogous to Gaussian split-valence 6-31G** basis set. In this method relativistic calculations are done with all electron relativistic rectification to valence orbitals *via* a local pseudo potential for direct inversion in a subspace method (DIIS) without symmetry constrains. Self-consistent field (SCF) methods are used with a convergence criteria of energy 1×10^{-5}Ha, maximum force gradient 2×10^{-3} Ha $Å^{-1}$ and displacement convergence 5×10^{-3} Å on the total energy and 10^{-6} A.U. on electron density are the boundary conditions. Vibrational frequency calculations are done to ensure the energy minima. Zero point vibrational energy correction is incorporated in all the calculated energies. Absence of imaginary frequencies for all geometries suggests their energy minima.

Average binding energy per atom is calculated with the subsequent equation

$$BE = -\frac{E_{tot}}{n} \quad \ldots [i]$$

$E_{tot} = E_n - nE_1$, E_{tot} = total energy of a cluster

E_1 = Energy of a single atom and E_n = Energy of optimized clusters where n is the number of atoms in the cluster.

In case of ionic clusters, the binding energy is calculated as

$$BE = -E_{tot}^{\pm} / n \quad \ldots [ii]$$

$$E_{tot}^{\pm} = E_n^{\pm} - (n-1)E_1 - E_1^{\pm}$$

$E_1^{\pm}$ and $E_n^{\pm}$ are the energies of the single charged atom ($Rh_1^{\pm}$) and Rh_n clusters, respectively.

Dissociation energy of a cluster of size n is evaluated from

$$D(n, n-1) = E(Rh_n - 1) + E(Rh_1) - E(Rh_n) \quad \ldots [iii]$$

E (Rh_1) = energy of single atom and E (Rh_n) = energy of optimized n atom rhodium.

3. Results and Discussion

3.1 Structural properties

Stable geometries of neutral Rh_n (n=21-30) clusters evaluated at BLYP/DNP level are shown in the Fig. 1. Sextet multiplicity is the lowest energy state for Rh_{21} with symmetric point group C_{4V} having average bond length 2.49 Å and caped cubical geometry. Four cubes are fused together with one rhodium atom is at the capping site in the case of Rh_{21} (Fig. 1). The binding energy per atom and average Rh−Rh bond distances of all lowest energy neutral and ionic clusters are given in Table 1 and Table 2, respectively.

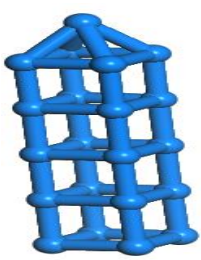

Rh_{21}

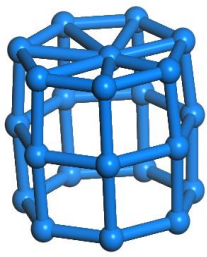

Rh22

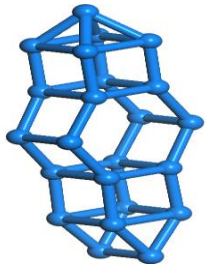

Rh_{23}

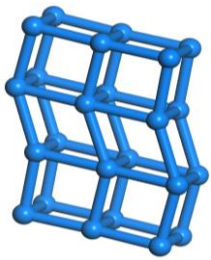

Rh_{24}

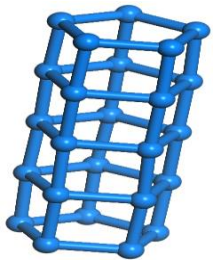

Rh_{25}

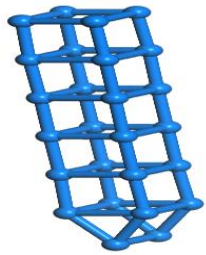

Rh_{26}

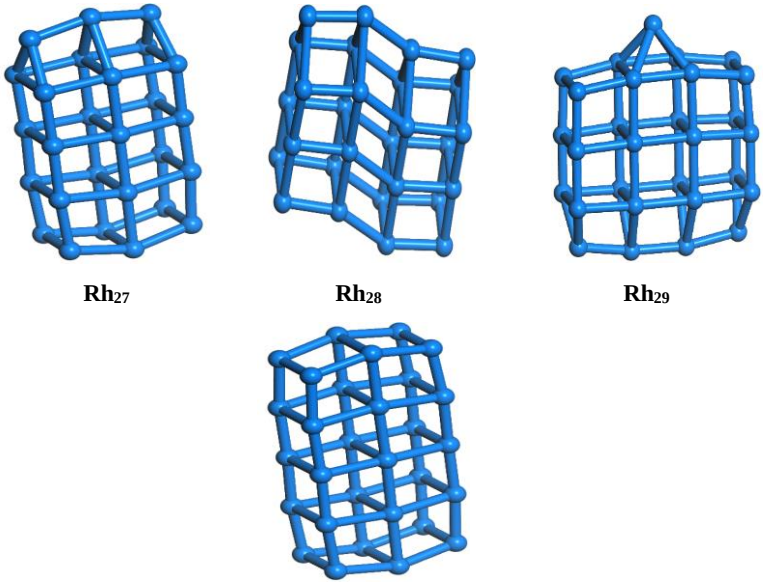

Fig 1: DFT evaluated ground state geometries of Rh_n (n=21-30) clusters

It is noticed from the Table 1 that the binding energy per atom of Rh_{21} is obtained to be 3.41 eV. For Rh_{22} cluster caped cyclic heptagon geometry with pentet multiplicity is the lowest energy isomer having average Rh-Rh bond length of 2.52 Å and C_1 symmetric point group. The binding energy per atom for the most stable Rh_{22} is calculated to be 3.50 eV. The lowest energy Rh_{22} consists of three fused heptagon with a capping atom. Granja *et al.* [19] observed average bond distance and binding energy per atom of Rh_{22} cluster are to be 2.69 Å and 4.13eV, respectively. Fused hexagonal bi-capped cubic geometry with quartet multiplicity is the ground state for the Rh_{23}. 3.47 eV and 2.47 Å are the binding energy per atom and average Rh-Rh bond length, respectively with symmetry point group, Cs for the ground state Rh_{23} cluster. Slightly higher values of average Rh-Rh bond length (2.71 Å) and binding energy (4.17 eV) are reported by Granja *et al*, [19]. While, Villasenor *et al*, [20] reported the binding energy and bond length values of Rh_{23} clusters are 2.52 eV and 2.50 Å, respectively. Pentet state with fused cubic geometry and symmetric point group C_{2h} is the lowest energy state for Rh_{24}. The average bond length and binding energy per atom of stable Rh_{24} cluster are 2.51 Å and 3.52 eV, respectively. Fused pentagonal geometry for Rh_{25} cluster in the sextet multiplicity with symmetric point group C_5 is examined to be the ground state having average bond length of 2.55 Å and binding energy 3.55eV/atom. It is observed from Fig. 1 that five pentagons are fused together for Rh_{25} cluster.

For Rh_{26} cluster, septet multiplicity with bi-capped fused cubic structure is found to be the most stable isomer with symmetric point group (C_1). The binding energy per atom and the average bond length Rh-Rh of this stable cluster are evaluated to be 3.68 eV and 2.58 Å, respectively. Granja *et al*, [19] reported the average bond length and binding energy per atoms of Rh_{26} cluster to be 2.72 Å and 4.22 eV respectively. Capped cubic geometry of Rh_{27} having quartet state is estimated to be the most stable isomer. This isomer has a symmetric point group (C_1), having average Rh-Rh bond length and binding energy per atom are 2.46 Å and 3.72eV, respectively. Pentet state with prismatic fused capped cubic geometry and symmetric point group C_S is the lowest energy state for Rh_{28}. In this case the, average bond length and binding energy per atom are found to be 2.54 Å and 3.94 eV, respectively. While, capped prismatic fused cubic geometry is found to be the ground state with C_1 symmetry and sextet multiplicity in the case of Rh_{29}. Average bond length and binding energy of Rh_{29} is calculated to be 2.55 Å and 4.01 eV/atoms. Pentet state with fused cubic geometry and symmetric point group C_{4v} is the lowest energy state for Rh_{30}. Calculated average bond length and binding energy per atom of stable Rh_{30} are evaluated to be 2.57 Å and 4.11 eV, respectively. Variation of the binding energy per atom with size is presented in the Fig. 2. It is noticed from Fig. 2 that binding energy of the rhodium clusters increases with increase in clusters size. However, slightly lower binding energy is found in the case of Rh_{23}. In this study, ionic (cationic and anionic) rhodium clusters are generated by removing or adding one electron to the lowest energy Rh_n (21-30) for evaluating significant geometrical and electronic properties. For this purpose, spin unrestricted geometry optimization with different multiplicities is performed. DFT evaluated binding energy values (eV/atom) of the ionic rhodium clusters are listed in the Table 1. Table1 reveals that the binding energy per atom of the ionic rhodium clusters increases with the cluster size like neutral clusters. However, binding energy per atom for the ionic Rh_n is found to be higher than the corresponding neutral clusters (Fig. 2). Again, calculated average Rh-Rh bond distance of the anionic rhodium clusters are found to be larger than the neutral and cationic rhodium clusters. Higher and lower average Rh-Rh bond distances are recorded in the case of neutral and ionic Rh_{26} and Rh_{27}, respectively. However, variations of all the bond lengths are not very smooth with the variation of size of all the neutral and ionic of Rh_n. Coordination number (α) evaluated at DNP/BLYP level in the case of neutral and ionic rhodium clusters are found to be same. Coordination number (α) of Rh_{21}, Rh_{22}, Rh_{23}, Rh_{24}, Rh_{25}, Rh_{26}, Rh_{27}, Rh_{28}, Rh_{29} and Rh_{30} clusters are calculated to be 3.81, 3.82, 3.74, 3.50, 3.60, 3.76, 3.66, 3.42, 3.72 and 3.60, respectively.

Table 1: DFT evaluated binding energies (eV) of Rh_n (n=21-30) clusters at BLYP/DNP level

Cluster Size	Neutral	Cationic	Anionic
Rh_{21}	3.41	3.51	3.56
Rh_{22}	3.50	3.59	3.60
Rh_{23}	3.47	3.57	3.62
Rh_{24}	3.52	3.70	3.66
Rh_{25}	3.55	3.72	3.70
Rh_{26}	3.68	3.79	3.76
Rh_{27}	3.72	3.83	3.85
Rh_{28}	3.94	4.09	3.98
Rh_{29}	4.01	4.13	4.16
Rh_{30}	4.11	4.22	4.25

Table 2: DFT evaluated average Rh-Rh bond lengths (Å) of Rh_n (n=21-30) clusters at BLYP/DNP level

Cluster Size	Neutral	Cationic	Anionic
Rh_{21}	2.49	2.47	2.51
Rh_{22}	2.52	2.49	2.55
Rh_{23}	2.47	2.50	2.50
Rh_{24}	2.51	2.54	2.48
Rh_{25}	2.55	2.53	2.57
Rh_{26}	2.58	2.57	2.61
Rh_{27}	2.46	2.48	2.52
Rh_{28}	2.54	2.56	2.58
Rh_{29}	2.55	2.52	2.50
Rh_{30}	2.57	2.56	2.59

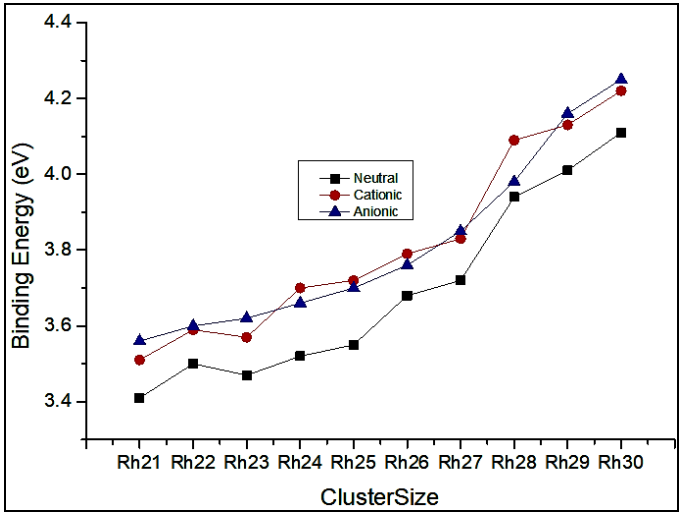

Fig 2: Binding energy (eV/atom) of neutral, cationic and anionic Rh_n clusters

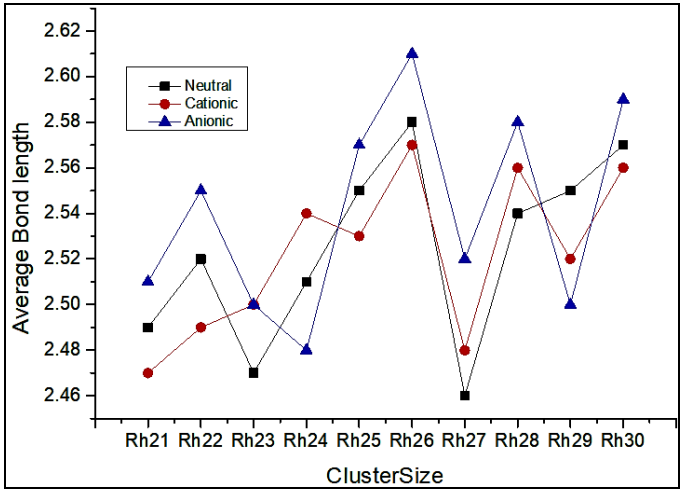

Fig 3: Bond length of neutral, cationic and anionic Rh_n clusters

3.2 Relative Stability

Second order finite difference of total energies $\Delta^2 E(n)$ of small clusters is evaluated to understand their relative stability. $\Delta^2 E(n)$ Represent the measure of stability function. The following mathematical formulation is used to define the stability function:

$$\Delta^2 E(n) = 2E(n) - E(n+1) - E\ (n-1)$$

$E(n)$ = energy of the cluster with n atom. Fig 4 represent the variation of stability function of rhodium clusters with cluster size. Even atomic rhodium clusters has higher stability function values and the highest peak of $\Delta^2 E(n)$ is noticed in the case of Rh_{28}. Bond dissociation energies i.e. energy required for fragmenting Rh_n cluster to Rh_{n-1} and Rh; of the rhodium clusters are plotted against the cluster size is shown in Fig 5. Fig 5 implies that even atomic cluster possesses higher values of dissociation energies than the odd. It is also observed that Rh_{28} possesses higher dissociation energy while, Rh_{29} possesses lower dissociation energy values.

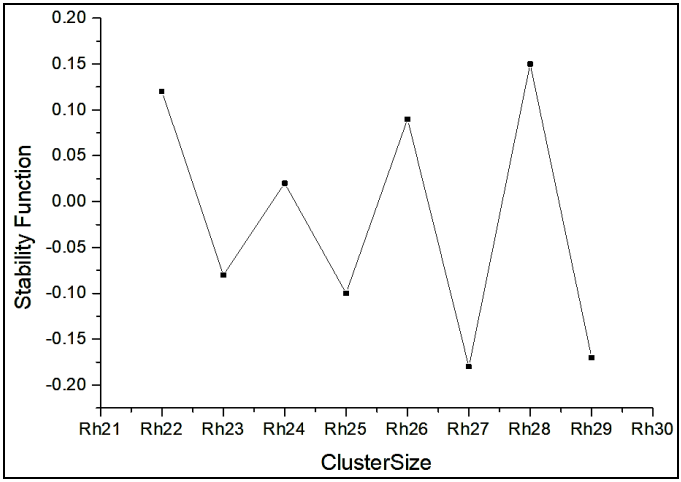

Fig 4: Stability function of neutral, cationic and anionic Rh_n

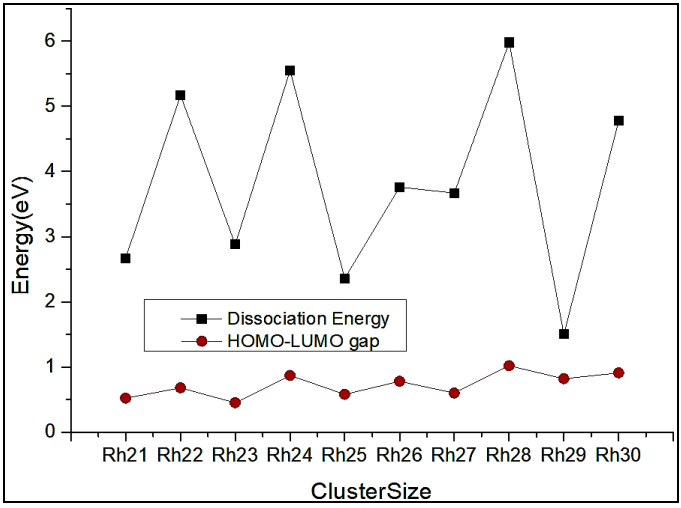

Fig 5: Dissociation Energy and HOMO-LUMO gap of neutral Rh_n clusters

3.3 Electronic Properties and Reactivity Parameters

A. Ionization Potentials and Electron Affinity

Vertical ionization potential and electron affinity of Rh_n (n=21-30) clusters are determined by using the following equations

$$IP = E_n^+ - E_n$$

$$EA = E_n - E_n^-$$

Where E_n^+ and E_n^- are the respective energies of the cationic and anionic rhodium clusters at the geometry of neutral cluster. Variations of ionization potential and electron affinity of all the clusters with size are plotted in Fig 6. Higher ionization potential suggests the stronger binding of nucleus with their electrons that gives a extra stability due to closed shell electronic arrangement. From the Fig 6, it is observed that Rh_{28} cluster has higher ionization energy than its neighbour. Again, it is also observed that Rh_{22} and Rh_{28} have lower electron affinity values. Lower electron affinity suggests lower affinity for accommodating the extra electron to acquired stability. Therefore, Rh_{28} cluster found to be the most stable because of its-highest value of ionization energy and lowest value of electron affinity.

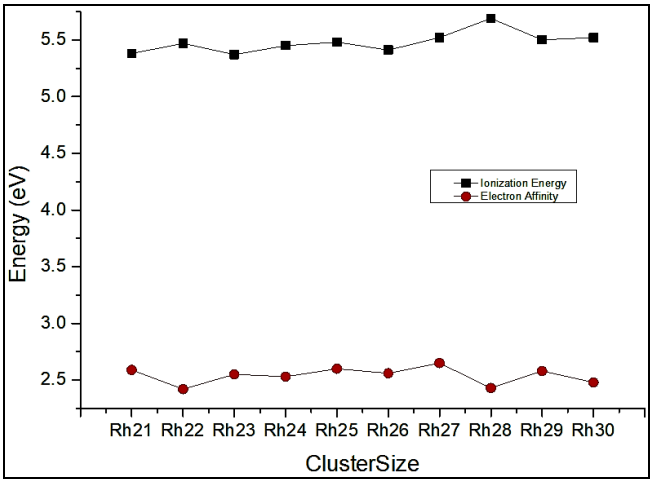

Fig 6: Variation of Ionization energy and Electron affinity of Rh_n (n=2-8) with size

B. HOMO-LUMO Gap, Global Hardness and Electronegativity

Variation of HOMO-LUMO gap of ground state isomer with cluster size is presented in Fig 5. Odd-even fluctuation of HOMO-LUMO gap is noticed with the variation to the cluster size (Fig 5). Even atomic clusters have higher HOMO-LUMO energy gap than the odd atomic clusters. Rh_{24} and Rh_{28} exhibit larger HOMO-LUMO energy difference. Larger HOMO-LUMO energy gap of the rhodium clusters represents higher stability. HOMO-LUMO of Rh_n reveals that Rh_{28} is more stable and Rh_{23} is less stable. DFT evaluated global hardness values of rhodium clusters with respect to cluster size are presented in Fig 8. Higher global hardness, (η) of any chemical species represents higher stability. Higher value of (η) is observed for Rh_{28}. Because of the close band gap structure larger clusters demonstrates lower hardness values. Electrons near the Fermi sections are loosely bounded because of the linear combination of large number of atomic orbitals in the case of larger rhodium clusters. That is why, larger cluster always have the tendency to change their electronic structure. Electronegativity and electrophilicity of the Rh_n clusters are derived by using DFT method at BLYP/DNP level and their variation with cluster size is shown in Fig 8. Higher electronegativity values suggest larger attraction between nucleus and electrons which reveals higher stability. It is seen from Fig 8 that Rh_{28} is more stable. Again, electrophilicity signifies the stabilization energy required by clusters when it acquires an additional electronic charge. It is noticed from Fig 8 that Rh_{28} has lower electrophilicity values than others *i.e.* this cluster has little requirement to get electrons from surrounding, which sustains the higher stability of Rh_{28} cluster than its neighbours.

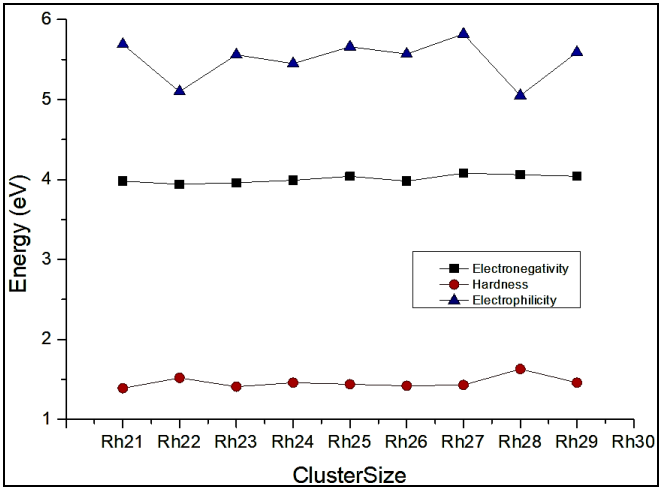

Fig 7: Chemical Hardness, Electronegativity and Electrophilicity plot of Rh_n (n=2-8)

3.4 Magnetic Properties

Magnetic moment of rhodium clusters are evaluated at BLYP/DNP level and the values are listed in the Table 3. It is observed from the Table 3 that magnetic moment of rhodium clusters changes discontinuously with size. All the Rh_n clusters possess a non-zero magnetic moment and the highest magnetic moment of 0.28 μ_B per atom is noticed for Rh_{21}. Calculated magnetic moment of the rhodium clusters correlate well with the experimental values [8, 44]. Experimental value of magnetic moment of Rh_{22}, Rh_{23} and Rh_{26} clusters are 0.27±0.14, 0.13±0.13 and 0.25±0.12 μ_B per atom, respectively. DFT evaluated electronic dipole moment (in Debye) of all the stable rhodium clusters is shown in the Table 9. Dipole moment of the larger Rh_n (n=21-30) clusters are found to be higher (Table 3) in comparison to the smaller rhodium clusters [21]. Higher dipole moment arises due to the increase in numbers of electrons with the increase of size of rhodium clusters. Higher delocalization of electrons is possible in the case of larger clusters which lead to the increase of the dipole moment.

Table 3: Magnetic and dipole moments values (μ_B /atom) of Rh_n (n=21-30) clusters calculated at BLYP/DNP level

Cluster Size	Magnetic Moment	Dipole Moments
Rh_{21}	0.28	2.59
Rh_{22}	0.22	2.42

Rh_{23}	0.17	2.55
Rh_{24}	0.21	2.53
Rh_{25}	0.24	2.60
Rh_{26}	0.26	2.56
Rh_{27}	0.14	2.65
Rh_{28}	0.17	2.43
Rh_{29}	0.21	2.58
Rh_{30}	0.16	2.48

3.5 Density of States (DOS) Study

DFT evaluated density of states at BLYP/DNP level are mentioned in Fig 9. It is observed from Fig 9 that d electrons have the maximum DOS values than other s and p electrons which suggest that d electrons are more involved in bonding than other s and p electrons. In the figure zero energy levels are named as Fermi energy. It is observed that except for Rh_{22} cluster all other clusters shows its s and p electrons state at Fermi energy that indicates the equal effects of both s and p electrons towards bonding among Rh-Rh. On the left side of Fermi level is bonding and on the right side is anti-bonding region. It is noticed from the Fig that all electrons density are maximum at bonding than on anti-bonding states. Density of d, s and p electrons are observed in anti-bonding regions. D-D transition is noticed for these clusters as the height of d electrons density is maximum in both bonding and anti-bonding region.

Density of states for spin contribution is also mentioned in Fig 10. Zero energy level is termed as Fermi level of energy. Negative values of spin density of states are basically for bonding zone and positive values of DOS are for anti-bonding zone. It is noticed from the Fig that for odd atomic clusters, d electron spin density is more whereas for even atomic clusters all s, p and d electrons are responsible for creating magnetic moment value of clusters. It is noticed that spin densities are not uniform on both side of Fermi level that means all spins are not properly cancels out that results for a little magnetic character in these clusters. s and p spin density is found to be maximum for even atomic clusters than the d spin density.

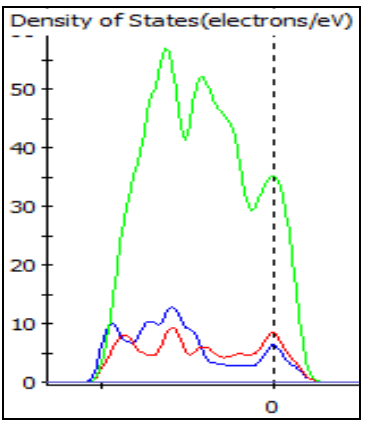

Rh_{21}

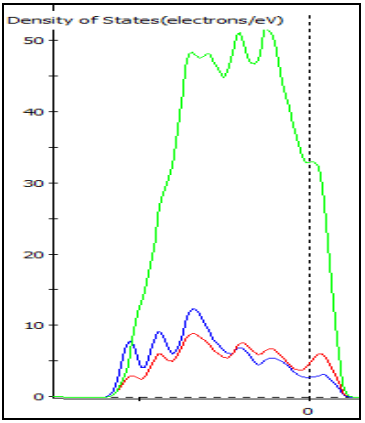

Rh_{22}

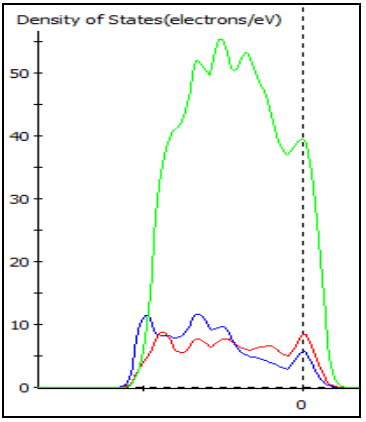

Rh_{23}

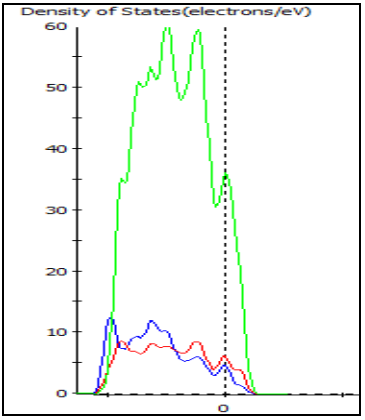

Rh_{24}

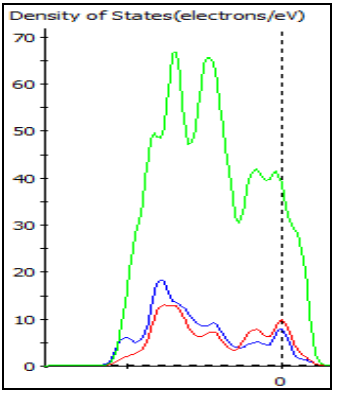

Rh_{25}

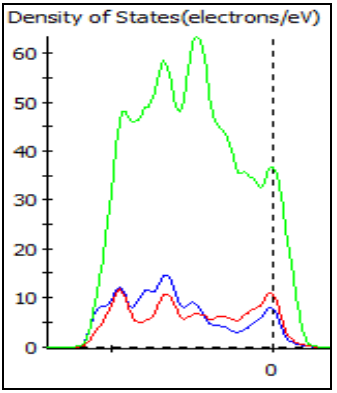

Rh_{26}

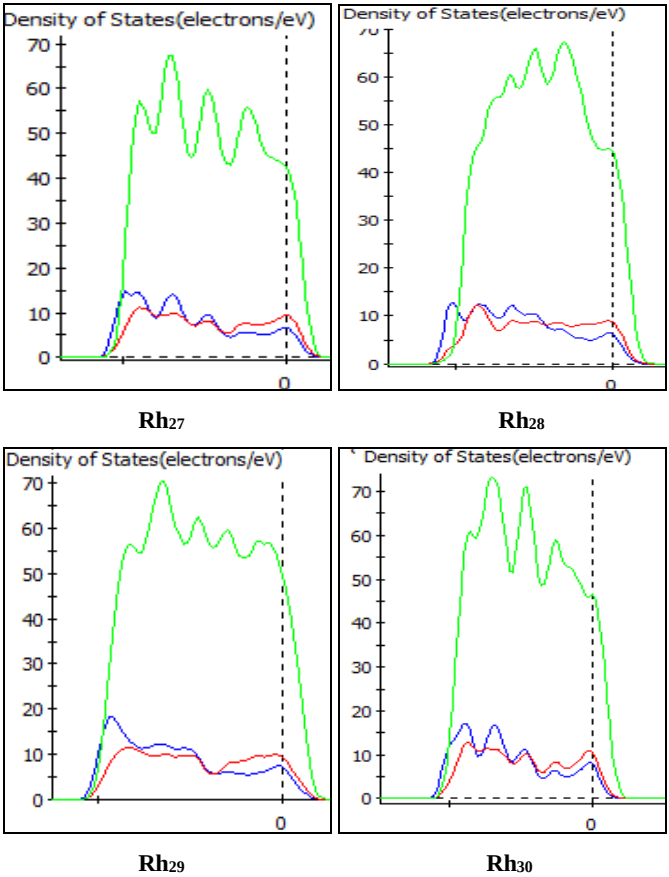

Fig 9: DFT evaluated DOS diagrams of Rh_n (n=21-30) clusters. Blue, red and green colour represents s, p and d electrons. In the graph energy is shown on X axis and density of states on Y

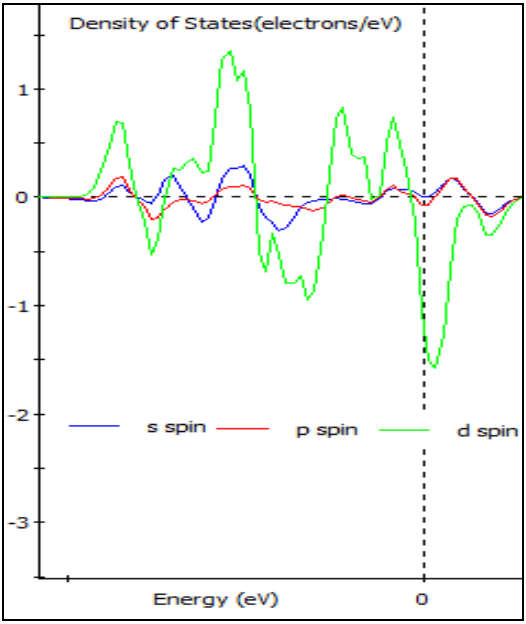

Rh_{21}

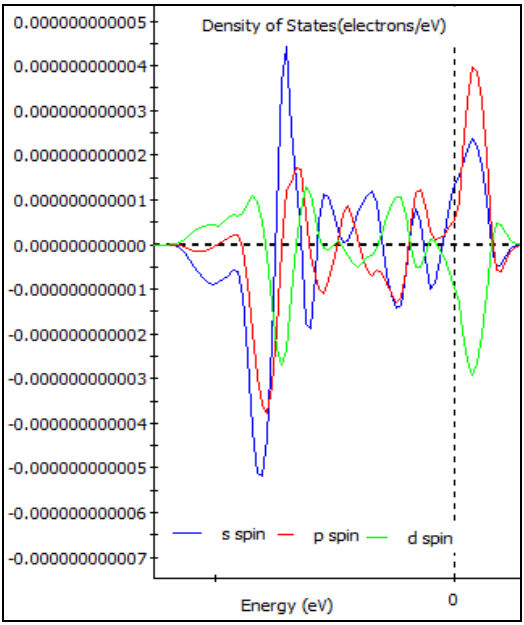

Rh_{22}

Fig 10: DFT evaluated spin density of states (DOS) diagrams of Rh_n (n=21-30) clusters

Deformed Electron and Spin Density Study

DFT evaluated deformed electron density and spin density analysis of the rhodium clusters are presented in Fig 11. Fig 12 reveals that electron densities are equally deformed on the constituent rhodium atoms as well as on the bonds in the case of Rh_{21}, Rh_{25} and Rh_{28}. Higher deformation density signifies greater stability of clusters because of the development of ionic character. Different type of deformed electron density in case of Rh_{28} suggests that all d as well as s and p orbitals are equally involved in the formation of Rh_{28}. This is not the case in Rh_{21} and Rh_{25} where only one type of density is deformed.

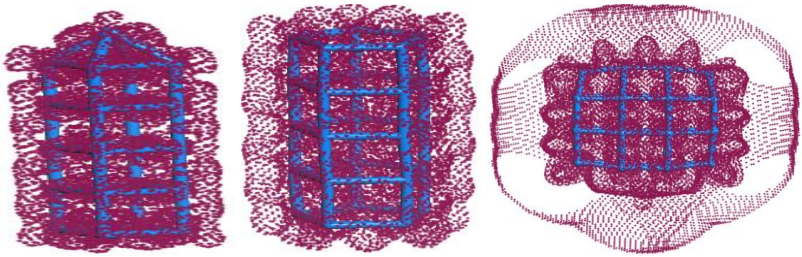

Rh_{21} **Rh_{25}** **Rh_{28}**

Fig 11: DFT evaluated deformed electron density of Rh_{21}, Rh_{25} and Rh_{28} clusters

From the Fig it is noticed that for Rh_{25} cluster intensity of one type of spin moment density is more than that of other, where as in Rh_{30} both types of spin moment densities are almost present. So in Rh_{30} cluster overall spin densities are somewhat nullified by both types of spin moments as their vectors are in opposite directions which results in a little magnetic moment of Rh_{30}. Where as in Rh_{25} cluster greater magnetic moment is noticed than Rh_{30} as some spin moment density remains after cancellation of both types of spin moment densities. It is the reason for which Rh_{25} has larger magnetic moment than Rh_{30} cluster.

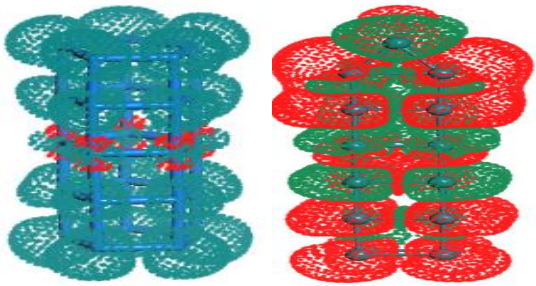

Rh_{25} **Rh_{30}**

Fig 12: DFT evaluated deformed spin density of Rh_{25} and Rh_{30} clusters

Conclusion

Systematic study is made on electronic, structural and magnetic properties of finite size Rh_n (n=21-30) clusters with different spin multiplicities. Important inference can be drawn on the stability of the rhodium clusters based on the calculated reactivity parameters such as stability function, dissociation energy, HOMO-LUMO gap, electron affinity. All the parameters reveal highest stability of Rh_{28} among all Rh_n (n=21-30) clusters. DOS study reveals that d electron spin density is more for odd atomic clusters whereas for even atomic clusters all s, p and d electrons are responsible for exhibiting magnetic moment. None zero magnetic moment obtained for all the Rh_n (n=21-30) clusters. Deformed electron density analysis suggests that p and d orbitals are equally deformed on all the atoms and bonds that increase the stability Rh_{28}in comparison to other rhodium clusters.

Acknowledgement

Authors thank Department of Science and Technology (DST), New Delhi, India for financial support (SB/EMEQ-214/2013).

Conflict of Interest

Authors have no conflict of interests.

References

1. Elkind JL, Weiss FD, Alford JM, Laaksonen RT, Smalley RE. Fourier transform ion cyclotron resonance studies of H_2 chemisorption on niobium cluster cations. J Chem. Phys. 1988; 88:5215. DOI: https://doi.org/10.1063/1.454596
2. Kalita B, Deka RC. Stability of small Pd*n* (*n*=1−7) clusters on the basis of structural and electronic properties: A density functional approach. J Chem. Phys. 2007; 127:244306. DOI: 10.1063/1.2806993
3. Wang H, Ko YJ, Garcia LG, Sen P, Beltra MR, Bowen KH. Joint photoelectron and theoretical study of $(Rh_mCo_n)^-$ (m = 1–5, n = 1-2) cluster anions and their neutral counterparts. Phys. Chem. Chem. Phys. 2011; 13:7685. DOI: 10.1039/C0CP01674H
4. Ibach H, Luth H. Solid State Physics, 2nd ed. Springer: Berlin, 1995.
5. Janak JF. Uniform susceptibilities of metallic elements. Phys. Rev. B. 1977; 16:255. DOI: https://doi.org/10.1103/PhysRevB.16.255
6. Pfandzelter R, Steierl G, Rau C. Evidence for 4d Ferromagnetism in 2D Systems. Ru Monolayers on C (0001) Substrates. Phys. Rev. Lett. 1996; 74:3467. DOI: 10.1103/PhysRevLett.74.3467

7. Goldoni A, Baraldi A, Comelli G, Lizzit S, Paolucci G. Experimental Evidence of Magnetic Ordering at the Rh (100) Surface. Phys. Rev. Lett. 1999; 82:3156. DOI: https://doi.org/10.1103/PhysRevLett.82.3156

8. Pastor GM, Davila JD, Benneman KH. Size and structural dependence of the magnetic properties of small 3*d*-transition-metal clusters. Phys. Rev. B. 1989; 40:7642. DOI: https://doi.org/10.1103/PhysRevB.40.7642

9. Liu F, Khanna SN, Jena P. Magnetism in small vanadium clusters. Phys. Rev. B. 1991; 43:8179. DOI: https://doi.org/10.1103/PhysRevB.43.8179

10. Galicia R. Rhodium clusters Study-13 by molecular orbitals. Rev. Mex. Fis. 1985; 32:51. DOI: 10.1103/PhysRevB.66.224410

11. Reddy BV, Khanna SN, Dunlap BI. Giant magnetic moments in 4d clusters. Phys. Rev. Lett. 1993; 70:3323. DOI: https://doi.org/10.1103/PhysRevLett.70.3323

12. Cox AJ, Louderback JG, Bloomfield LA. Experimental observation of magnetism in rhodium clusters. Phys. Rev. Lett. 1993; 71:923. DOI: https://doi.org/10.1103/PhysRevLett.71.923

13. Cox AJ, Louderback JG, Bloomfield LA. Magnetism in 4*d*-transition metal clusters. Phys. Rev. B. 1994; 49:12-295. DOI: https://doi.org/10.1103/PhysRevB.49.12295

14. Delley B. From molecules to solids with the DMOL3 approach J Chem. Phys. 2000; 113:7756. DOI: https://doi.org/10.1063/1.1316015

15. Delley B. An all-electron numerical method for solving the local density functional for polyatomic molecules. J Chem. Phys. 1990; 92:508. DOI: https://doi.org/10.1063/1.458452

16. Becke AD. Density-functional exchange-energy approximation with correct asymptotic behaviour. Phys. Rev. A. 1988; 38:3098. DOI: https://doi.org/10.1103/PhysRevA.38.3098

17. Lee C, Yang W, Parr RG. Development of the Colle-Salvetti correlation-energy formula into a functional of the electron density. Phys. Rev. B. 1988; 37:785. DOI: https://doi.org/10.1103/ PhysRevB.37.785

18. Delly B, Ellis DE. Efficient and accurate expansion methods for molecules in local density models J Chem. Phys. 1982; 76:1949. DOI: https://doi.org/10.1063/1.443168

19. Aguilera-Granja F, Rodriguez-Lopez JL, Michaelian K, Berlanga-Ramirez EO, Vega A. Structure and magnetism of small rhodium clusters. Phys. Rev. B 2002; 66:224410. DOI: 10.1103/PhysRevB. 66.224410

20. Villasenor-Gonzalez P, Dorantes-Davila J, Dreysse H, Pastor GM. Size and structural dependence of the magnetic properties of rhodium clusters. Phys. Rev. B. 1997; 55**:**15084. DOI: 10.1103/PhysRevB.55.15084

21. Dutta A, Mondal P. Structural evolution, electronic and magnetic manners of small rhodium $Rh_n^{+/-}$ (n = 2-8) clusters: a detailed density functional theory study. RSC. Adv. 2016; 6:6946. DOI: 10.1039/C5RA21600A

Chapter - 5
Nano-Structured Metals, Metal Oxides and Composites: An Overview

Authors

Dr. Bishal Bhuyan
Department of Chemistry, North Lakhimpur College (Autonomous), Lakhimpur, Assam, India

Rajashree Newar
Department of Chemistry, Indian Institute of Technology, Delhi Hauz Khas, New Delhi, India

Chapter - 5

Nano-Structured Metals, Metal Oxides and Composites: An Overview

Dr. Bishal Bhuyan and Rajashree Newar

Abstract

Nanochemistry is the study of manipulating matter on an atomic and molecular scale. As quoted by Geoffrey Ozin, a pioneer in the field of nanochemistry, it is "an emerging subdiscipline of solid state chemistry that emphasizes the synthesis rather than the engineering aspects of preparing little pieces of matter with nanometer sizes in one, two or three dimensions". The nanomaterial chemistry has been applied in biomedical chemistry, polymer chemistry, product synthesis and development of various products which are already available commercially. This chapter is designed to give an overview of general terminology of nanochemistry and synthesis of nanoparticles from metals, metal oxides and their composites, and their applications in various fields.

Keywords: Nanoparticles, Synthesis, Noble metal nanoparticles, Tungsten Oxide, Adipic acid.

1. Nanoparticles: Historical Background

It has been scripted in literature that the idea of nanotechnology was first recognized by Nobel Prize awardee Sir Richard Feynman, back in the year, 1959. Amidst one meeting, he quoted "There is plenty of room at the bottom", suggesting the immense possibilities of an emerging field in the near future. Then onwards, a new horizon towards material science has begun. However, the historical background of nanoparticles is surprisingly long [1]. Interestingly, the existence of nanoparticles and their varied useful utilizations can be traced from many ancient sculptures and decorations. Some fine works of ceramic decorations with metal nanoparticles can be observed from the 9^{th} century in Mesopotamia. (Fig. 1) [2].

Besides silver, gold has also a fascinating history in decorative purposes. One of the finest use of this metal can be observed in the British Museum. The Romans manufactured the Lycurgus Cup in the 4^{th} century.

Interestingly, it appears green in daylight, however, on illuminating from inside, it becomes red (Fig. 2). In the 19th century, Michael Faraday first described the preparation of gold nanoparticles as well as their intense red-violet colour as a function of the particles. Thus, nano-particle has fascinated men from time immemorial and still continues to do so.

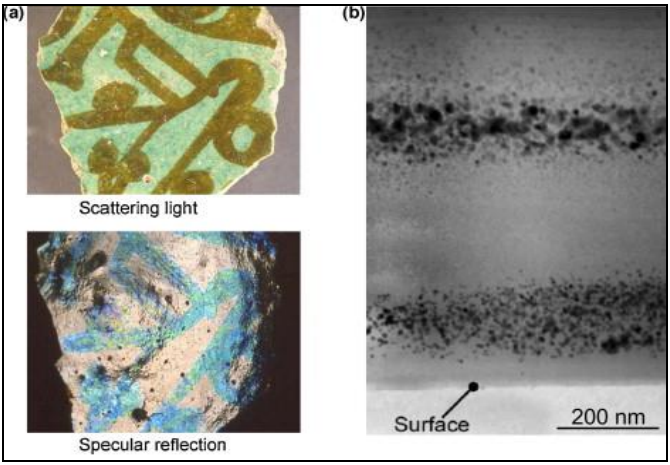

Fig 1: (a) Photograph of a medieval piece of a glazed ceramic observed by scattered light and specular reflection. (b) TEM image of the double layer of silver nanoparticles

2. Nanoparticles: Definition and Synthesis

Precisely, nanomaterials are study of particles at a specific scale less than about a hundred nanometer. The measurement of length scale is considered to be vital for numerous reasons. By patterning matter on the nanoscale, it is possible to vary the fundamental properties of materials viz. melting points, magnetization, charge capacity, etc. and chemical properties. These tailored materials have found their utility in fields of different technological, chemical biological applications as semiconductors, sensors, catalysts, drug-delivery probe, anti-microbial agents, to name a few. Such versatile use of nano-materials in every aspect of societal development are comprehended to be a revolution in itself. Among the preparative approaches undertaken for synthesis, 'Top-down' and 'bottom-up' methods are considered to be the pioneers in the field of nanotechnology. In Top-down method, the nano sized particles are obtained *via* slicing or breaking of larger bulk sized materials, while for bottom-up route, the nanoparticles are obtained from molecules or atoms. Ball-milling protocol is one of the refereed top-down method whereas, colloidal dispersion method is a typical bottom-up approach for preparation of nanoparticles.

Fig 2: The Lycurgus Cup in reflected (left) and (b) in transmitted (right) light.

Apart from the above mentioned approaches, nanoparticles are generally synthesized by two additional methods *viz.* physical and chemical. Physical methods are generally used for metal deposition through techniques such as thermal evaporation, laser ablation and sputter deposition [3-10]. These techniques, though produce nanoparticles with specific functionalities, but fails to produce in bulk amount. Additionally, it require sophisticated experimental setup and are costly [11]. Chemical approaches, on a contrary, are user-friendly and limits the expenditures. Co-precipitation, sol-gel, hydrothermal and solvothermal methodologies are some of the well documented and accepted processes for synthesizing nanoparticles.

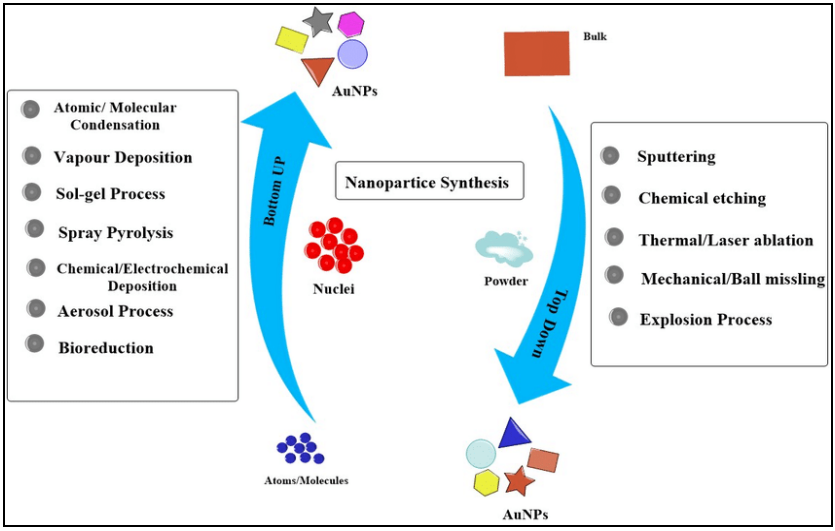

Fig 3: Schematic representation of Top-down and Bottom-up approaches

3. Classification of Nanoparticles and Their Synthesis

Any materials can be synthesized into their nano dimensions. However, from the viewpoint of the content of the thesis, it is deemed necessary to discuss some aspects of metal and metal oxide NPs. Metallic nanoparticles, among others, have definitely fascinated scientists for over a century now. In recent times, they have been extensively used in biomedical applications and engineering. They are considered to be a focus of interest owing to their promising features. Numerous methods including chemical and physical approaches have been employed for their synthesis. However, very recently, biosynthesis route is observed to gather much appreciation among scientist. Low cost processing, abundant availability of natural feedstock such as plant extracts, fungi, algae, bacteria, etc. and simple methodology are some noted salient features, which adds to its high demand. Moreover, the proficiency of these bio-source mediated processes are excellent and exhaustive research are under way to understand their mechanistic phenomenon. It is noteworthy to mention that noble metal NPs such as Au, Ag and Cu find their applicability in numerous fields including biomedical and catalysis, owing to their unique localized surface plasmon resonance (LSPR) properties. Surface Plasmon resonance are defined as electromagnetic waves trapped at the metal/dielectric interface due to the collective oscillations with the free electrons of the metal. SPR is confined to materials having negative real and positive imaginary dielectric constants.

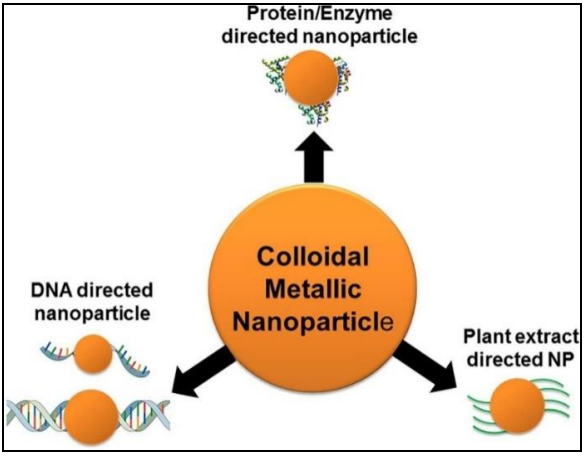

Fig 4: Classification of Colloidal metallic nanoparticles

Evidently, it is observed that Au, Ag and Cu NPs have a definite SPR in the visible region of the spectrum. Apart from metals, metal oxide nanoparticles also have garnered immense interest among the research

community. Metal oxide NPs are regarded as an important class of inorganic materials amongst a broad array of functional materials. The metal elements react with enriched oxygen species to generate a large variety of nanostructured metal oxides with fascinating structures and properties. As a result, they find their extensive use in emerging fields of catalysis, photocatalysis, storage devices, sensors, etc. Pivotal interest in these oxide materials stems from the fact that their new acquired properties can be largely altered by virtue of size and shape based on the choice of the synthetic routes. Henceforth, numerous methodologies have been pursued in context of controlling the size and shape of the nanostructured metal oxides materials. One of such approaches is capping agent assisted synthesis. The organic molecules alleviate the surface of the materials and also enhance the

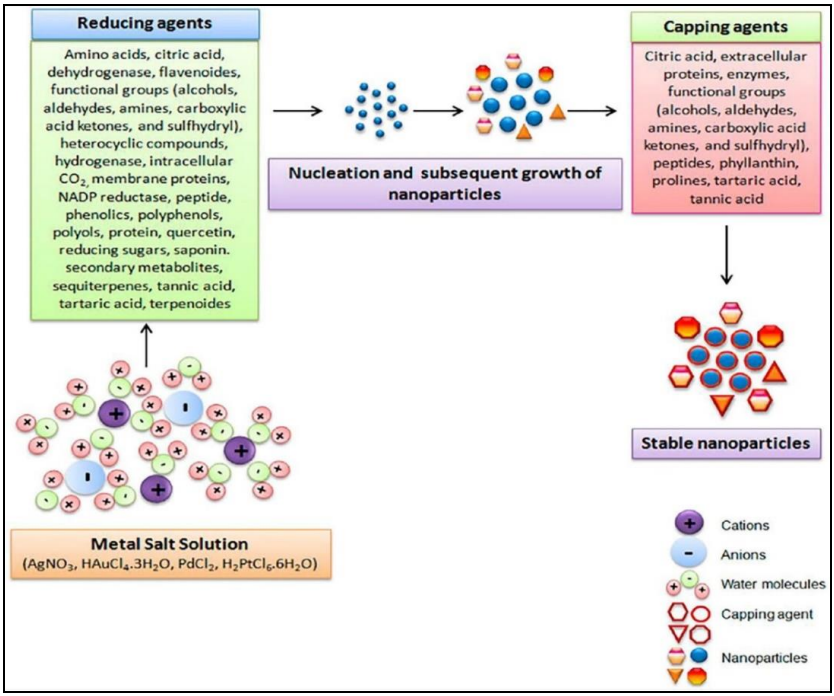

Fig 5: Schematic representation of the mechanistic behaviour of formation of nanoparticles

Surface functionalization of the nano-structured oxide materials. Moreover, other synthetic methods such as hydrothermal and co-precipitation techniques are also performed to obtain nanomaterials with desired properties. Attention of the readers may be drawn to the fact that much advancement has been achieved in the domain of nanocatalysts in

recent times. Supported ionic liquid catalyst (SILC) is a new concept which embraces both the quality of ionic liquids and versatility of nanomaterials. We are familiar of the fact that ionic liquids are popular reaction media owing to their thermal stability, very low pressure and ability to dissolve various compounds. Therefore, exhaustive works have been pursued taking into consideration the advantages of ILs. In SILC, they not only retain the salient features of ILs and supports, but also generate a new series of properties and performance due to synergistic effect. Metal/metal oxides have proved to be a promising support for immobilizing ILs, because of their high surface area, low toxicity, good stability and easy preparation approaches.

In a similar pattern, now-a-days, great emphasis has been put on utilization of waste/natural feedstocks in important organic transformations in combination with metal and metal oxides NPs. Recently, a few interesting works on such potential use of waste and/or natural feedstocks have been well documented in literature. The inherent abundance of minerals and other necessary components in natural feedstocks makes them a promising alternative to conventional catalysts. Moreover, these approaches are observed to be green, efficient and involves very low cost and sophistications. As a result, this emerging field provides humongous promise to withstand the standards of sustainable chemistry in near future.

4. Nanomaterials in Photocatalysis, Catalysis and Biological Applications

Nanomaterials have gathered enormous attraction owing to their interesting properties as well as utility in diverse areas. Among many areas, nanostructured materials have been extensively explored in the fields of photocatalysis, catalysis and biological applications. For instance, in case of semiconductors, when the dimensions get reduced to a certain size, quantum confinement leads to an increase in the bandgap. The bandgap thus obtained can be simply controlled by monitoring the dimensions of the nanomaterials. These changes result in the modification of the optical absorption and the emission spectra of the synthesized nanomaterials. Metal oxide NPs, have been heavily explored in the field of photocatalysis. However, single-component metal oxide NPs fail to absorb light in the visible region. For example, TiO_2 photocatalyst can only absorb light of wavelength less than 387 nm. As a result, numerous efforts are pursued for improved absorption of visible light including doping, introduction of noble metals, etc. Doping technique involves the immobilization of another metal/metal oxides with matching band gaps. Here, the heterojunction thus formed have a bandgap

which is tuned in such a manner that lifetime of the photogenerated electron hole pairs get extended. This ultimately results in an improved photocatalytic activity. Another well-known method is the incorporation of noble metals (NM) with metal oxides (MO) NPs. Metals such as Ag and Au, when incorporated with MO NPs are regarded as an effective way to prepare nanoparticles that can absorb visible light efficiently. This process in actual, prolongs the lifetime of the photogenerated charge carriers and enhances the photoactivity. In this context, it is worthwhile to mention that graphitic carbon nitride (g-C_3N_4), an allotrope of carbon has found enormous popularity in the field of photocatalysis. It is inherently photoactive with a band gap of 2.73 eV. Several works on the use of g-C_3N_4/metal oxide/metal NPs as photocatalysts have been documented in the literature [12-16]. Therefore, all in all metal and/or metal oxides NPs with or without g-C_3N_4constitute a major domain of photocatalysis.

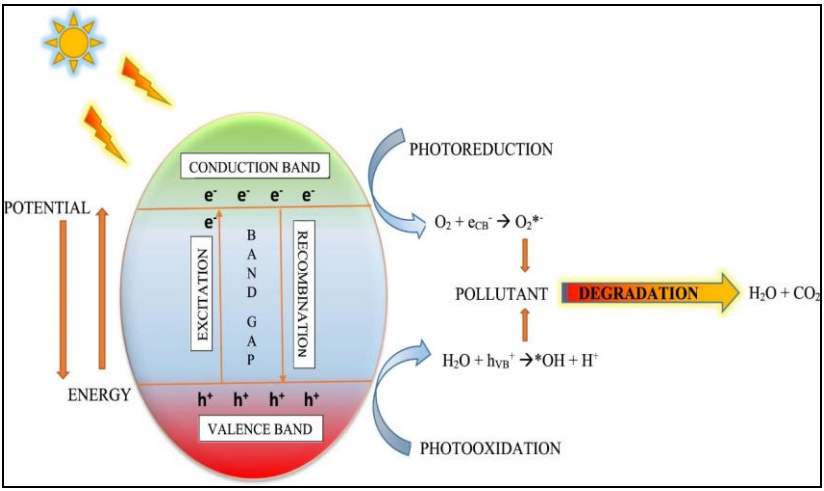

Fig 6: Illustrative diagram on mechanistic behaviour of semiconductors materials

It is noteworthy to mention that to a great extent, the present and future prospects of human life depends on catalytic technologies. From conversion of crude oil, natural gas to production of petrochemical and chemical stuffs, all rely on catalytic technologies. Development in catalytic field thus, is regarded to be a pioneering step towards fulfilling the necessities. In general, catalyst can be termed as a substance that increases the rate of a reaction by lowering the barrier of activation energy (E_a), which is required to convert the reactants into their desired products without consuming itself in the reaction. Precisely, it can be defined as the acceleration of the chemical reactions by the presence of foreign substances which are not consumed. In

catalysis domain, active surface area of a catalyst holds immense importance. It is evident that the active surface area increases when the size of the catalyst decreases. Hence, the smaller the catalyst particles, the greater is the surface to volume ratio. Additionally, the higher the active surface area of the catalyst, the higher is the efficiency of the catalyst. With nanoparticles, the benefits of the materials lies on being in the smaller size range [17]. The smaller dimension of nanomaterials unambiguously supports its skill as a catalyst. Numerous reports are available on the efficiency of nanoparticles as catalysts, which validates the previous conjecture [18, 19]. In addition, it is noteworthy to mention that the nanoparticles acts as a bridge between the homogeneous and heterogeneous catalysts. Among other features, it nullifies some disadvantages of the conventional homogenous counterparts. The ease of catalyst separation, recyclability and retention of excellent catalytic activity even after reuse are some noted features of nanoparticles as catalysts. Reports reveal that numerous catalytic organic transformations have been availed by researchers using nanocatalysts [20-22]. Some of the practised reactions are Oxidation-reduction, Coupling reactions, Heck coupling, Suzuki coupling, C-H activation, Henry reaction, Hydrogen production reactions, Aldol condensation reactions, etc. Thus, these observations suggest the growing importance of nanoparticles in the field of catalysis.

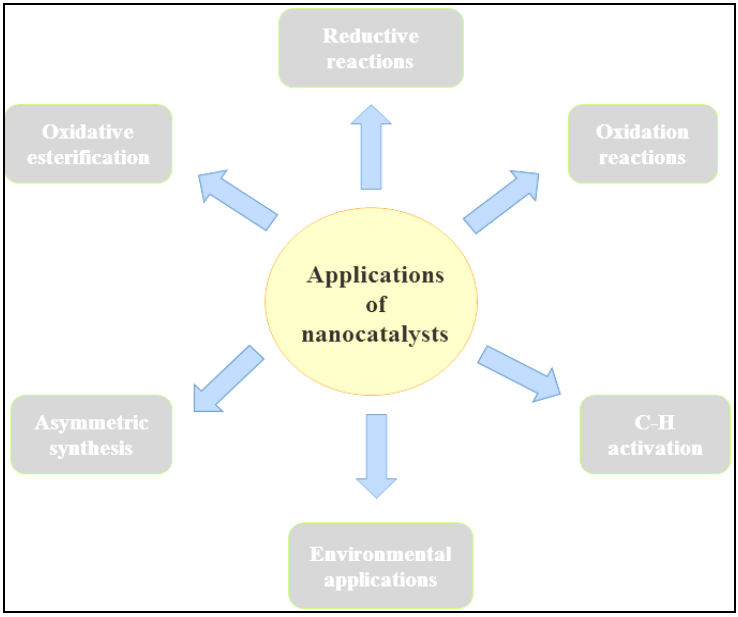

Fig 7: Illustrative representation of varied applications of nanocatalysts

Likewise, development of newer improved therapeutic agents with efficient antimicrobial activities continues to draw attention among researchers. In this context, it is relevant to mention that nanoparticles are being widely used in biological applications *viz.* biosensing, cancer therapeutics, etc. Precisely, Au and Ag NPs are reported to be used for gene delivery and treatment of cancers. Moreover Ag NPs are also documented to possess anti-fungal, anti-viral, anti-inflammatory and anti-platelet activity. A wealth of literature are available which establishes Ag NPs to have excellent antibacterial activity [23-26]. However, it remains still disputable how silver employs antibacterial activity to kill bacteria. Few researchers speculate that there are three hypothesis to elucidate the antibacterial activity of Ag NPs. The first hypothesis speaks about the attachment of Ag NPs with the cellular membrane of the bacteria. Owing to its attachment, Ag NPs can penetrate inside the cell wall of the bacteria and disrupt the enzymatic functions, leading to death of the cell. The other hypothesis, as suggested by Wang *et al.* [27] discusses about reactive oxygen species (ROS) generation. An increase in ROS leads to bacterial death by damaging the proteins and DNA of the bacteria. Different from the above two, the third hypothesis propose that the antibacterial activity of Ag NPs is solely dependent on Ag^+ ions encounter. Presence of Ag^+ in the cellular membrane of bacteria results DNA to lose its replication power and also inactivation of the cellular proteins. Thus, a detailed insight into the anti biological activities of noble metal NPs reveals that significant works have been performed in this field.

As mentioned previously, nanoparticles have been utilized extensively as catalyst cum reaction media for a variety of organic transformations, therefore it is deemed necessary to make a discussion on such organic reactions. There are several organic transformations which are considered to be synthetically useful and industrially important. A few such reactions that are relevant to the content of the thesis are discussed in the following section.

Cross-Aldol Condensation Reactions

Aldol and crossed-aldol condensation reactions are known a long time as synthetically important reactions. They are powerful tools for formation of C-C bond in several carbonyl compounds. A host of literature are available which represent sincere development in the field of aldol condensation reactions under catalytic conditions. For instance, Gawande and his co-workers in 2011, synthesized a heterogeneous versatile MgO-ZrO_2 and tested its catalytic efficacy in cross-aldol condensation of aromatic aldehydes with cyclic ketones [28]. In the condensation reactions, the corresponding

products were obtained in excellent yields under solvent free conditions (Scheme 1).

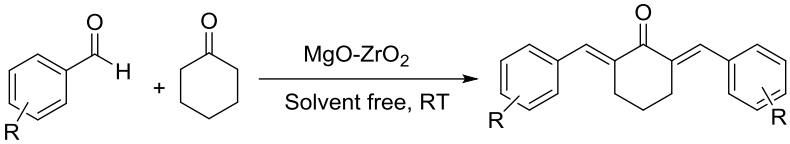

Scheme 1: Cross-aldol condensation using $MgO\text{-}ZrO_2$ as catalysts

Previously, self and cross-aldol condensation reactions of aldehydes and ketones were carried out with large excess of reagents and an inorganic base, usually NaOH and/or KOH. But, to great dismay, these bases are harmful and also needed in large quantity to manifest good results. Moreover, they are quite difficult to remove from the reaction mixtures after completion of reaction and yield of the desired products are not high due to the formation of by-products.

Synthesis of Adipic Acid

Adipic acid (AA) is regarded as one of the most significant aliphatic dicarboxylic acids produced industrially. The reason behind this lies in the fact that it is used as a raw material in the production of abundant valuable materials like polyurethanes, polyamides, plasticizers, intermediates for pharmaceuticals and insecticides, etc. It is mainly used for the manufacture of nylon 6, 6 (Scheme 2). The polycondensation with hexamethylenediamine (HMDA) towards nylon 6, 6 accounts for around 85% of all adipic acid produced, with the remainder used for polyurethanes and adipic esters. Industrially, the production of adipic acid is achieved by the oxidation of a cyclohexanol/cyclohexanone mixture or cyclohexane with nitric acid. Though very well practised, these processes are associated with co-production of substantial amount of ecologically unfavourable greenhouse gases like N_2O.The emergence of such noxious gases contribute enormously to severe cases of global warming and ozone depletion. Consequently, development of greener methodologies has become an important concern and has already witnessed large improvements.

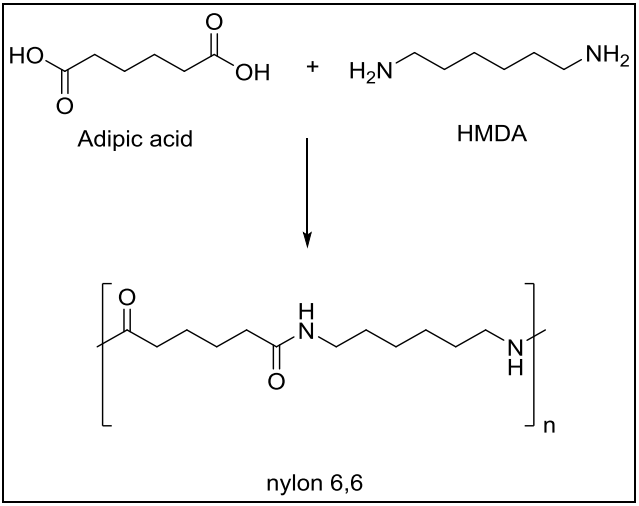

Scheme 2: Synthesis of nylon 6, 6 using Adipic acid and HMDA

In the year 1975, first alternative routes to production of adipic acid was achieved [29]. In that successful endeavour, hydrocarboxylation of 1, 3 butadiene afforded adipic acid without any nitrous oxide waste.

In another report, Noyori *et al*. formulated a halide free biphasic process for direct conversion of cyclohexene to adipic acid. A phase transfer catalyst in presence of H_2O_2 was used for the aforementioned conversion, giving a high yield of 90%. Later on, Freitag and his co-workers used Na_2WO_4 as a catalyst in presence of microwave radiation to afford adipic acid. The resultant product was obtained in a very short reaction time of 90 min with 68% yield.

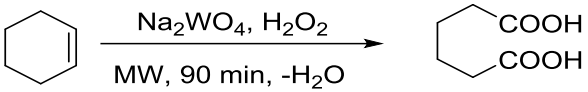

Scheme 3: Synthesis of Adipic acid *via* Na_2WO_4 catalyst

Dehydrogenation of Alcohols

Oxidation of alcohols to carbonyl compounds is a fundamental organic transformation of great interest. To achieve economic and environmental acceptability, a great deal of effort has been devoted on developing heterogeneous based catalytic systems involving noble metals such as Ru, Pd, Pt and Au for aerobic oxidation of alcohols. However, from the standpoint of atom efficiency, economic viability and safety of the reaction, oxidant-free dehydrogenation of alcohols to carbonyl compounds may be

considered ideal. Additionally, this oxidant free protocol is also a potential method for hydrogen production from biomass products. A detailed study revealed that several catalytic systems based on homogeneous and heterogeneous materials have been used for oxidant free dehydrogenation of alcohols [212-214].

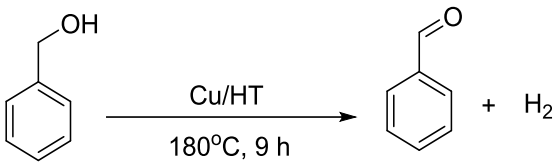

Scheme 4: Oxidant free dehydrogenation of alcohols using Cu/HT catalyst

Hydroxylation of Benzene

Direct hydroxylation of benzene is a sustainable and promising strategy to synthesize phenol. Phenol is considered to be an important organic intermediate used in the synthesis of polymer resins, pharmaceutical products along with its widespread application in preservatives and fungicides. The annual production of phenol is estimated to be nearly about 7 million metric tonnes, which accounts to its wide applicability in numerous fields. Hock and Lang, in the year 1944, first reported the synthesis of phenol via cumene process. However, requirements of high pressure and temperature conditions were considered to be among its few limitations. In accordance of newer, improved catalysts, metal free catalysts have also been recently exploited as catalysts for the generation of phenol. For instance, Yang *et al*. reported a highly efficient graphene catalysed reaction process for one step conversion of benzene to phenol. Graphene was chemically converted to afford the catalyst. They further demonstrated that the direct oxidation was achieved with good conversion and selectivity at a moderate reaction temperature using H_2O_2 as oxidant.

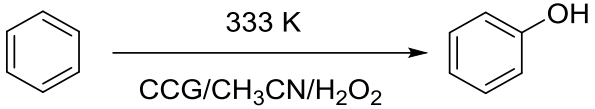

Scheme 5: One step oxidation of benzene to phenol *via* chemically converted graphene (CCG) as catalysts

In 2013, Zhang *et al*. developed a catalysis protocol for the direct oxidation of benzene to phenol using $FeCl_3$/mpg-C_3N_4 and visible light irradiation.

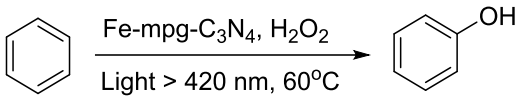

Scheme 6: One step oxidation of benzene to phenol *via* chemically converted graphene (CCG) as catalysts

Interestingly, superior selectivity of the reaction was observed for these catalysts, but poor conversion rates prevailed as a serious problem. Even the involvement of less active metals such as Fe, V, Cu, etc. as catalysts still required high temperature. Immobilization of these metals over porous silica surface and polymeric support manifested good catalytic performance, however, required longer reaction time. As a result, it is reasonably important to develop newer catalysts for the catalytic generation of phenol under milder conditions with high yield and selectivity.

What therefore emerges out of the foregoing overview on the chemistries of metal and/or metal oxide NPs and their various applications is that though these areas have matured quite considerably, yet there remains sufficient amount of scope for important works.

References

1. Wheeler JA, Feynman R. Interaction with the Absorber as the Mechanism of Radiation. Rev. Mod. Phys. 1945; 17:157.
2. Kreuter J. Nanoparticles- a historical perspective, Int. J Pharm. 2007; 331(1):1-10.
3. Lead JR, Wilkinson KJ. Aquatic colloids and nanoparticles: current knowledge and future trends. Environ. Chem. 2006; 3(3):159-171.
4. Hough RM, Noble RRP, Reich M. Natural gold nanoparticles. Ore Geol. Rev. 2011; 42(1):55-61.
5. Heiligtag FJ, Neiderberger M. The fascinating world of nanoparticle research. Mater. Today. 2013; 16(7-8):262-271.
6. Colomban P, Gouadec G. The ideal ceramic composite with oxide matrix, or how to reconcile contradictory physical and chemical criteria. Ann. Chim. Sci. Mater. 2005; 30(6):673-688.
7. Colomban P. The use of Metal nanoparticles to produce Yellow, Red, and Iridescent Colour, from Bronze Age to present times in Lustre pottery and glass: Solid State Chemistry, Spectroscopy and Nanostructure. J Nano Res. 2009; 8:109-132.

8. Sciau P, Mirguet C, Roucau C, Chabanne D, Schvoerer M. Double nanoparticle layer in a 12th century Lustreware Decoration: Accident or Technological Mastery?. J Nano Res. 2009; 8:133-139.

9. Leonhardt U. Optical metamaterials: Invisibility Cup. Nat. Photon. 2007; 1:207-208.

10. Becht S, Ernst S, Bappert R, Feldmann C. Nanomaterialien zum Anfassen. Do-it-yourself. Chem. Unserer Zeit. 2010; 44(1):14-23.

11. Love SA, Marquis BJ, Haynes CL. Recent advances in nanomaterial plasmonics: fundamental studies and applications. Appl. Spectrosc. 2008; 62(12):346A-362A.

12. Cheng NY, Tian JQ, Liu Q, Ge CJ, Qusti AH, Asiri AM *et al*. Au-Nanoparticle-Loaded Graphitic Carbon Nitride Nanosheets: Green Photocatalytic Synthesis and Application toward the Degradation of Organic Pollutants. ACS Appl. Mater. Interfaces. 2013; 5(15):6815-6819.

13. Ge L, Han CC, Liu J, Li YF. Enhanced visible light photocatalytic activity of novel polymeric g-C_3N_4 loaded with Ag nanoparticles. Appl. Catal. A. 2011; 409-410, 215-222.

14. He YM, Zhang LH, Teng BT, Fan MH. New Application of Z-Scheme Ag_3PO_4/g-C_3N_4 Composite in Converting CO_2 to Fuel. Environ. Sci. Technol. 2015; 49(1):649-656.

15. Katsumata H, Tachi Y, Suzuki T, Kaneco S. Z-scheme photocatalytic hydrogen production over WO_3/g-C_3N_4 composite photocatalysts. RSC. Adv. 2014; 4:21405-21409.

16. He YM, Zhang LH, Fan MH, Wang XX, Walbridge ML, Nong QY *et al*. Z-scheme SnO_2-x/g-C_3N_4 composite as an efficient photocatalyst for dye degradation and photocatalytic CO_2 reduction. Sol. Energy Mater. Sol. 2015; 137:175-178.

17. Dong G, Schuth F. Synthesis of non-siliceous mesoporous oxides. Chem. Soc. Rev. 2014; 43:313-344.

18. Lim CW, Lee IS. Magnetically recyclable nanocatalyst systems for the organic reactions. Nano Today. 2010; 5(5):412-434.

19. Mornet S, Vasseur S, Grasset F, Duguet E. Magnetic nanoparticle design for medical diagnosis and therapy. J Mater. Chem. 2004; 14:2161-2175.

20. Zhang S, Shen XT, Zheng ZP, Ma YY, Qu YQ. 3D graphene/nylon rope as a skeleton for noble metal nanocatalysts for highly efficient heterogeneous continuous-flow reactions. J Mater. Chem. A. 2015; 3:10504-10511.

21. Polshettiwar V, Asefa T. Nanocatalysis synthesis and applications. John Wiley & Sons, 2013.

22. Tian K, Liu W, Zhang S, Jiang H. One-pot synthesis of a carbon supported bimetallic Cu-Ag NPs catalyst for robust catalytic hydroxylation of benzene to phenol by fast pyrolysis of biomass waste. Green Chem. 2016; 18(20):5643-5650.

23. Baeck SH, Choi KS, Jaramillo TF, Stucky GD, McFarland EW. Enhancement of Photocatalytic and Electrochromic Properties of Electrochemically Fabricated Mesoporous WO_3 Thin Films. Adv. Mater. 2003; 15(15):1269-1273.

24. Zhang D, Wang S, Zhu J, Li H, Lu Y. WO_3 Nanocrystals with tunable percentage of (001)-facet exposure. Appl. Catal. B. 2012; 123-124, 398-404.

25. Chen D, Ye J. Hierarchical WO_3 Hollow Shells: Dendrite. Sphere, Dumbbell, and Their Photocatalytic Properties. Adv. Funct. Mater. 2008; 18(13):1922-1924.

26. Xu H, Wang W, Zhu W. Shape Evolution and Size-Controllable Synthesis of Cu_2O Octahedra and Their Morphology-Dependent Photocatalytic Properties. J Phys. Chem. B. 2006; 110(28):13829-13834.

27. Hudson R, Feng Y, Varmab RS, Moores A. Bare magnetic nanoparticles: sustainable synthesis and applications in catalytic organic transformations. Green Chem. 2014; 16:4493-4505.

28. Gawande MB, Branco PS, Parghi K, Shrikhande JJ, Pandey RK, Ghumman CAA *et al*. Synthesis and characterization of versatile MgO-ZrO_2 mixed metal oxide nanoparticles and their applications. Catal. Sci. Technol. 2011; 1:1653-1664.

29. Castellan A, Bart J, Cavallaro S. Nitric acid reaction of cyclohexanol to adipic acid. Catal. Today. 1991; 9(3):255-283.

Chapter - 6
Synthesis of Heterocycles over Nanoporous Zeolites

Authors

B. Sarmah
Department of Chemistry, Indian Institute of Technology, Ropar, Punjab, India

R. Srivastava
Department of Chemistry, Indian Institute of Technology, Ropar, Punjab, India

Chapter - 6

Synthesis of Heterocycles over Nanoporous Zeolites

B. Sarmah and R. Srivastava

Abstract

Heterocyclic moieties are the integral part of a wide range of natural products and synthetic compounds. Approximately 60% of all chemical products and 90% of chemical process worldwide depend on the catalysis. Although conventional routes using mineral acid or base are available for the synthesis of heterocyclic compounds, but the waste generated for every steps required for purification, and isolation make the process not ecofriendly from environmental and safety point of view. Zeolites are solid acid, recyclable, and nonpolluting heterogeneous catalysts that could be used for various chemical transformations. This chapter presents the role of nanoporous zeolites namely Nano-ZSM-5, and other large pore zeolites in the synthesis of bulkier heterocycles. A plethora of heterocyles namely three, five, six, and seven-membered of pharmaceutical importance can be synthesized from Brönsted or Lewis acid site promoted zeolites shall be demonstrated here. Finally, the authors' view on the perspective of synthesis of a wide range of heterocyclic compounds using nanoporous zeolites are given.

Keywords: Nanoporous zeolite; nano-ZSM-5; titanosilicate (TS-1); H-Beta, H-Y, epoxides; pyrrole; pyrrolidine; pyrazole; imidazole; imidazoline; tetrazole; triazole; benzo thiazole; benzothiazoline; 1, 2-methylenedioxybenzene (MDB); indole; benzimidazole; indolizine; oxazole; thiazole; thiazolidinone; cyclic carbonate; tetrahydrofuran; thiophene; thiolane; solketal; pyridine; β- picoline; 2,6-lutidine; 2,4,6-collidine; piperidine; pyran; piperazine; pyrazine; 1,4-diazabicyclo [2.2.2] octane; 3,4-dihydropyrimidin-2(1H)-ones; quinoline; isoquinoline; 2-methylquinoxaline; quinazoline-2,4(1H,3H)- dione; 2,3-dihydro 1,5-benzothiazepine; benzodiazepine, ε-caprolactam, 4H-benzo[b]pyrans, pyrano [c] chromene, flavonoids, coumarin, 1,5-diazabicyclo-[4.3.0]non-5-ene (DBN), 1,8-diazabicyclo[5.4.0]undeo7-ene (DBU), 5-hydroxymethylfurfural (HMF), 2-pyrrolidinone, 2-thiolandione, butenolides, δ- valerolactone, ε-caprolactone, and N-methylpyrrolidine (NMP).

1. Introduction

Zeolites belong to microporous aluminosilicates with high crystallinity. Petrochemical and fine-chemicals market are governed by solid acid catalyst "Zeolites" since its kinetic diameters are less than 10Å. Microporous crystalline Zeolites are built from TO_4 (T=Si, or Al) tetrahedron as primary building unit, and these are connected through corner sharing of oxygen atoms to form three dimensional porous framework structure [1]. Synthesis of zeolite is a complex phenomenon. Zeolites are synthesized in highly basic medium using silica source, alumina source, and inorganic/organic cation through a kinetically controlled hydrothermal crystallization process. Initially, the primary building units for example silica, and aluminum tetrahedral condenses to give the secondary building units (pentasil units or pentasil chains). Then this secondary building units undergo self assemble in presence of various organic and inorganic structure directing agent to afford the Meta stable phase of zeolites. After certain duration, crystalline zeolites are filtered off from the synthesis mixture. A wide range of zeolites with various framework structures can be synthesized by changing the synthesis composition and the cation (inorganic and/or organic). Two most common zeolites for example ZSM-5 comprise of 10 membered oxygen ring channel with 5.5 Å medium pores and Beta zeolite 12 membered oxygen ring channel having disordered type structure with 7.4Å large pore. Nanoporous materials can be grouped into three categories depending on the pore diameter: microporous (<2 nm), mesoporous (2–50 nm), and macroporous (>50 nm) [2]. Zeolites have application in several fields owing to its tunable interconnected porous network structure, textural properties, silica to alumina ratio, and acidity etc.

There are 230 framework of zeolite structures are known till today [3]. It may be noted that conventional microporous zeolites have pore diameter less than 2 nm, which restricts the diffusion constraints of bulkier molecules. Therefore, to conduct larger molecular transformations, zeolite should have additional mesoporosity. Hence, reduction in the size of zeolite nanocrystal during the synthesis of zeolites using additives (for example alkyl triethoxy silane) has gained significant preference over various strategies reported in literature [4, 5, 6, 7, 8]. To prepare zeolites having interconnected micropores and mesopores (nanocrystalline zeolites) with high acidity, crystallinity and hydrothermal stability is a challenging task. This can be achieved by introducing additives as mentioned above since it contains three hydrolysable alkoxysilyl moieties and a hydrophobic alkyl chain, which resist in the formation of extended tetrahedral silica linkages. Hence, this

lead to retardation of zeolite growth at the organic-inorganic interface, results in the formation of nanocrystalline zeolites. Another advantage of nanocrystalline zeolites over conventional zeolites is that they don't undergo quick deactivation.

2. Classification of Zeolites

Classification of zeolites are based on two categories namely, (i) oxygen ring channel [9] and (ii) silica to alumina ratio. Based on oxygen ring channel, Zeolites are groups as small pore (8 membered), medium pore (10 membered), large pore (12 membered), and ultra-large pore (14 or 18 membered) (Table 1). Similarly, when silica to alumina content is considered, Zeolites are grouped as low silica (1-1.5), intermediate silica (2-5), high silica (10-100), and silica molecular sieves. High silica zeolites are very good for catalytic activity because of their stability.

Table 1: Zeolite classification based on oxygen ring size [9]

Molecular Sieve Type	Framework Structure	Example of Zeolites	Ring Size
Small pore	LTA	A, SAPO-42	8
	CHA	Chabazite, SAPO-34	8
	AEI	ALPO-18	8
	AFX	ALPO-56, SSZ-16	8
	RTH	ITQ-3	8
Medium pore	MFI	ZSM-5, Silicate	10
	MEL	ZSM-11	10
	FER	Ferrierite, ZSM-48	10
	TON	ZSM-22	10
	AEL	ALPO-11, SAPO-11	10
	AFO	ALPO-41	10
	MWW	MCM-22, ITQ-1	10
Large pore	FAU, EMZ	Faujasite, SAPO-37	12
	BEA	Beta	12
	MOR	Mordenite	12
	MTW	ZSM-12	12
	LTL	Linde type L	12
	AFI	ALPO-5, SAPO-5	12
	ATO	ALPO-31	12
	IFR	MCM-48	12
Ultra-large pore	UFI	MCM-9, ALPO-54	18
	AET	ALPO-8, MCM-37	14
	DON	UTD-1	14

3. Application of Nanoporous Zeolites for Synthesis of Heterocycles

The emerging applications of zeolites are ion-exchange capacity that depends on the number and nature of cation exchange sites and their

accessibility. Furthermore, zeolites can also be used in detergents, soaps, water softening device, and to remove radioactive ion from polluted water. Another important application is in the area of gas separation and sorption that depend on the size of the pore opening and volume of void. In general, low silica to alumina zeolites (e.g. A, and X) are good for this type of applications. Furthermore, utilization and transformation of carbon dioxide gas into value-added chemicals is another thrust application of nanocrystalline zeolites. Zeolites are robust heteterogeneous catalyst for various chemical reactions such as cracking, isomerizations, hydrocarbon synthesis, acid-base condensation, and metal induced redox reactions. In most of the cases, reaction takes place within the pores, or on surface acid site where acid sites are located. Catalytic activity of zeolites depend on silica to alumina ratio, the pore opening, dimension of channel and shape/size selectivity, spacing of cages to host reactants & intermediates [10].

Some important features that make nanoporous zeolite a sustainable heterogeneous catalyst for chemical transformations are summarized in table 2.

Table 2: Summary of salient features of nanoporous zeolites that make suitable for organic transformations

1	Large number of surface silanol groups present on the surface of nanocrystalline zeolite facilitates grafting or anchoring of various organic moieties.
2	Large Surface area, external surface area, total pore volume, and mesopore volume.
3	Reduction in the size of zeolite nanocrystal, a boon for bulk molecular transformations.
4	Transition metal framework substituted Zeolites, excellent for redox catalysis.
5	Strong acidity due to presence of Brönsted acid, and Lewis acid sites.
6	Shape selectivity due to tunable interconnected porous network structure.
7	Favorable interaction of active site, reactants, and diffusion of products from its pore aperture.
8	High thermal stability.
9	Excellent reusability.

In this chapter, acid catalyzed reaction furnished by parent medium pore zeolites such as ZSM-5, large pore zeolites Beta, MOR, and HY zeolites and redox reaction mediated by surface modified/metal substituted zeolites shall be discussed.

There are numerous reactions that could be catalyzed using zeolites to synthesize three, five, six, and seven-membered heterocycles of pharmaceutical importance [11].

3.1 Synthesis of Three-Membered Heterocycle

Among three membered heterocycles, epoxides gain considerable interest because they are versatile intermediates or reagents in organic chemistry [12]. This structural scaffold is also present in various biologically active compounds [13]. Epoxides viz. propylene oxides are prepared on industrial scale using homogeneous catalyst e.g. hypochlorous acid that lead to generation of waste salt by-product (NaCl or $CaCl_2$), high cost, and poor atom economy. However, the highly reactive three membered oxirane rings could be synthesized using TS-1 zeolite in presence of H_2O_2 as oxidant in methanol (Scheme 1) [14]. The positive outcome of this reaction is the formation of water as a byproduct and propylene oxide selectivity upto 95%.

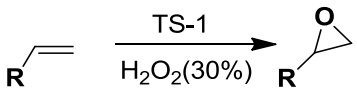

Scheme 1: Route for synthesis of epoxide using TS-1.

However, for larger alkene, epoxidation using TS-1 is less effective; in that case Ti substituted BEA or Zr substituted Nano-ZSM-5 is more effective [15].

3.2 Synthesis of Five-Membered Heterocycles Containing One Nitrogen Atom

Nitrogen containing heterocycles can be classified in to following categories depending upon the number and position of nitrogen atom in the five membered rings. These are pyrroles, pyrazoles, imidazoles, triazoles, indoles and so on.

Pyrroles, an important heterocycle moiety that are present in many natural products and alkaloids such as heme, chlorophyll etc. It shows numerous biological activities and appears in the core structure of several drugs molecules [16]. Two potent examples that contain pyrrole as active pharmacophore mecamylamine, pempidine (antihypertensive) and amantadine (antiviral agents). Pyrroles can be synthesized through well known Knorr-Paal condensation reaction of primary amines with 1, 4-diketone in presence of solid acid zeolites (Scheme 2) [17].

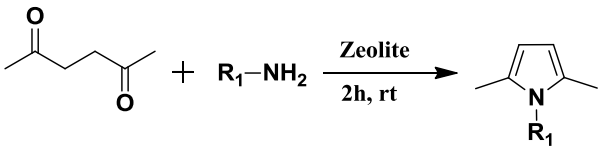

Scheme 2: Route for synthesis of pyrrole using zeolite.

N-alkyl pyrrolidine is another five-membered nitrogen containing heterocycle that can be synthesized via reaction between 1, 4-butanediol or tetrahydrofuran and ammonia under vapor phase at 300 ^{o}C using various metal containing ZSM-5 zeolites (M-ZSM-5, M=Cr > V > Mn > Mo > Pb= Cu > W). However, Cr-ZSM-5 zeolite showed superior result under this vapor phase condition (Scheme 3) [18]. To obtain the high yield of NMP, excess amount of ammonia was used. Interestingly, VAPO, SAPO, did not afford NMP. The higher activity of Cr-ZSM-5 could be due to its bi-functional nature with $[Cr\ (OH)]^{2+}$ and H^{+} as active centres and the polarizabilty of cation.

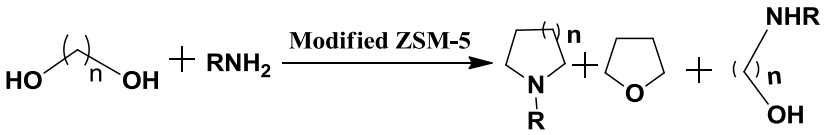

Scheme 3: Route for synthesis of N-alkyl pyrrolidine using zeolite.

It may be noted that, Brönsted acid centers were formed as a result of dissociation of water. Here, main driving force for the dissociation of water that resulted in the formation of bi-functional nature of the catalyst Cr-ZSM-5 is the polarizability of Cr^{3+} cation. In another report, Brönsted acid site present in the zeolites namely HY, that afforded 82% selective formation of NMP product with 61% conversion of THF under vapor phase condition (Scheme 4) [19].

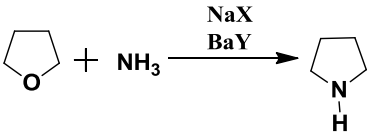

Scheme 4: Route for synthesis of pyrrolidine using zeolite.

However, under these circumstances, alkali metal-exchanged zeolite namely BaY were totally inactive [19].

3.3 Synthesis of Heterocycles Containing More Than One Nitrogen Atoms

Pyrazole is one of the important heterocycles that contains two nitrogen atoms in the five membered ring. Pyrazole derivatives are important constituents of various agrochemicals and pharmaceutical such as herbicides [20]. Pyrazole an alkaloid, has many medicinal activities namely anti-inflammatory, analgesic, anticancer, anticonvulsant, antibacterial, antimicrobial, anti-viral, antimalarial, hypoglycemia, and antineoplastic

agent etc. This can be prepared through intermolecular cyclization of β-diketones with hydrazine derivatives in presence of zeolite HY, and EMT [17] as catalyst. Another, route to prepare pyrazole is the cyclization reaction of E-chalcone and hydrazine followed by dehydrogenation using OMS (30%)/Nano-ZSM-5-nanocomposites [21] as catalyst (Scheme 5). Kobayashi *et al*. reported that pyrazole could also be prepared by the reaction between ethyl propionate with ethyl dizao acetate at room temperature using NaY as catalyst (Scheme 5) [22].

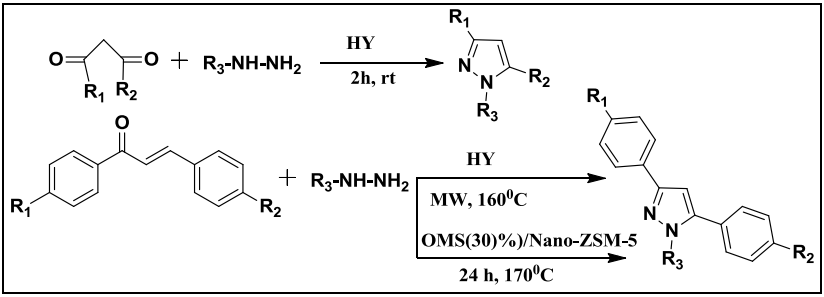

Scheme 5: Route for synthesis of pyrazole using zeolite

Another five membered heterocycle such as imidazole that plays a crucial role for the synthesis of agrochemicals, and pharmaceuticals [23]. Furthermore, it also acts as curing agent, anti-rust agent for epoxy resin [20]. Moreover, imidazoles are also utilized as active component in the light or heat sensitive area. Substituted imidazoles can be synthesized by the multicomponent condensation reaction of benzil or benzoin, primary amines, and ammonium acetate using HY zeolite-silica gel under microwave irradiation (Scheme 6) [24].

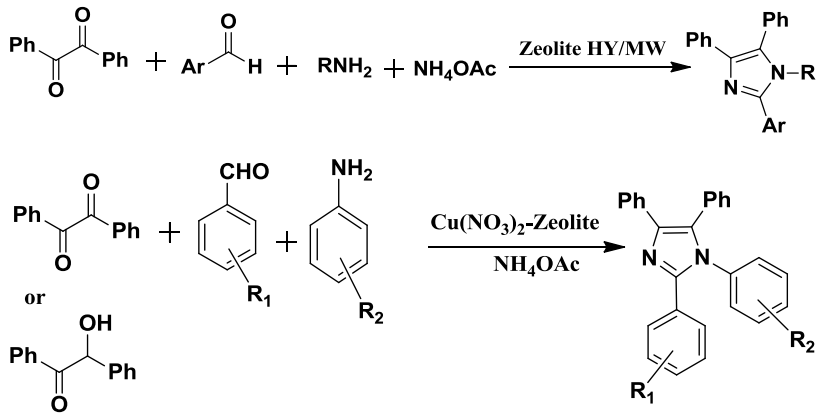

Scheme 6: Routes for the synthesis of imidazole using zeolite

This reaction can also proceed with benzoin, benzaldehyde, aniline, and ammonium acetate using zeolite supported copper nitrate [25]. Triarylimidazoles can also be prepared by a mixture of benzil, benzaldehyde, and ammmoniumacetate under microwave in presence of HY zeolite-silica gel as catalyst [26].

Imidazolines are pharmaceutically important building motifs that are found in many biologically active compounds [27] or in existing drugs acting that act as antiproliferative agent, antihypertensive agent etc. [28]. Apart from its medicinal importance, these are also used as synthetic intermediates [29], chiral ligands [30], chiral auxiliaries [31] in organic synthesis. Imidazolines can be synthesized by the reaction of aromatic carboxylic acid and ethylenediamine in xylene using Ersorb-4 (E4), a clinoptylolite–type zeolite as catalyst (Scheme 7) [32].

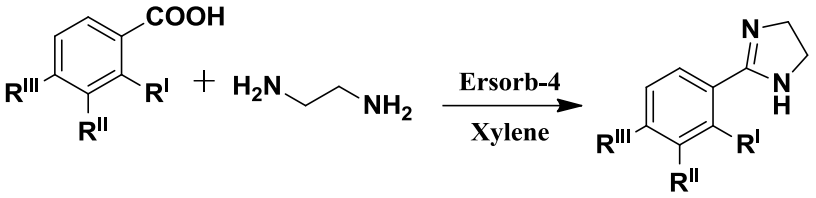

Scheme 7: Route for the synthesis of imidazoline using zeolite.

Tetrazoles are nitrogen containing heterocycles that play a crucial role in the pharmaceutical industry. Tetrazoles especially 5-aminotetrazoles are used as anti allergic, anti-asthmatic [33], antiviral, anti-inflammatory [34], and anti-neoplastic [35]. Furthermore, tetrazoles scaffold have ability to act as ligand in coordination chemistry [36]. It also finds application as explosives and rocket propellants [37]. Tetrazoles can be synthesized through two ways: (i) by treating cyanamide, and sodium azide in dimethylformamide or refluxing in water for a stipulated time, (ii) by reacting primary amine, sodium azide, and triethyl orthoformate in absence of solvent at 120 ^{o}C using Natrolite zeolite as catalyst (Scheme 8) [38-39].

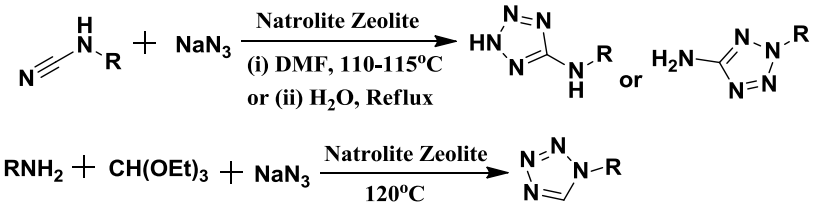

Scheme 8: Route for synthesis of tetrazole using zeolite.

Triazoles are nitrogen containing five membered heterocyclic

compounds. Triazoles are known to exhibit biological activities for example anti-HIV, anti-allergic, and antifungal activity [40]. Moreover, they are also used as photostabilizer, optical brighteners, and agrochemicals and so on [41]. Triazoles are generally prepared through [3+2] cycloaddition reaction between aromatic azide and phenylacetylene using copper nanoparticles supported mesoporous zeolite (Scheme 9) [42]. Substituted triazole can also be synthesized by the treating epoxide, sodium azide, and phenyl acetylene in presence of copper supported mesoporous ZSM-5 catalyst (Scheme 9) [42]. Triazole can be synthesized when alkylazide and alkyne react in presence of copper (I) exchanged zeolite (Mordenite, USY, ZSM-5, Beta) as catalyst (Scheme 9) [43].

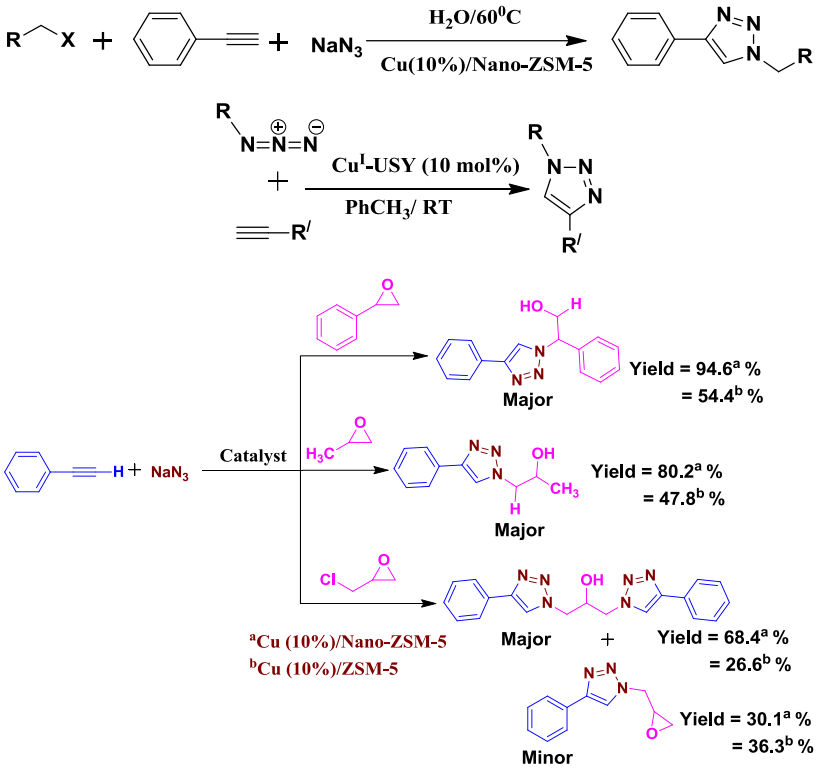

Scheme 9: Various routes for the synthesis of substituted triazole using zeolite.

3.4 Synthesis of Fused Heterocycles Containing Hetero Atoms (O, N, or S Etc.)

Two important fused heterocycles namely benzoxazole and benzothiazole that exhibit diverse pharmacological activities such as

antibacterial, antiulcers, antihypertensive, antiviral, antifungal, anticancer, and antihistamines activity [44]. Moreover, these bioactive molecules also act as ligand for asymmetric transformation [45] and shows optical [46], and luminescent properties [47]. Benzoxazole can be prepared through two ways: (i) Beckman rearrangement of salicylaldoxime under down-flow reactor at 493 K using zeolite (MOR, Beta, ZSM-5, HY etc.) as catalyst [48]; (ii) treatment of *o*-amino phenol and benzaldehyde under reflux using zeolite as catalyst (Scheme 10) [49]. Similarly, benzothiazole can be synthesized through reaction between benzaldehyde and *o*-aminothiophenol using zeolite as catalyst (Scheme 11) [50].

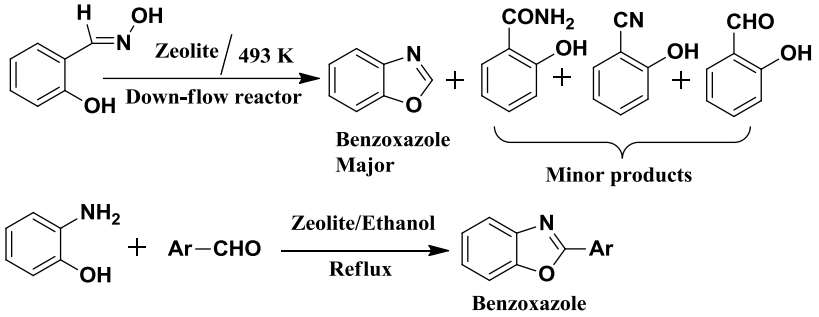

Scheme 10: Routes for the synthesis of benzoxazole using zeolite.

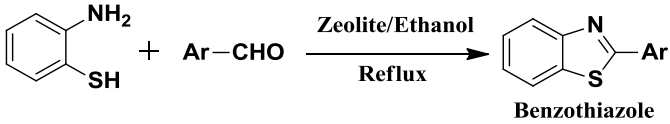

Scheme 11: Route for synthesis of benzothiazole using zeolite.

Benzothiazoline is a fused heterocyle that exhibit diverse pharmacological activities. As, Sb, Ga, and in derivatives [51] of benzothiazolines are bifunctional tridente ligands. Benzothiazoline can be prepared via one-pot cyclization reaction between *o*-aminothiophenol and ketone derivatives over Nano-ZSM-5 or Nano-Beta zeolites (Scheme 12) [52].

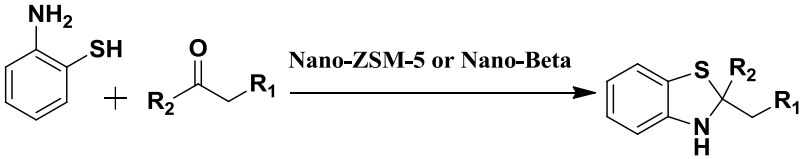

Scheme 12: Route for synthesis of benzothiazoline using zeolite.

1, 2-methylenedioxybenzene (MDB) is a fused heterocyle, where the

methylenedioxy-core acts as an active ingredient especially in agrochemical and household products. For example, Piperonyl butoxide an insecticide, drugs (Tadalafil^{TM}, and Paroxetine^{TM}) or fragrances (Piperonal, Helional^{TM}) [53] where MDB core is present. MDB can be prepared through reaction between catechol and diethoxymethane under vapor-phase using TS-1 catalysts (Scheme 13) [54].

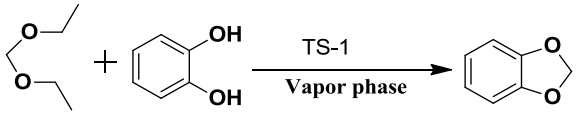

Scheme 13: Route for synthesis of 1, 2-methylenedioxybenzene using zeolite.

Indole scaffold is present in many natural products, polymers, and pharmaceutical agents [55]. Fischer-Indole synthesis (FIS) route is one of the classical routes to synthesize indole. First step of FIS include condensation reaction between phenyl hydrazine and ketones that result in the formation of phenylhydrazone intermediate. Next step is the formation of another intermediate enehydrazine, facilitated by Brönsted or Lewis acid site present in zeolite. Finally, phenylhydrazine tautomer undergoes [3, 3]-sigmatropic rearrangement thereby liberating ammonia and furnishes indole as product (Scheme 14) [56]. Another route to prepare substituted indole is the annulations of *o*-iodoanilide with phenylacetylene catalyzed by palladium (II) supported Na-Y zeolite (Scheme 14) in presence of LiCl and CS_2CO_3 at 140 ^oC [57].

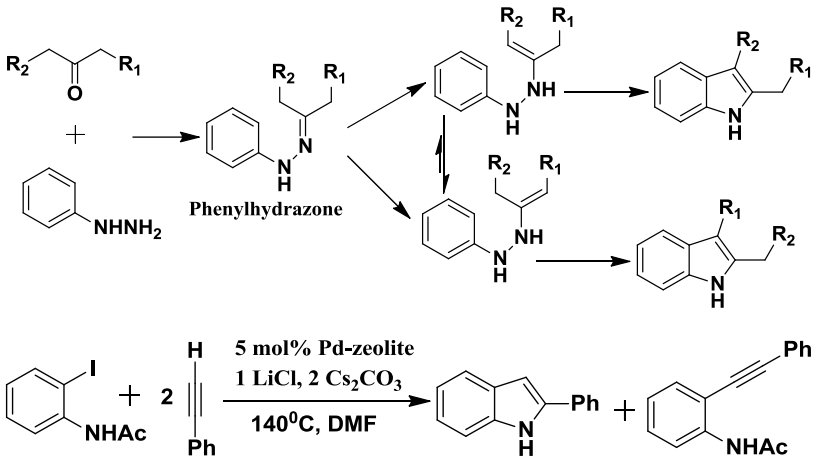

Scheme 14: Various routes for synthesis of indole using zeolite.

Benzimidazoles are important nitrogen containing heterocyclic motifs.

These are present in agrochemicals, dyestuffs, and polymeric products [58]. They exhibit many pharmacological activities such as inhibition of phosphodiesterase IV [59], anti-arrhythmic, antiviral indications [60], anthelmintics, proton pump inhibitors, antihistaminic [61], antiulcer, antihypertensive, anticoagulant, anti-allergic, analgesic, anti-inflammatory, antipyretic, antibacterial, antifungal, antiparasitic, antioxidant, anticancer and anti-anxiolytic activity [62]. Benzimidazoles namely 2-phenylbenzimidazole could be prepared through reaction of 1, 2-diaminobenzene with benzoyl chloride via heterocyclization of N-benzoyl-1, 2-diaminobenzene over zeolite catalyst (Scheme 15) [63]. It can also be prepared through condensation reaction between *o*-phenylenediamine and aldehyde [64] or carboxylic acid [65] over zeolite catalyst as shown in Scheme 15.

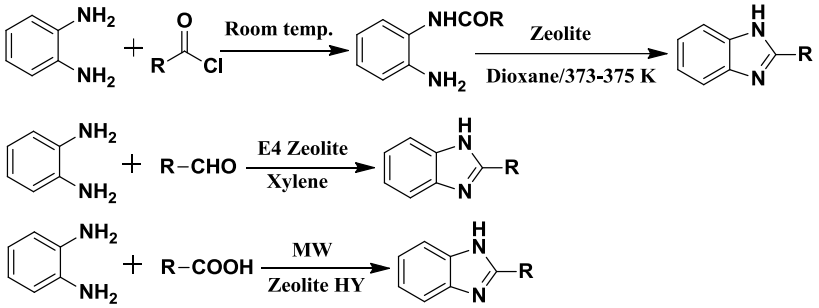

Scheme 15: Various routes for synthesis of benzimidazoles using zeolite.

Indolizine scaffold is present in many natural and synthetic bioactive molecules [66]. It exhibits biological properties such as inhibition of 5-hydroxytryptamine (5-HT_3) receptor [67], phospholipase [68], aromatase [69], 15- lipoxygenase [70], cancer cell [71], and topoisomerase I activity [72]. It also shows fluorescent activities therefore it is utilized in material science. Indolizine can be synthesized via one-pot multi-component C-C coupling strategy in presence of copper nanoparticles supported zeolite catalyst (Scheme 16) [73].

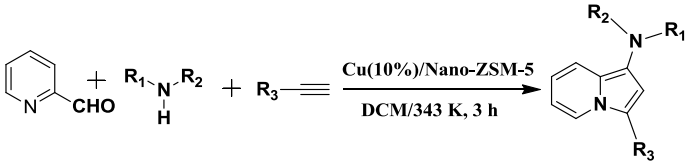

Scheme 16: Route for synthesis of indolizine using zeolite.

4H-benzo[b]pyrans and pyrano[c]chromene are fused pyran derivatives that have gained considerable interest due to their wide range of therapeutic

properties, such as anticoagulant, antimicrobial, anticancer, and diuretic activities [74, 75]. 4H-benzo[b] pyran and pyrano[c] chromene can be synthesized through multicomponent condensation reaction involving 1,3-diketones or 4-hydroxycoumarin with aromatic aldehydes and malononitriles over ruthenium supported imine-functionalized zeolite beta catalyst (Scheme 17) [76].

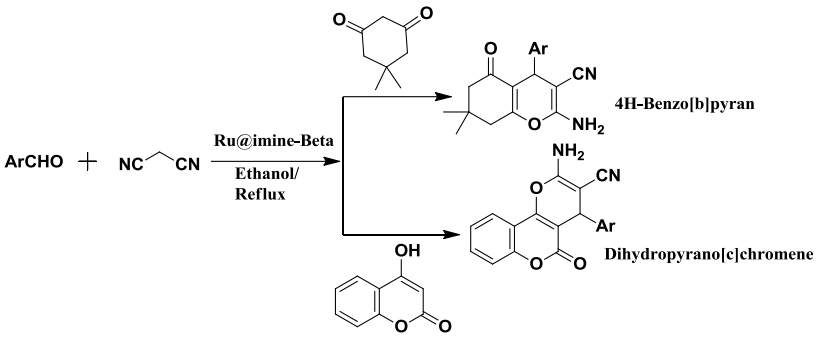

Scheme 17: Routes for synthesis of pyran and chromene derivatives using zeolite.

Flavonoids, are polyphenolic compounds that exhibit biological activities such as anti-inflammatory, anti-microbial, anti-carcinogenic, anti-HIV, cardioprotective and neuroprotective activities [77]. Flavonoids can be synthesized through cyclization reaction between benzaldehyde and 2-hydroxyacetophenone in presence of zeolite catalyst (Scheme 18).

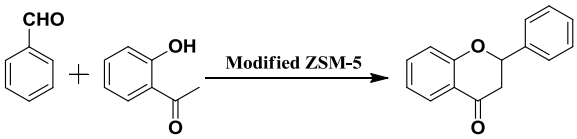

Scheme 18: Route for synthesis of flavonoid using zeolite.

Coumarin is another fused heterocycle present in many natural substances. They are utilized in the production of agrochemicals, pharmaceuticals, and fragrance industry (Scheme 19) [78].

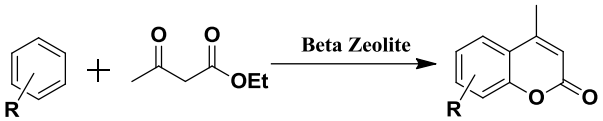

Scheme 19: Route for synthesis of coumarin using zeolite.

DBN, DBU are two nitrogen based fused heterocycles that can be synthesized through cyclization reaction between pyrrolidinone or caprolactam and 1, 3-diaminopropane over HY zeolite (Scheme 20) [79].

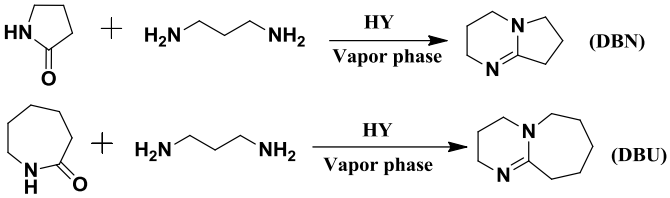

Scheme 20: Routes for synthesis of DBN and DBU using zeolites

3.5 Synthesis of Five Membered Heterocycles Containing Heteroatoms (N, O, and S Etc.)

Oxazole is an important five membered heterocyle, where oxygen and nitrogen are located at 1, 3 position. It shows different biological activities such as antiviral, antimalarial, antifungal, anti tuberculosis, and antibacterial agent [80]. Oxazole can be prepared through two ways: (i) first route being condensation reaction between substituted benzoic acid and 2-amino ethanol or o-aminophenol over E4 zeolite as catalyst in xylene solvent [32]; (ii) second route involves two steps methodology, first step being condensation between propargyl alcohol and acetamide (propargylation) forming alkynyl amide. In the second step, alkynyl amide undergoes cycloisomerization in presence of acidic site of H-Beta zeolite to form oxazole as major product (Scheme 21) [81]. Isoxazole is another five membered heterocycle where, oxygen and nitrogen atoms are located at 1, 2 position. It is found in many natural products such as ibotenic acid, and drugs including COX-2 inhibitor. Isoxazole can be prepared from nitroaldolic condensation of aromatic aldehydes with nitroalkanes over basic zeolite for example CsNaX (Scheme 21) [82].

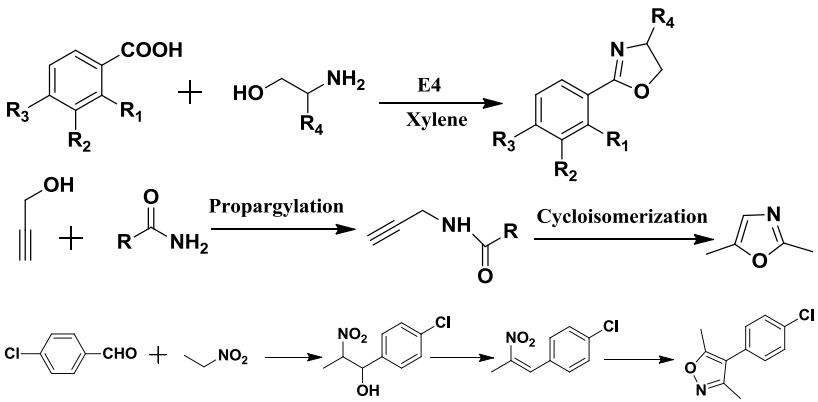

Scheme 21: Various routes for synthesis of oxazole using zeolite.

Thiazole is a five membered heterocycle, where sulfur and nitrogen

atoms are located at 1, 3 position. It exhibits various medicinal activities namely anti-inflammatory, anticancer, anti-hyperlipidemia, and antihypertensive activities [83]. Thiazole can be prepared in two-steps strategies under vapor phase route: initially, acetone reacts with methyl amine and forms imine as intermediate. Next step, furnishes attack of imine with sulfur dioxide over basic zeolite namely CsX to afford thiazole product (Scheme 22) [84].

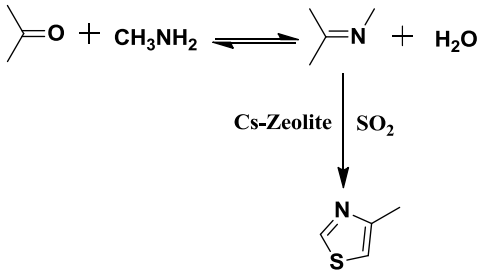

Scheme 22: Route for synthesis of thiazole using zeolite.

Thiazolidinone is a five membered heterocycle that contains sulphur and nitrogen as sole heteroatoms. It shows diverse pharmacological properties, such as antibacterial, anticancer, antitubercular, antioxidant, anti-inflammatory, COX-1 inhibitory and anti-HIV activities [85]. This could be prepared through multicomponent reaction of thioglycolic acid, benzaldehyde, aniline over ZSM-5 zeolite as catalyst (Scheme 23) [56].

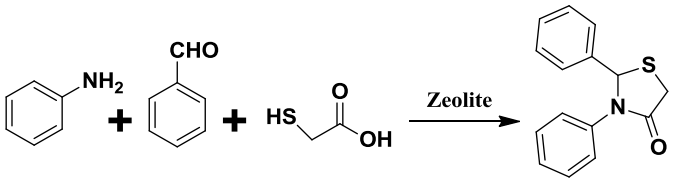

Scheme 23: Route for synthesis of thiazolidinone using zeolite.

Cyclic carbonate is a five membered heterocycle that exhibits various biological activities such as antagonist, anticonvulsants, antibacterial, antihypertensive, anticancer, and anti-inflammatory. Cyclic carbonate could be prepared from epoxide using various surface modified zeolite catalysts namely, basic zeolite functionalized with ILs /bases (1^0, 2^0, 3^0 amine) [86] or metal phthalocyanine complexes (M= Cu^{2+}; Co^{2+}; Ni^{2+} and Al^{3+}) encapsulated in zeolite-Y (Scheme 24) [87].

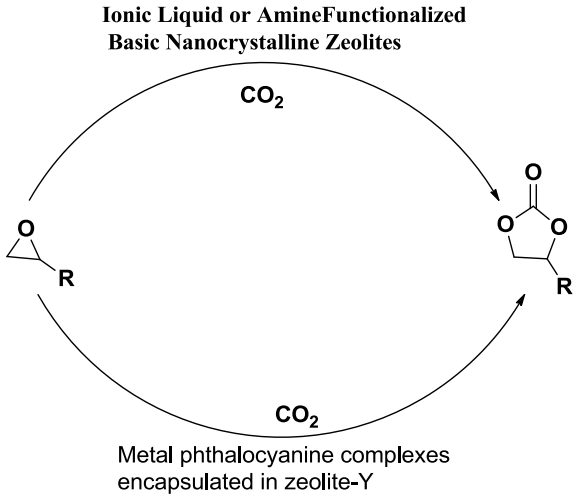

Scheme 24: Zeolite assisted route for synthesis of cyclic carbonate.

Tetrahydrofuran is a five membered saturated heterocycle. It is an important precursor for the synthesis of elastomer copolyester, polyurethanes, elastic fibers and a suitable medium for many polymers [88]. THF can be prepared using various zeolite based solid acid catalysts (namely H-ZSM-5, CrZSM-5, SAPO, and VSAPO) under vapor phase condition. For example, when 1, 4-butanediol reacts with aniline at 300 ^{o}C over chromium substituted ZSM-5 Zeolite, THF is formed as exclusive product (Scheme 25) [18].

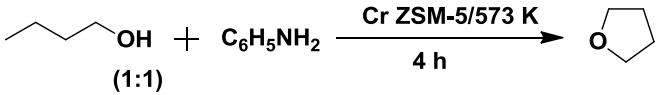

Scheme 25: Route for synthesis of tetrahydrofuran using zeolite.

Thiophene is a five membered heterocycle where sulfur is present as sole heteroatom. Thiophene and its derivative exhibit many medicinal activities such as antimicrobial activity, anticancer activity, anti-inflammatory, antihypertensive, analgesic, CNS activity, and so on. Thiophene can be prepared through vapor phase reaction between furan and hydrogen sulphide at 603 K over basic zeolite such as NaX, or BaY (Scheme 26) [89].

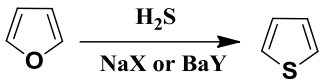

Scheme 26: Route for synthesis of thiophene using zeolite.

Thiolane is a five membered saturated heterocycle where sulphur is present as heteroatom. Synthesis of thiolane doesn't proceed with with acidic zeolite such as HY, ZSM-5 [90]. However, basic zeolite such as NaX affords thiolane almost quantitatively when tetrahydrofuran reacts with hydrogen sulphide under vapor phase condition (Scheme 27) [91].

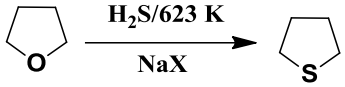

Scheme 27: Route for synthesis of thiolane using zeolite.

Cyclic ketal (Solketal) is a five membered dioxygen containing heterocycle. Solketal is an important raw material for the synthesis of fragrances, food, beverage additives, pharmaceuticals, detergents, and lacquers products [92]. Solketal can be prepared through two ways: (i) by reaction of glycerol and acetone at room temperature over acidic zeolites [93, 52]; (ii) other route being the cyclization reaction between activated styrene oxide and acetone at 353 K (Scheme 28) [94].

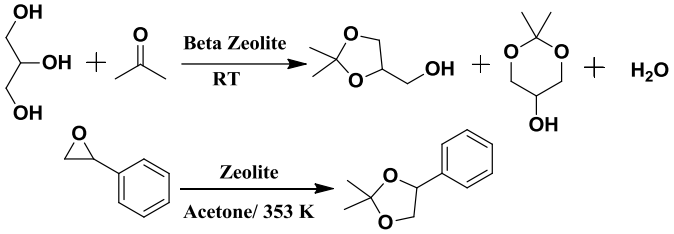

Scheme 28: Routes for synthesis of solketal using zeolite.

5-hydroxymethylfurfural (HMF) is a five membered furan based heterocycle. It is an important building block for the production of biofuels, polymeric products namely polyurethane, and polyamide [95]. It can be synthesized through zeolite mediated dehydration of carbohydrates (Scheme 29) [96, 97].

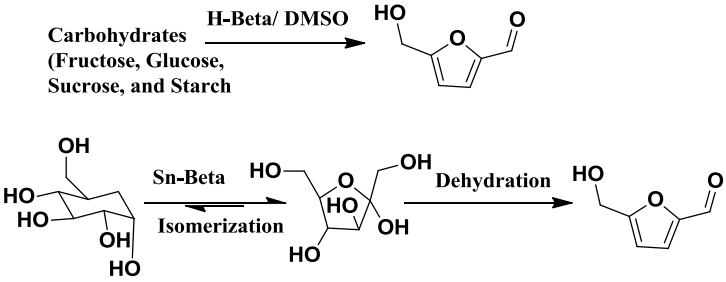

Scheme 29: Zeolite assisted synthesis of HMF.

2-pyrrolidinone or 2-thiolandione are five membered heterocyles that can be synthesized through oxygen/sulphur transformation of γ-butyrolactone over basic zeolites (Scheme 30) [98, 99].

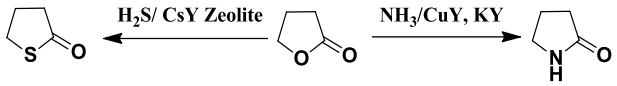

Scheme 30: Synthesis of 2-pyrrolidinone or 2-thiolandione using metal exchanged basic zeolites

Butenolides are five membered furanone heterocycle that are found in many natural products, and drugs [100, 101, 102]. It exhibits many pharmacological activities such as antifungal, anti-inflammatory, ant-cancer, anti-HIV, antimicrobial, and anticancer activities [103, 104, 105, 106]. Butenolide can be synthesized through multicomponent reaction of aromatic amine, acetylenic esters, and aldehyde under reflux condition using HY zeolite (Scheme 31) [107].

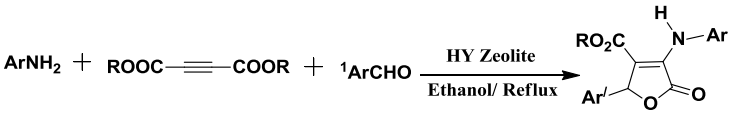

Scheme 31: Route for synthesis of butenolide using zeolite

3.6 Synthesis of Six Membered Heterocycles Containing Heteroatoms (N, and O)

Pyridine, picolines, and their derivatives are important intermediates in the preparation of various pharmaceuticals, surfactants, herbicides, and other fine chemicals [108, 109]. Six membered nitrogen containing heterocycle namely pyridine can be synthesized through two routes under vapor phase condition. First one being the multi-component reaction of Acrolein, acetaldehyde, and ammonia using ZSM-5 catalyst (Scheme 32); (ii) Second route involves the chemical reaction of acetaldehyde, formaldehyde, and ammonia to give selectively pyridine (Scheme 32).

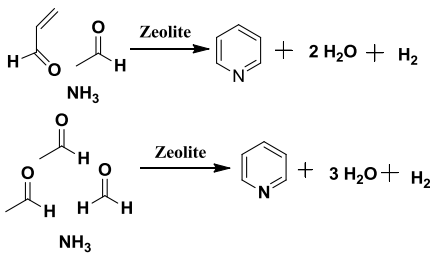

Scheme 32: Routes for synthesis of pyridine using zeolite.

Similarly, when two molecules of acrolein react with ammonia, β-picoline is formed as exclusive product in presence of acidic Zeolite (Scheme 33). B-picoline can also be prepared through multicomponent reaction of acetaldehyde, formaldehyde, and ammonia over zeolite (Scheme 33).

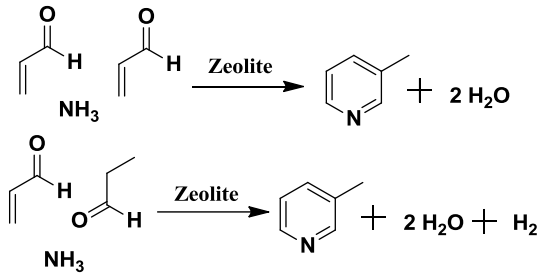

Scheme 33: Routes for synthesis of β-picoline using zeolite.

Other heterocycles such as 2, 6-lutidine, and 2, 4, 6-collidine can be synthesized under vapor phase condition using zeolite catalyst as shown in (Scheme 34).

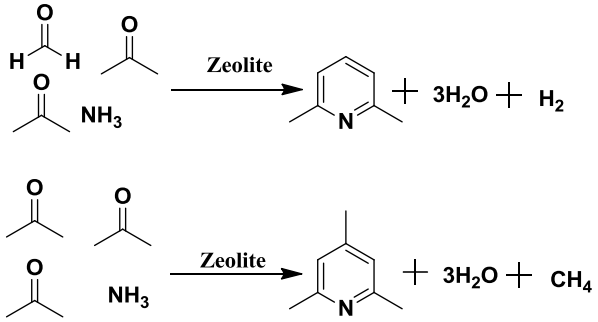

Scheme 34: Routes for synthesis of 2, 6-lutidine, and 2, 4, 6-collidine using zeolite.

Piperidine and pyran are six membered heterocyles that contain nitrogen, and oxygen as heteroatom. Piperidine and pyran are produced from the vapor phase reaction between 1, 5-pentanediol and ammonia over various ZSM-5 catalysts (Scheme 35).

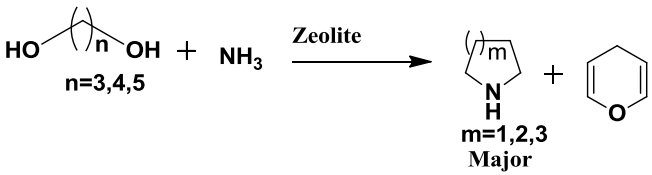

Scheme 35: Route for synthesis of piperidine and pyran using Zeolite.

Piperazine and pyrazine are both nitrogen containing six membered heterocycles. They are employed mainly in perfumes, various drugs, and agrochemicals. These can be synthesized from dehydrocyclization of N-(2-Hydroxyethyl) ethylenediamine to afford piperazine as major product over zeolites at 533 K (Scheme 36) [108, 110].

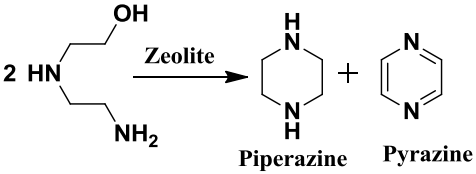

Scheme 36: Route for synthesis of piperazine and pyrazine using zeolite.

1, 4-diazabicyclo [2.2.2] octane (DABCO) is a saturated six membered nitrogen containing heterocycle. It can be synthesized from intermolecular cyclization of ethanolamine over modified zeolite ZSM-5 under vapor phase condition at 573 K (Scheme 37) [108, 110].

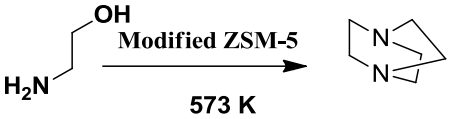

Scheme 37: Route for synthesis of DABCO using zeolite.

3, 4-dihydropyrimidin-2(1H)-ones (DHPM), a sixmembered nitrogen containing heterocycle, which is present in many natural products. It exhibits broad range of therapeutic and pharmaceutical properties [111]. DHPM can be synthesized through cyclocondensation reaction of aromatic aldehydes, β-ketoester, and urea over zeolite (H-ZSM-5, HY) in toluene under reflux condition (Scheme 38).

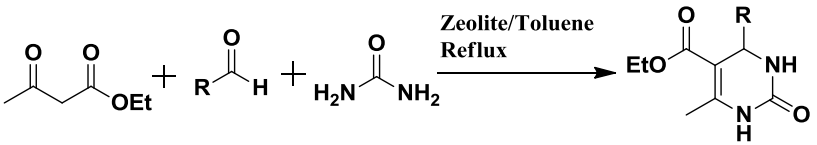

Scheme 38: Route for synthesis of DHPM using zeolite.

Quinoline is a fused sixmembered nitrogen containing heterocycle that exhibits promising anti bacterial and antifungal activity [112]. Substituted quinoline namely 4-methyl quinoline can be synthesized predominantly over 2-methylquinoline when aniline reacts with crotonaldehyde under vapor phase condition using zeolite as catalyst (Scheme 39) [113].

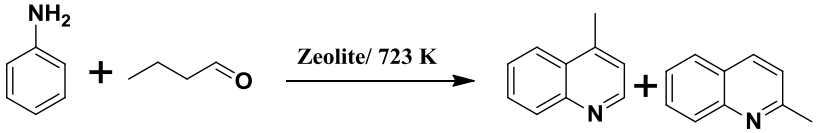

Scheme 39: Route for synthesis of quinoline using zeolite.

Isoquinoline shows a wide range of pharmacological activities against cancer, rheumatoid arthritis, tumor, diabetes, stroke, hemorrhagic shock, and retro-viral infections [114]. This bioactive molecule can be synthesized from the Beckmann rearrangement of cinnamaldoxime over zeolite to afford isoquinoline as major product, and cinnamonitrile as minor product (Scheme 40).

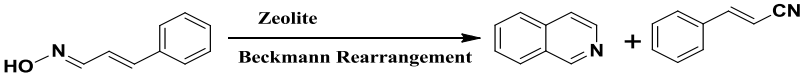

Scheme 40: Route for synthesis of isoquinoline using zeolite.

2-Methylquinoxaline is a fused sixmembered nitrogen containing heterocycle that exhibits several medicinal activities such as antimicrobial, anticancer, antiviral, antibacterial, and kinase inhibitory activities etc. This can be prepared from the reaction between *o*-phenylenediamine and 1, 2 propanediol or 2-bromo acetophenone using modified zeolite catalyst (Scheme 41) [52].

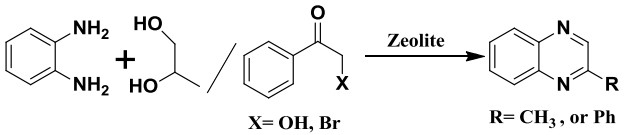

Scheme 41: Route for synthesis of substituted quinoline using zeolite.

Quinazoline-2, 4 (1H, 3H)-diones is another fused heterocycle that shows various medicinal activities [115]. It can be prepared through cycloaddition reaction of activated carbon dioxide and 2-aminobenzonitrile over ionic liquid or base functionalized nanocrystalline ZSM-5 catalyst (Scheme 42) [86].

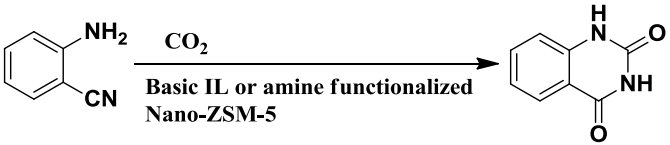

Scheme 42: Route for synthesis of quinazoline-2, 4 (1H, 3H)-Dione using Zeolite.

Δ-Valerolactone, an important precursor for polyamide synthesis is a six

membered cyclic ester [116]. Δ-Valerolactone can be synthesized at ambient temperature from pentanone using zeolite H-ZSM-5 (Si/Al=70) as catalyst (Scheme 43) [116, 84].

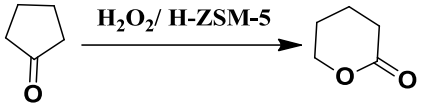

Scheme 43: Route for synthesis of δ-Valerolactone using zeolite.

3.7 Synthesis of seven membered heterocycles

E-caprolactam, an important monomer of Nylon-6 fibers and resin is a seven membered cyclic amide. It can be synthesized through Beckmann rearrangement of cyclohexanone oxime over zeolite catalyst at temperature >350 ^{o}C (Scheme 44) [117].

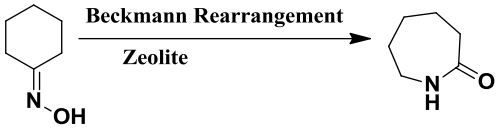

Scheme 44: Route for synthesis of ε-caprolactam using zeolite.

Benzoheterozepines are seven membered heterocycles that contain either nitrogen or sulphur as heteroatom. 2,3-Dihydro 1,5-benzothiazepine shows wide range of pharmacological activities namely CNS depressant, anticancer, Ca^{2+} channel antagonistic, antiplatelet aggregator, anti-HIV, antimicrobial, cardiovascular, and cholinesterase inhibitory activity [118]. Similarly, benzodiazepine also exhibits diverse medicinal activities namely anti-inflammatory, antidepressants, sedatives, anticonvulsant, anti-anxiety and so on [119]. The reaction of *o*-phenylenediamine and acetone using nano-ZSM-5 results in the formation of benzodiazepine [52]. Benzohetreozepine can be synthesized through treatment of (E)-chalcone with substituted aniline in presence of Nano-ZSM-5 catalyst (Scheme 45) [52].

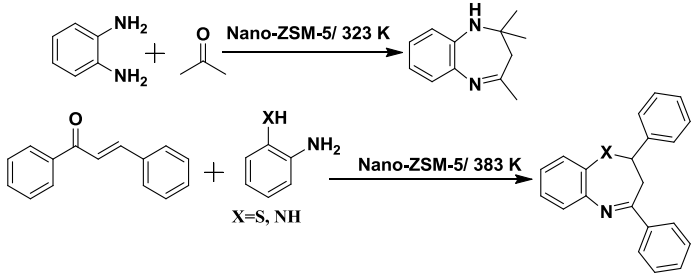

Scheme 45: Route for synthesis of benzodiazepine using zeolite.

Similarly, ε-caprolactone an important precursor for polymer industry is a seven membered cyclic ester [120]. It can be synthesized through oxidation of cyclohexanone using hydrogen peroxide in presence of ZSM-5 as catalyst (Scheme 46) [121].

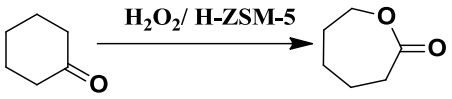

Scheme 46: Route for synthesis of ε-caprolactone using ZSM-5 catalyst.

4. Concluding Remarks and Future Perspectives

Nanoporous zeolites play a dominant role in the selective synthesis of a wide range of three, five, six, and seven membered heterocycles. The excellent activity of nanoporous zeolites are attributed to the facile approach of reactant molecules to the acidic sites situated at the pore-mouth or inside the channel, and the diffusion of reactant/products molecules facilitated by its inter-crystalline mesopores. Furthermore, these catalysts can be easily separated from the reaction mixture, thus make the process sustainable. Moreover, presence of large external surface area, high total pore volume, and large number of surface silanol groups cause nanocrystalline zeolites a promising candidate for multifunctional activities. Therefore, it facilitates the high dispersion of metal nanoparticles, optimum loading of metal oxide, and grafting of ionic liquids on the external surface of Nano-ZSM-5.

Besides, showing catalytic activities, nanoporous or nanocrystalline zeolites also exhibit other thrust applications especially in the area of energy, health care, bio-sensing, and environmental protection. It may be noted that conventional zeolites are not suitable for aforesaid activities. Soft templates mediated routes are one of the advanced methodology to synthesize nanoporous zeolites, however need of soft templates (mesopore directing agent) is not commercially available, and their synthesis is often cumbersome. Therefore, from industrial point of view, it is necessary to develop nanoporous zeolites using commercially viable templates or additives. Therefore, nanocrystalline ZSM-5 would be a better option as it can be synthesized in large scale using cheap, easily available additives n-propyltriethoxysilane.

Finally, this chapter summarizes various benign routes for the synthesis of heterocyles (three, five, six, and seven membered) using nanoporous zeolite as solid acid/base catalyst. In conventional approach, mineral acid/base is required to accomplish this task. Furthermore, the waste generated at the end of process cause serious threat to the environment.

Therefore, nanoporous zeolites is far better candidate to synthesize a wide range of heterocycles of medicinal importance. These eco-friendly routes will definitely encourage the synthetic chemist or chemical forum to pursue their own research in this area as it satisfies the important aspect of green chemistry.

References

1. Egeblad K, Christensen CH, Kustova M, Christensen CH. Templating mesoporous zeolite. Chem. Mater. 2008; 20:946-960.
2. White RJ, Luque R, Budarin VL, Clark JH, Macquarrie DJ. Supported metal nanoparticles on porous materials: Methods and applications. Chem. Soc. Rev. 2009; 38:481-494.
3. http://www.iza-structure.org/databases/; Database of Zeolite Structures.
4. Corma A. From microporous to mesoporous molecular sieve materials and their use in catalysis. Chem. Rev. 1997; 97:2373-2420.
5. Corma A, Domine ME, Nemeth L, Valencia S. Al-free Sn-beta zeolite as a catalyst for the selective reduction of carbonyl compounds (Meerwein-Ponndorf-Verley Reaction). J Am. Chem. Soc. 2002; 124:3194-3195.
6. Cavani F, Teles JH. Sustainability in catalytic oxidation: An alternative approach or a structural evolution. Chem Sus Chem. 2009; 2:508-534.
7. Schoonheydt RA, Geerlings P, Pidko EA, Van Santen RA. The framework basicity of zeolites. J Mater. Chem. 2012; 22:18705-18717.
8. Fricke R, Kosslick H, Lischke G, Richter M. Incorporation of gallium into zeolites: Syntheses, properties and catalytic application. Chem. Rev. 2010; 100:2303-2406.
9. McAteer CH, Murugan R, Rao YVS. Heterogeneously catalyzed synthesis of heterocyclic compounds, Advances in heterocyclic chemistry, Elsevier, 2016, 120.
10. Srivastava R. Synthesis and applications of ordered and disordered mesoporous zeolites: Present and future prospective. Catal. Today. 2018; 309:172-188.
11. Bacolini G. Topic's heterocycle. Syst. Synth. React. Prop. 1996; 1:103.
12. Gilchrist TL. Heterocyclic Chemistry, third ed. Addison Wesley Longman Ltd. London, 1997.
13. Pillai UR, Sahle-Demessie E, Varma RS. Microwave-expedited olefin

epoxidation over hydrotalcites using hydrogen peroxide and acetonitrile. Tetrahedron Lett. 2002; 43:2909-2911.

14. Wang J, Xu L, Zhang K, Peng H, Wu H, Jiang JG *et al*. Multilayer structured MFI-type titanosilicate: Synthesis and catalytic properties in selective epoxidation of bulky molecules. J Catal. 2012; 288:16-23.
15. Sarmah B, Srivastava R, Satpati B. Highly efficient silver nanoparticles supported nanocrystalline zircon silicate catalyst for the epoxidation and hydration reactions Chemistry Select. 2016; 5:1047-1056.
16. Sheikh KD, Banerjee PP, Jagadeesh S, Grindrod SC, Zhang L, Paige M *et al*. Fluorescent epigenetic small molecule induces expression of the tumor suppressor ras-association domain family 1A and inhibits human prostate xenograft. J Med. Chem. 2010; 53:2376-2382.
17. Sreekumar R, Padmakumar R. Simple, efficient and convenient synthesis of pyrroles and pyrazoles using zeolites. Synth. Commun. 1998; 28:1661-1665.
18. Rao YVS, Kulkarni SJ, Subrahmanyam M, Rao AVR. Modified ZSM-5 catalysts for the synthesis of five-and six-membered heterocyclic compounds. J Org. Chem. 1994; 59:3998-4000.
19. Ono Y, Hatada K, Fujita K, Halgeri A, Keii T. Type L zeolites as selective catalysts for the ring transformation of cyclic ethers into cyclic imines J Catal. 1976; 41:322-328.
20. Katritzky AR, Rees CW, Scriven EFV. Comprehensive Heterocyclic Chemistry II. 1996; 2:207-257.
21. Sarmah B, Srivastava R. Octahedral MnO_2 molecular sieve-decorated meso-ZSM-5 catalyst for eco-friendly synthesis of pyrazoles and carbamates. Ind. Eng. Chem. Res. 2017; 56:15017-15029.
22. Kobayashi K, Igura Y, Imachi S, Masui Y, Onaka M. 1, 3-Dipolar cycloaddition of ethyl diazoacetate to alkynes in the pores of zeolite NaY. Chem. Lett. 2007; 36:60-61.
23. Shalini K, Sharma PK, Kumar N. Imidazole and its biological activities: A review. Der Chemica Sinica. 2010; 1:36-47.
24. Teimouri A, Chermahini AN. An efficient and one-pot synthesis of 2, 4, 5-trisubstituted and 1, 2, 4, 5-tetrasubstituted imidazoles catalyzed via solid acid nano-catalyst. J Mol. Catal. A: Chem. 2011; 346:39-45.
25. Balalaie S, Arabanian A. One-pot synthesis of tetrasubstituted

imidazoles catalyzed by zeolite HY and silica gel under microwave irradiation. Green Chem. 2000; 2:274-276.

26. Balalaie S, Arabanian A, Hashtroudi MS. Zeolite HY and silica gel as new and efficient heterogeneous catalysts for the synthesis of triarylimidazoles under microwave irradiation. Monatshefte fuÈr Chemie. 2000; 131:945-948.

27. Greenhill JV, Lue L. Progress in Medicinal Chemistry. Ellis GP, Luscombe DK. (Eds.) Elsevier, New York, NY, 1993, 3.

28. Williams DA, Lemke TLF. Principles of Medicinal Chemistry, fifth ed.; Lippincott Williams & Wilkins: Philadelphia, 2002.

29. Jones RCF, Nichols JR. Thiamine coenzyme models: Imidazolinium ylides and the reactions of 2-(hydroxyalkyl) imidazolines. Tetrahedron Lett. 1990; 31:1771-1774.

30. Morimoto T, Tachibana K, Achiwa K. Chiral thioimidazoline ligands for palladium-catalyzed asymmetric allylation. Synlett, 1997, 783-785.

31. Jones RCF, Turner I, Howard KJ. A new route to homochiral piperidines. Tetrahedron Lett. 1993; 34:6329-6332.

32. Hegedüs A, Hell Z, Potor A. Zeolite-catalyzed environmentally friendly synthesis of benzimidazole derivatives. Synth. Commun. 2006; 36:3625-3630.

33. Ford RE, Knowles P, Lunt E, Marshall SM, Penrose AJ, Ramsden CA *et al*. Synthesis and quantitative structure-activity relationships of antiallergic 2-hydroxy-N-(1H-tetrazol-5-yl) benzamides and N-(2-hydroxyphenyl)-1H-tetrazole-5-carboxamides. J Med. Chem. 1986; 29:538-549.

34. Girijavallabhan VM, Pinto PA, Genguly AK, Versace RW. Eur. Patent EP 274867, Chem. Abstr. 1988, 1989; 110:23890.

35. Taveras AG, Mallams AK, Afonso A. Int. Patent WO 9811093, Chem. Abstr. 1998; 128:230253.

36. Ek F, Wistrand LG, Frejd T. Synthesis of fused tetrazole- and imidazole derivatives via iodocyclization. Tetrahedron. 2003; 59:6759-6769.

37. Jursic BS, Leblanc BW. Preparation of tetrazoles from organic nitriles and sodium azide in micellar media. J Heterocycl. Chem. 1998; 35:405-408.

38. Habibi D, Nasrollahzadeh M, Kamali TA. Green synthesis of the 1-

substituted 1H-1, 2, 3, 4-tetrazoles by application of the Natrolite zeolite as a new and reusable heterogeneous catalyst. Green Chem. 2011; 13:3499-3504.

39. Nasrollahzadeh M, Habibi D, Shahkarami Z, Bayat Y. A general synthetic method for the formation of arylaminotetrazoles using natural natrolite zeolite as a new and reusable heterogeneous catalyst. Tetrahedron. 2009; 65:10715-10719.

40. Droumaguet CL, Wang C, Wang Q. Fluorogenic click reaction. Chem. Soc. Rev. 2010; 39:1233-1239.

41. Shao C, Zhu R, Luo S, Zhang Q, Wang X, Hu Y. Copper(I) oxide and benzoic acid on water: A highly practical and efficient catalytic system for copper(I)-catalyzed azide-alkyne cycloaddition. Tetrahedron Lett. 2011; 52:3782-3785.

42. Sarmah B, Satpati B, Srivastava R. Cu ion-exchanged and Cu nanoparticles decorated mesoporous ZSM-5 catalysts for the activation and utilization of phenylacetylene in a sustainable chemical synthesis. RSC Adv. 2016; 6:87066-87081.

43. Chassaing S, Kumarraja M, Sido ASS, Pale P, Sommer J. Click Chemistry in Cu^{I}-zeolites: The Huisgen [3 + 2]-cycloaddition. Org. Lett. 2007; 9:883-886.

44. Huang ST, Hsei IJ, Chen C. Synthesis and anticancer evaluation of bis (benzimidazoles), bis (benzoxazoles), and benzothiazoles. Bioorg. Med. Chem. Lett. 2006; 14:6106-6119.

45. Figge A, Altenbach HJ, Brauer DJ, Tielmann P. Synthesis and resolution of 2-(2-diphenylphosphinyl-naphthalen-1-yl)-1-isopropyl-1*H*-benzoimidazole: A new atropisomeric P, N-chelating ligand for asymmetric catalysis. Tetrahedron: Asymmetry. 2002; 13:137-144.

46. Costa SPG, Batista RMF, Cardoso P, Belsley M, Raposo MMM. 2-Arylthienyl-substituted 1, 3-benzothiazoles as new nonlinear optical chromophores. Eur. J Org. Chem, 2006, 3938-3946.

47. Day JC, Tisi LC, Bailey MJ. Evolution of beetle bioluminescence: The origin of beetle luciferin. Luminescence. 2004; 19:8-20.

48. Thomas B, George J, Sugunan S. Synthesis of benzoxazole via the beckmann rearrangement of salicylaldoxime on protonated zeolites: A green continuous process. Ind. Eng. Chem. Res. 2009; 48:660-670.

49. Teimouri A, Chermahini AN, Salavati H, Ghorbanian L. An efficient

and one-pot synthesis of benzimidazoles, benzoxazoles, benzothiazoles and quinoxalines catalyzed via nano-solid acid catalysts. J Mol. Catal. A: Chem. 2013; 373:38-45.

50. Durgashanker R, Audhesh K, Singh Y. Synthesis and characterisation of some new organoarsenic (V) schiff bases derivatives derived from bifunctional tridentate benzothiazolines. Main Group Metal Chem. 2006; 29:65-72.

51. Agrawal M, Trandon JP, Mehrotra RC. Synthesis of some new gallium and indium complexes with some sulphur containing ligands. J Inorg. Nucl. Chem. 1981; 43:1070-1073.

52. Sarmah B, Srivastava R. Sustainable catalytic process with a high eco-scale score for the synthesis of five-, six-, and seven-membered heterocyclic compounds using nanocrystalline zeolites. Asian J Org. Chem. 2017; 6:873-889.

53. Vanelle P, Meuche J, Maldonado J, Crozet MP, Delmas F, Timon-David P. Functional derivatives of 5-benzo[1, 3]dioxol-5-yl-1-methyl-*1H*-imidazole-2-carbaldehyde and evaluation of leishmanicidal activity. Eur. J Med. Chem. 2000; 35:157-162.

54. Giugni A, Impalà D, Piccolo O, Vaccari A, Corma A. An eco-friendly synthesis of 1, 2-methylenedioxybenzene in vapour phase. Appl. Catal., B. 2010; 98:72-78.

55. March J. Advanced Organic Chemistry. Fourth edition. Wiley-Interscience, New York, 1992, 11-41.

56. Douglas AW. In situ studies of chemical reactions by carbon-13 Fourier transform nuclear magnetic resonance. Application to the Fischer Indole synthesis. J Am. Chem. Soc. 1978; 100:6463-6469.

57. Hong KB, Lee CW, Yum EK. Synthesis of 2-substituted indoles by palladium-catalyzed heteroannulation with Pd-NaY zeolite catalysts. Tetrahedron Lett. 2004; 45:693-697.

58. Rasmussen PG. Imidazole and benzimidazole synthesis. J Chem. Educ. 1999; 76:13-45.

59. Cheng JB, Cooper K, Duplantier AJF, Karaus KG, Marshall SC, Marfat A *et al*. Synthesis and *in vitro* profile of a novel series of catechol benzimidazoles. The discovery of potent, selective phosphodiesterase type IV inhibitors with greatly attenuated affinity for the [^{3}H] rolipram binding site. Bioorg. Med. Chem. Lett. 1995; 5:1969-1972.

60. Ellingboe JW, Spinelli W, Winkley MW. Class III antiarrhythmic activity of novel substituted 4-[(methylsulfonyl) amino] benzamides and sulfonamides. J Med. Chem. 1992; 35:705-716.

61. Joule JA, Mills K, Smith GF. Heterocyclic Chemistry. Chapman & Hall, London, 1995.

62. Pozherskii AF, Soldatenkov AT, Katritzky AR. Heterocycles in Life and Society. Wiley, New York, 1997.

63. Hegedüs A, Hell Z, Potor A. Zeolite-catalyzed environmentally friendly synthesis of benzimidazole derivatives. Synth. Commun. 2006; 36:3625-3630.

64. Heravi MM, Tajbakhsh M, Ahmadi AN, Mohajerani B. Zeolites efficient and eco-friendly catalysts for the synthesis of benzimidazoles. Monatshefte für Chemie. 2006; 137:175-179.

65. Saberi A, Rangappa KS. Zeolite HY catalyst for the synthesis of benzimidazole and its 2-alkyl, aryl and heteroaryl derivatives under microwave irradiation and solvent-free condition. Synthesis and Reactivity in Inorganic, Metal-Organic, and Nano-Metal Chemistry. 2009; 39:425-427.

66. Michael JP. Indolizidine and quinolizidine alkaloids. Nat. Prod. Rep. 2008; 25:139-165.

67. Bermudez J, Fake CS, Joiner GF, Joiner KA, King FD, Miner WD *et al*. 5-Hydroxytryptamine (5-HT3) receptor antagonists. Indazole and indolizine-3-carboxylic acid derivatives. J Med. Chem. 1990; 33:1924-1929.

68. Weide T, Arve L, Prinz H, Waldmann H, Kessler H. 3-Substituted indolizine-1-carbonitrile derivatives as phosphatase inhibitors. Bioorg. Med. Chem. Lett. 2006; 16:59-63.

69. Sonnet P, Dallemagne P, Guillon J, Enguehard C, Stiebing S, Tanguy J, Bureau R, Rault S, Auvray P, Moslemi S, Sourdaine P, Seralini GE. New aromatase inhibitors. Synthesis and biological activity of aryl-substituted pyrrolizine and indolizine derivatives. Bioorg. Med. Chem. 2000; 8:945-955.

70. Teklu S, Gundersen LL, Larsen T, Malterud KE, Rise F. Indolizine 1-sulfonates as potent inhibitors of 15-lipoxygenase from soybeans. Bioorg. Med. Chem. 2005; 13:3127-3139.

71. Shen YM, Lv PC, Chen W, Liu PG, Zhang MZ, Zhu HL. Synthesis and

antiproliferative activity of indolizine derivatives incorporating a cyclopropylcarbonyl group against Hep-G2 cancer cell line. Eur. J Med. Chem. 2010; 45:3184-3190.

72. Marco E, Laine W, Tardy C, Lansiaux A, Iwao M, Ishibashi F *et al*. Molecular determinants of topoisomerase I poisoning by lamellarins: Comparison with camptothecin and structure-activity relationships. J Med. Chem. 2005; 48:3796-3807.

73. Sarmah B, Satpati B, Srivastava R. Cu ion-exchanged and Cu nanoparticles decorated mesoporous ZSM-5 catalysts for the activation and utilization of phenylacetylene in a sustainable chemical synthesis. RSC Adv. 2016; 6:87066-87081.

74. Bonsignore L, Loy G, Secci D, Calignano A. Synthesis and pharmacological activity of 2-oxo-(2H) 1-benzopyran-3-carboxamide derivatives. Eur. J Med. Chem. 1993; 28:517-520.

75. Al-Haiza MA, Mostafa MS, El-Kady MY. Synthesis and biological evaluation of some new coumarin derivatives. Molecules. 2003; 8:275-286.

76. Tabatabaeian K, Zanjanchi MA, Mamaghani M, Dadashi A. Anchoring of ruthenium onto imine-functionalized zeolite beta: an efficient route for the synthesis of 4*H*-benzo[*b*]pyrans and pyrano[*c*]chromenes. Can. J Chem. 2014; 92:1086-1091.

77. Beretz A, Anton R, Stoclet JC. Flavonoid compounds are potent inhibitors of cyclic AMP phosphodiesterase. Beretz A, Anton R, Stoclet JC. Experimentia. 1977; 34:1054-1055.

78. Weinmann I. in Coumarins: Biology, Applications and Mode of Action Kennedy R. O, Thornes RD. (Eds): Wiley, Chichester, UK, 1997, 1-22.

79. Hesse M, Holderichm W, Gallei E. Preparation of cyclic amidines on zeolites. Chem. Ing. Tech. 1991; 63:1001-1003.

80. Swellmeen L. 1, 3-Oxazole derivatives: A Review of biological activities as antipathogenic. Der Pharma Chemica. 2016; 8:269-286.

81. Venkatesha NJ, Bhat YS, Prakash BSJ. Manifestation of zeolitic pore characteristics of modified montmorillonite in oxazole synthesis by propargylation and cycloisomerization reactions. Appl. Catal., A. 2015; 496:3148-3151.

82. Ballini R, Bigi F, Gogni E, Maggi R, Sartori G. Zeolite as base catalyst: Nitroaldolic condensation. J Catal. 2000; 191:348-353.

83. Germain P, Gronemeyer H, De Ler AR. A Synthesis of the PPARβ/δ-selective agonist GW501516 and C4-thiazole-substituted analogs. Bioorg. Med. Chem. Lett. 2006; 16:49-54.

84. Dam CB, Davis ME. Applications of zeolites to fine chemicals synthesis. Catal. Today. 1994; 19:151-186.

85. Palekar VS, Damle AJ, Shukla SR. Synthesis and antibacterial activity of some novel bis-1,2,4-triazolo[3,4-*b*]-1,3,4-thiadiazoles and bis-4-thiazolidinone derivatives from terephthalic dihydrazide. Eur. J Med. Chem. 2009; 44:5112-5116.

86. Sarmah B, Srivastava R. Activation and utilization of CO_2 using ionic liquid or amine-functionalized basic nanocrystalline zeolites for the synthesis of cyclic carbonates and quinazoline-2,4(1H,3H)-dione. Ind. Eng. Chem. Res. 2017; 56:8202-8215.

87. Srivastava R, Srinivas D, Ratnasamy P. Synthesis of cyclic carbonates from olefins and CO_2 over zeolite-based catalysts. Catal. Lett. 2003; 89:81-85.

88. Weissermel K, Arpe HJ. Industrial Organic Chemistry, third edition. Wiley-VCH: Weinheim, Germany, 1997.

89. Venuto PB, Landis PS. Organic catalysis over crystalline aluminosilicates. Organic catalysis over crystalline aluminosilicates Adv. Catal. 1968; 18:259-371.

90. Ono Y, Mori T, Hatada K. Ring transformation of tetrahydrofuran into tetrahydrothiphene over alkali metal cation exchanged zeolites. Acta Phys. Chem. 1978; 24:233-237.

91. Dartt CA, Davis ME. Applications of zeolites to fine chemicals synthesis. Catal. Today. 1994; 19:151-186.

92. Nethravathi BP, Reddy KRK, Mahendra KN. Synthesis of 2,2-dimethyl-4-phenyl-[1, 3]-dioxolane using zeolite encapsulated Co(II), Cu(II) and Zn(II) complexes. Bull. Chem. Soc. Ethiop. 2010; 24:295-298.

93. Venkatesha YS, Bhat BSJP. Dealuminated BEA zeolite for selective synthesis of five-membered cyclic acetal from glycerol under ambient conditions. RSC Adv. 2016; 6:18824-18833.

94. Zatorski LW, Wierzchowski PT. Zeolite-catalyzed synthesis of 4-phenyl-1, 3-dioxolanes from styrene oxide. Catal. Lett. 1991; 10:211-214.

95. Roman-Leshkov Y, Barrett CJ, Liu ZY, Dumesic JA. Production of dimethylfuran for liquid fuels from biomass-derived carbohydrates. Nature. 2007; 447:982-985.

96. Sarmah B, Satpati B, Srivastava R. One-pot tandem conversion of monosaccharides and disaccharides to 2, 5-diformylfuran using a Ru nanoparticle-supported H-beta catalyst. Catal. Sci. Technol. 2018; 8:2870-2882.

97. Nikolla E, Roman-Leshkov Y, Moliner M, Davis ME. One-pot synthesis of 5-(hydroxymethyl) furfural from carbohydrates using tin-beta zeolite. ACS Catal. 2011; 1:408-410.

98. Hatada K, Shimada M, Ono Y, Keii T. Ring transformation of γ-butyrolactone into 2-pyrrolidinone over synthetic zeolites. J Catal. 1975; 37:166-173.

99. Ono Y. Heterocycles: A review. 1981; 16:1755-1771.

100. Clark B, Capon RJ, Lacey E, Tennant S, Gill JH, Bulheller B *et al.*: Aromatic butenolides from an Australian Isolate of the soil ascomycete gymnoascus reessii. J Nat. Prod. 2005; 68:1226-1230.

101. Seitz M, Reiser O. Synthetic approaches towards structurally diverse γ-butyrolactone natural-product-like compounds. Curr. Opin. Chem. Biol. 2005; 9:285-292.

102. Jusseau X, Chabaud L, Guillou C. Synthesis of γ-butenolides and α, β-unsaturated γ-butyrolactams by addition of vinylogous nucleophiles to Michael acceptors. Tetrahedron. 2014; 70:2595-2615.

103. Levy LM, Cabrera GM, Wright JE, Seldes AM. 5H-furan-2-ones from fungal cultures of aporpium caryae. Phytochemistry. 2003; 62:239-243.

104. Pour M, Spulak M, Balsanek V, Kunes J, Kubanova P, Butcha V. Synthesis and structure–antifungal activity relationships of 3-aryl-5-alkyl-2, 5-dihydrofuran-2-ones and their carbanalogues: Further refinement of tentative pharmacophore group. Bioorg. Med. Chem. 2003; 11:2843-2866.

105. Padakanti S, Pal M, Yeleswarapu KR. An improved and practical synthesis of 5, 5-dimethyl-3-(2-propoxy)-4-(4-methanesulfonylphenyl)-2-(5H)-furanone (DFP-a selective inhibitor of cyclooxygenase-2). Tetrahedron. 2003; 59:7915-7920.

106. Choudhury A, Jin F, Wang D, Wang Z, Xu G, Nguyen D *et al.* A concise synthesis of anti-viral agent F-ddA, starting from (S)-dihydro-5-

(hydroxymethyl)-2 (3H)-furanone. Tetrahedron Lett. 2003; 44:247-250.

107. Bahramian F, Fazlinia A, Mansoor SS, Ghashang M, Azimi F, Biregan MN. Preparation of 3, 4, 5-substituted furan-2 (5*H*)-ones using HY zeolite nano-powder as an efficient catalyst. Res. Chem. Intermed. 2016; 42:6501-6510.

108. Golunski SE, Jackson D. Heterogeneous conversion of acyclic compounds to pyridine bases- A review. Appl. Catal. 1986; 23:1-14.

109. Subrahmanyam M, Muralidhar G, Kulkarni SJ, Viswanathan V, Srinivas B, Yadav JS *et al*. Ind. Patent, 281/DEL/92, 1992.

110. Srinivas N, Gopal DV, Srinivas B, Kulkarni SJ, Subrahmanyam M. Intermolecular cyclization of ethanolamine to 1,4-diazabicyclo (2.2.2) octane over modified pentasil zeolites. Microporous Mesoporous Mater. 2002; 51:43-50.

111. Rovnyak GC, Kimall SD, Beyer B, Cucinotta G, DiMarco JD, Gougoutas J *et al*. Calcium entry blockers and activators: Conformational and structural determinants of dihydropyrimidine calcium channel modulators. J Med. Chem. 1995; 38:119-129.

112. Kharb R, Kaur H. Therapeutic significance of quinoline derivatives as antimicrobial agents. Int. Res. J Pharm. 2013; 4:63-69.

113. Ishitani H, Kobayashi S. Catalytic asymmetric aza Diels-Alder reactions using a chiral lanthanide Lewis acid. Enantioselective synthesis of tetrahydroquinoline derivatives using a catalytic amount of a chiral source. Tetrahedron Lett. 1996; 37:7357-7360.

114. Watson CY, Whish WJD, Threadgill MD. Synthesis of 3-substituted benzamides and 5-substituted isoquinolin-1 (2H)-ones and preliminary evaluation as inhibitors of poly (ADP-ribose) polymerase (PARP). Bioorg. Med. Chem. 1998; 6:721-734.

115. Seitz LE, Suling WJ, Reynolds RC. Synthesis and antimycobacterial activity of pyrazine and quinoxaline derivatives. J Med. Chem. 2002; 45:5604-5606.

116. Bhattacharyya SK, Nandi DK. High pressure synthesis of delta-valerolactone and adipic acid. Ind. Eng. Chem. 1959; 51:143-146.

117. Zhang Y, Wang Y, Bu Y. Vapor phase Beckmann rearrangement of cyclohexanone oxime on Hβ-zeolites treated by ammonia. Microporous Mesoporous Mater. 2008; 107:247-251.

118. Ambrogi V, Furlani A, Grandolini G, Papaioannou A, Perioli L, Scarcia V *et al*. Synthesis, antimicrobial and cytostatic activities of some derivatives of indolo [2, 3-*b*]-1,5-benzothiazepine, a novel heterocyclic ring system. Eur. J Med. Chem. 1993; 28:659-667.

119. Chakraborty S, Shah NH, Fishbein JC, Hosmane RS. A novel transition state analog inhibitor of guanase based on azepinomycin ring structure: Synthesis and biochemical assessment of enzyme inhibition. Bioorg. Med. Chem. Lett. 2011; 21:756-759.

120. Weissermel K, Arpe HJ. Industrial Organic Chemistry, fourth edition. Wiley-VCH, Weinheim, 2003.

121. Chang CD, Hellring D, Production of lactones and omega-hydroxycarobxylic acids, U.S. Patent 4. 1989; 870:192.

Chapter - 7
Doping Mechanism and Charge Transfer in Polyaniline

Authors

Ferooze Ahmad Rafiqi
Department of Chemistry, National Institute of Technology Srinagar, Hazratbal, Srinagar, Jammu and Kashmir, India

Syed Kazim Moosvi
School Education Department Jammu & Kashmir Government, Jammu and Kashmir, India

Waseem Naqash
Department of Chemistry, National Institute of Technology Srinagar, Hazratbal, Srinagar, Jammu and Kashmir, India

Chapter - 7

Doping Mechanism and Charge Transfer in Polyaniline

Ferooze Ahmad Rafiqi, Syed Kazim Moosvi and Waseem Naqash

Abstract

Conducting polymers have received considerable attention among scientific community as versatile materials for various applications ranging from polymer based electronics to biomedical engineering. The discovery of conducting polymers and the ability to dope these polymers over the full range from insulator to metal is particularly exciting because it created a new field of research on the boundary between Chemistry and Condensed-matter physics. Among various conductive polymers, Polyaniline (PANI) is the most promising conductive polymers owing to its good conductivity, electrochemical reversibility, high polarizability, ease of preparation, and possible tailoring to the specific needs of the material applications. It can become highly conductive simply by proton doping. Chemical method, charge injection doping, photodoping and by metal insulator sandwich (MIS) type of doping are commonly methods of doping in conducting polymers. However, redox chemical doping is the most common method of doping in polyaniline. Polarons, bipolarons and solitons are the main charge carriers in polyaniline.

Keywords: Polyaniline, conductivity, doping, oxidative polymerization

Introduction of Conducting Polymers (Polyaniline)

Conventional polymers like plastics have saturated electronic structures and are therefore insulators. In 1960, an astonishing outcome was surfaced when an inorganic polymer polysulfur nitride (SN) x was found to have metallic character [1]. Its room temperature conductivity was found 10^3 $(\Omega\ cm)^{-1}$, which is too proximate to that observed for copper $(6\times 10^5(\Omega\ cm)^{-1})$ and too high to that of polyethylene $(10^{-14}\ (\Omega\ cm)^{-1})$. Polysulfur nitride behaves as a superconductor at below a critical temperature of 0.3 K. Conductivity in $(SN)_x$ is believed to be due to the presence of one unpaired electron from each S-N unit and virtually no forbidden gap between HOMO and LUMO levels of $(SN)_x$. However, this polymer was soon discarded from

commercial use due to its explosive nature. The conductivity of $(SN)_x$ was reported to increase by an order of magnitude upon exposure to Br_2 and similar oxidizing agents. These advancements were of fastidious significances since they demonstrated the presence of profoundly conducting polymers and empowered the enormous measure of work required to produce other polymeric conductors.

Their search in conducting polymers began nearly a quarter of a century ago, when an intrinsically insulating organic polymer polyacetylene was found capable of conducting electricity after doping with bromine and iodine vapours [2]. This revelation got significance to the extent that the Noble prize for chemistry was awarded to H. Shirakawa, A. G. Mac Diarmid and A. J. Heeger for their work on conducting polymers [3-5]. This revelation diverted the attention of researchers towards other organic polymers owing to their π - conjugated electronic structures and low forbidden energy gap between HOMO and LUMO. Since then a number of organic polymers like polyaniline, polythiophene, polypyrrole etc. have been synthesized prosperously utilizing this fundamental principle of redox mechanism.

Amongst the family of conducting polymers, polyaniline (PANI) has attracted the interest of researchers owing to its ease of availability, environmental stability and doping chemistry. PANI was first elucidated in the mid-nineteenth century by Henry Letheby who contemplated the electrochemical and chemical oxidation products of aniline in acidic media [6]. Improvement of various properties in PANI can be accomplished by forming composites or by doping [7, 8]. Polyaniline has low photophysical properties, less significant electrical conductivity, low ability of processability and poor thermal stability [9]. From literature survey it is evident that PANI has been doped with CNTs, metallic oxides, metallic salts, metals, zeolites, inorganic moieties, as a result properties of these polymers have ameliorated.

Aniline is a six membered ring system with functional group $-NH_2$ attached to one of the carbon atom and has aromatic character. Oxidation of aniline is the most commonly used synthetic route to polyaniline. The reaction is usually carried out in acidic medium with oxidising agent ammonium persulfate. Polyaniline can occur in a number of well-defined oxidation states. The different states range from the fully reduced leucoemeraldine via protoemeraldine, emeraldine and nigraniline to the fully oxidized pernigraniline. In the moderately oxidized states, polyaniline turns from insulating emeraldine base to conducting emeraldine salt. In the proton acidic doping, neither electrons are removed nor added in the polyaniline

backbone. However charge carriers are generated by this method. The conduction mechanism is believed to involve polarons. In the case of protonated emeraldine a delocalized poly (semiquinone radical cation) is the polaronic character.

Synthesis of Polyaniline

There are two major approaches to the synthesis of polyaniline and its composites. One is the chemical oxidative polymerisation method and the other is the electrochemical method. Both the methods have merits and demerits associated with them. However, chemical method is usually preferred over electrochemical method owing to cost efficacy and bulk quantity of polymer that can be prepared through this method [10].

Synthesis of Polyaniline (PANI) in Non-Aqueous Medium

Polyaniline in its conducting and most common, emeraldine salt state in non-aqueous medium is synthesised by chemical oxidative polymerisation method [11, 12]. This involves the use of aniline monomer in aqueous acidic medium using ammonium persulphate as the oxidant. However, non-aqueous DMSO is also used as the medium for polymerisation. In a typical procedure, 1 ml aniline is added to 10 ml of 2-5N solution of HCl in DMSO and is then cooled at 10 °C to give solution 'A'. A solution of 1.2 g of ammonium persulphate dissolved in 10 ml of DMSO (solution B) is then added gradually to the previous cooled solution 'A' for a period of 15-20 min with continuous stirring. The polymerisation reaction is then allowed to proceed at 10 °C temperature for 12-24 h with occasional stirring. The polymer is formed as a stable, thick dark green dispersion which is collected as a precipitate by filtration under pressure or through centrifugation method. It is washed 2-3 times with a mixture of acetone and HCl till a colourless filtrate is obtained and is then dried in an oven at a temperature of 30-50 °C. The overall reaction involved in the synthesis of emeraldine salt form of PANI (polyaniline hydrochloride) is depicted in Figure 1.

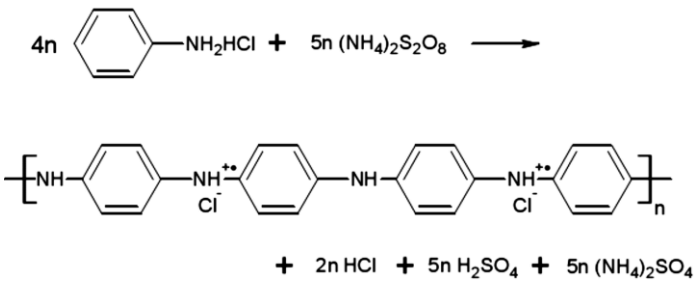

Fig 1: Reaction involved in the synthesis of emeraldine salt from PANI

Synthesis of Polyaniline in Aqueous Medium

Polyaniline in aqueous medium is synthesised by oxidative chemical polymerization method [13]. This involves the use of ammonium persulphate $(NH_4)_2S_2O_8$ as an oxidising agent and aniline as monomer. Distilled aniline (10 mL) and concentrated HCl (10 mL) is first cooled in a refrigerator for 10 minutes. After cooling, it is dissolved in 150 mL of distilled water. 4.5 g of $(NH_4)_2S_2O_8$ dissolved in 30 mL of water is added drop wise to this aniline-HCl solution with constant stirring. The stirred solutions after 2 h are allowed to stand for 1hour more. The greenish black precipitate obtained from this solution is filtered and washed repeatedly with distilled water. Then the precipitate is dried in an oven at 40 ^oC.

Electrochemical Synthesis

Electrochemical synthesis of polyaniline involves oxidation of the aniline in electrolyte solutions by applied electric potential. This involves the formation of electroactive films of polyaniline on electrodes. This method involves polymerization by potentiodynamic cyclic voltammetry, oxidations at constant potential or current, galvanostatic and potentiostatic methods. Polymerization of aniline via cyclic voltammetry is carried out by using a two electrode or three electrode systems [14]. Indium tin oxide, noble metals such as gold, silver or platinum, glassy carbon, etc. acts as a working electrode and saturated calomel electrode or silver chloride electrode as reference electrode. This is set up for two electrode system. However in three electrode system, besides the electrodes present in two electrode system, a counter electrode from electrochemically inert materials such as gold, platinum, or carbon is coupled with the working electrode. Inorganic acids like sulphuric acid, perchloric acid, nitric acid dissolved in water or solutions of organic acids like p-toluenesulfonic acid is used as a medium in the electropolymerization of aniline [15-18]. Electrictro Chemical synthesis can additionally be achieved in aqueous solutions of polymeric acids, such as poly (styrenesulfonic acid) or poly (2-acrylamido-2-methyl-1-propanesulfonic acid) [19]. Like chemical oxidation, adequate acidity is an essential requisite for the synthesis of polyaniline during electrochemical synthesis. Organic solvents like acetonitrile or dichloromethane have likewise been utilized for carrying out the electrochemical synthesis of PANI [20]. The reaction progress and result depends on sundry factors like concentration of aniline, current density, nature of solvent used etc. During electrochemical polymerization counter ions from the solution are additionally incorporated in the polyaniline matrix.

Electrochemical method is limited for the preparation of polyaniline films on electrode arrays but may be of choice for desired applications.

Theory of Conductivity in Conducting Polymers

The electrical conductivity of conducting polymers is not well expounded on the basis of simple band theory which is utilized to explicate the conduction mechanism of conventional inorganic semiconductors. It should be noted that the mechanism of charge transport process in polymers is quite complex. Band transport and hopping are the main mechanisms of charge transport in conjugated polymers [21]. As per band theory [22], each atom provides atomic orbital for overlapping with the same atomic orbitals of their neighbourhood atoms in all orientations generating molecular orbitals kindred to those in small molecules. After overlapping of atomic orbitals, energy bands are formed, with each band associated with a definite amount of energy range. The highest occupied electronic levels constitute the valence band (VB) and the lowest unoccupied levels constitute conduction band (CB). When the bands are completely filled or unfilled, no conduction happens. If the band gap is narrow at room temperature, as in case of semiconductors, thermal excitation of electrons from the valence band to the conduction band offers ascend to conductivity. When the band gap is too wide, thermal excitation at room temperature is inadequate to exhilarate electrons across the gap and the solid is an insulator. The high conductivity of metals is due to the overlapped valence and conduction bands with zero band gap energy. Conductive polymers are peculiar in that they conduct current without having a partially empty or partially filled band. The conduction mechanism and the nature of charge carriers in conducting polymers is explicated on the basis of conjugational or topological defects which are engendered as a consequence of doping. These include polarons, bipolarons and solitons which are formed in conducting polymers due to its partial oxidation or partial reduction with congruous dopants. Initially it was thought that upon doping, the oxidant takes away electrons from the filled valance band and reductant adds electrons into the vacant conduction band. However, this model was not satisfactory to expound the conduction mechanism in polyacetylene and other conducting polymers, because from experiments, it was found that the conduction is due to the charge carriers that do not have free spins [23]. To expound the conduction mechanism in conducting polymers, a new model called soliton model was presented [24]. In this model, charged solitons are supposed to be the conducting species for charge. Charged solitons are a kind of charge defects introduced in a polymer chain on doping with electron acceptors or

electron donors. This model was initially appealing because charged solitons have no spin and the conducting polymers are found to possess spineless transport. The conducting mechanism of polyacetylene acceded with soliton theory because polyacetylene has a degenerate ground state (i.e., two geometric structures corresponding to the same energy) as depicted in Fig. 2. But all other conducting polymers have non-degenerate ground state. The failure of soliton hypothesis prompted another hypothesis called polaron-bipolaron hypothesis. According to this concept the polymer chain is ionised on doping and this ionisation process engenders a polaron (radical ion) on the chain [25]. It stabilizes itself by polarizing the medium around it. The energy level associated with this radical ion represents a destabilized bonding orbital and in this way has a higher energy than the energies in the valence band. At low doping level these polarons are the transporters of electricity. On increasing the doping level the concentration of polaron increases and this result in a probability of interaction with each other, that can be either attractive or repulsive. As a result of attraction, two polaron may get coupled to compose a bipolaron. Bipolarons are doubly charged but spineless species. A bipolaron is thermodynamically more stable than two polarons. Both polarons and bipolarons cause structural deformations in the polymer chains as they move along the polymer chain by the rearrangement of double and single bonds in the conjugated system in an electric field. The polaron form and bipolaron forms of PANI are depicted in Fig.3. In the case of polyacetylene, it is thought that due to the degenerate ground state, the bipolarons initially formed disintegrate into polarons which further decay into spineless charged solitons. Charge transfer in molecularly doped polymers is accepted to be carried out by a hopping mechanism [26]. The mechanism of hopping has been explicated by using two centres model where the carriers hop between the two centres [27]. Diverse factors such as temperature (T), partition between shopping centres (R), distribution of hopping energy and electric field (f) increases the hopping probability and consequently govern this type of charge convey.

Fig 2: degenerate ground state of trans-polyacetylene

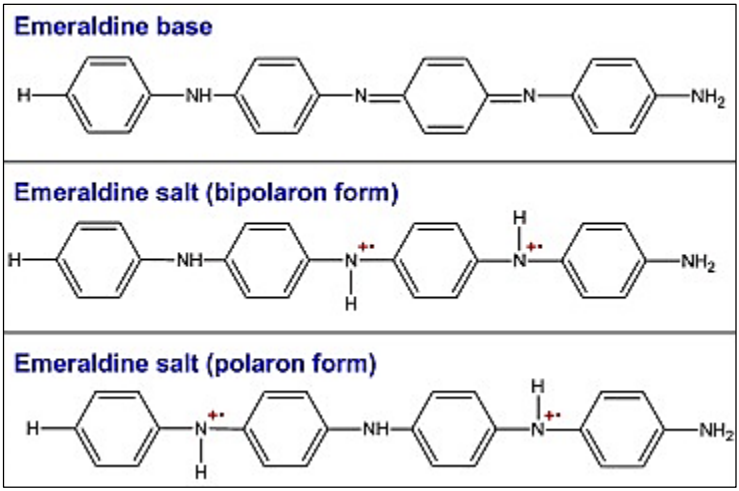

Fig 3: Polaron and bipolaron formation in polyaniline

Doping in Conducting Polymers

The term "doping" as applied to inorganic semiconductors does not rigorously apply to the organic semiconductor field because the processes are fundamentally different. Nevertheless, the term is commonly applied to polyacetylene and other conducting polymers. Conjugated organic polymers are either electrical insulators or semiconductors. These polymers can become highly electrically conductive after carrying out a structural modification; a process called as “doping”. Doping is simply considered as addition or removal of electrons to or from the π system of the polymer backbone chain. In comparison to conventional polymers, the conducting polymers have conjugated π-electrons in the backbone. These conducting polymers can facilely be oxidized or reduced owing to their low ionization potential and high electron affinity. Doping results in a dramatic transmutation in the electrical, electronic, magnetic, optical and structural properties of polymers. Doping of conjugated polymers leads to the formation of conjugational defects viz solitons, polarons or bipolarons in the polymer backbone. These conjugational defects are responsible for high electrical conductivity of conducting polymers. Doping method is the most conspicuous factor which effects conductivity of conjugated polymers. The degree of improvement in electric conductivity of a polymer mainly depends on the chemical reactivity of the dopant with the polymer. The rearrangements of the polymer chains occur upon doping; consequently new ordered structures are formed. Moreover, incorporation of the dopant molecules in the quasi one-dimensional polymer systems considerably

perturbs the chain order leading to the reorganization of the polymer chains [28]. Thus the ultimate conductivity in conducting polymers depends on various factors like nature and concentration of dopants, homogeneity of doping, carrier mobility, crystallinity, morphology and purity of polymers. The most commonly used doping methods [29] are described as:

1) **Chemical Doping:** Conducting polymers like Polypyrrole, Polythiophene, Polyaniline, etc. undergo redox doping. Redox doping leads to change in the number of electrons, associated with the polymer backbone. It is essentially of two types:

a) **P-Doping:** It is an oxidation process in which partial oxidation of the polymer backbone occurs with felicitous electron acceptor species (oxidizing agent).For example, when trans-polyacetylene is exposed to oxidizing agents like iodine, it brings out the doping reaction and a consequential increase in conductivity of about 10^{-5} to 10^{2} S/cm is witnessed.

$$\text{Polymer} + X \longrightarrow (\text{Polymer})^{n+} + X^{n-} \quad X = I_2, Br_2, ASF_5, \ldots$$

b) **N-Doping:** It is a reduction process in which the reduction of the polymer backbone chain occurs with congruous electron donating species (reducing agent). For example, the treatment of trans-polyacetylene with reducing agent such as sodium naphthalide leads to increase in its conductivity.

$$\text{Polymer} + M \longrightarrow (\text{Polymer})^{n-} + M^{n+} \quad M = Na, Li, \ldots$$

2) **Electrochemical Doping:** Conjugated polymers have extensiveπ-conjugation of electrons in the polymer chains and hence can easily be oxidized (p-doping) or reduced (n-doping) through electrochemical doping method. These conjugated polymer act as either an electron source or an electron sink during the process. The doping reaction can be achieved by applying a dc power source between a trans-polyacetylene coated positive electrode and a negative electrode. Both of them are immersed in a solution of $LiClO_4$ in propylene carbonate [30].

$$\text{Trans-}(CH)_x + xy\,(ClO_4)^- \rightarrow [(CH)^+_y\,(ClO_4)^-_y]\,x + xy\,e^-$$

Electrochemical doping has various advantages over chemical doping. For instance, doping level can be attained the polymer matrix simply by passing a definite quantity of electricity through it. Doping- doping processes in the polymeric network are achieved without any chemical product

elimination as both processes are reversible in nature. However, counter dopant ions stabilize the polymer chains in both the methods. The introduction of counter ions along the polymer backbone can be both an obstruction and an advantage. Although the counter ions may cause an undesirable structural distortion and a deteriorated effect on conductivity, they facilitate conjugated conducting polymers for actuation applications. In order to eradicate the introduction of counter ions in both chemical and electrochemical doping, other doping methods viz, "photo-doping" and "charge-injection doping" have been exploited.

3) **Photo-Doping:** Light of energy greater than the band gap present in conjugated polymers (e.g. trans-polyacetylene) excites electrons from the valence band into the conduction band [30]. Albeit the photo engendered charge carriers disappear after the removal of photo irradiated source still separation of electrons from holes leads the photoconductivity in the polymer by the application of a felicitous potential during irradiation.

4) **Charge Injection Doping:** A metal/insulator/semiconductor (MIS) configuration is used to carry out the doping process. In this configuration, a metal and a conducting polymer is separated by a thin layer of a high dielectric strength insulator. A surface charge layer appears on the multilayer structure when an appropriate potential is applied across it and accordingly charge carriers are injected into the band gap of conjugated polymers like polyacetylene, poly (3-hexylthiophene), etc. All the doping methods discussed above fall in the category of redox doping which involves alteration in the number of electrons associated with the polymer backbone chain. However, non-redox doping does not cause any change in the number of electrons associated with the polymer backbone, but simply a rearrangement of the energy levels. For example, polyaniline can be doped through a non-redox process where the number of electrons in the polymer back bone structure remains unchanged, making the doping process simpler [3]. Different doping methods are schematized in Fig. 4.

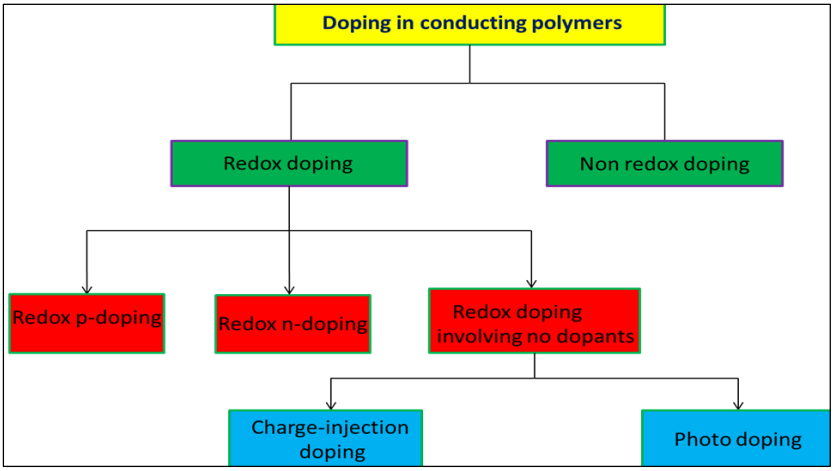

Fig 4: Different doping methods

1.5. Types of Doping Agents

Dopants may be classified as shown in Fig. 5

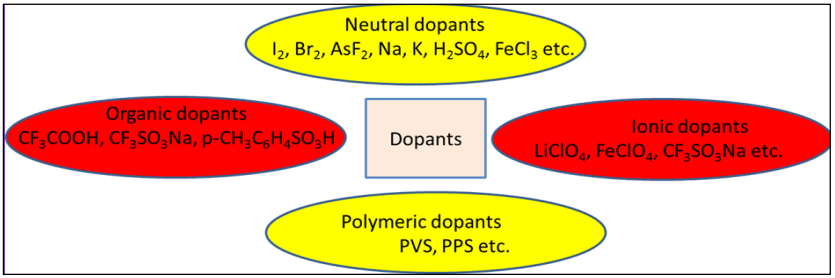

Fig 5: Classification of dopants.

During the process of doping, negative or positive ions are generated from neutral dopants with or without chemical modifications. Oxidation or reduction of ionic dopants occurs via the electron transfer mechanism between the polymer and dopant component. The charge on the polymer backbone is stabilized by the counter ions that remain attached with it. Anionic dopants are mostly organic molecules that get impregnated into the polymer chains during the anodic deposition of the polymer chains. Polymers are blended with other polymers in the solid state, in solution and in gel state.

1.6 Doping Techniques

Doping in polymers can be achieved through following techniques as shown in Fig.6

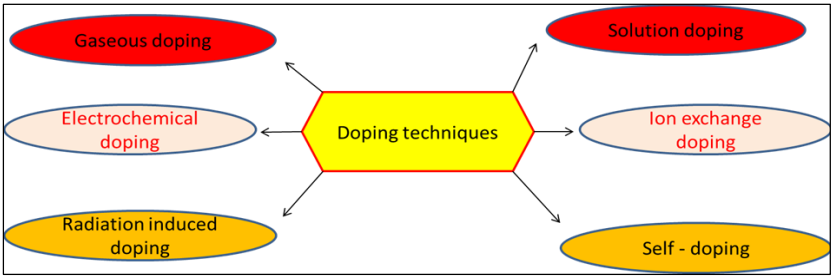

Fig 6: Various techniques of doping in polymers

Gaseous, solution and electrochemical doping are utilized widely because of the facileness in carrying out the doping process and economic efficacy. Gaseous doping process involves the exposure of vapours of dopant to the polymer under vacuum. Solution doping involves the use of polar solvents in which all the products of doping are soluble. Solvents such as acrylonitrile, tetrahydrofuran and nitromethane are used during solution doping. The polymer is treated with dopant solution. In the electrochemical doping technique usually polymerization as well as doping occurs at a time. During this process only ionic dopants are utilized as the electrolytes in polar solvents. In self-doping those ionisable groups which are covalently linked to the polymer chain act as dopants. Doping can also be done by simply irradiating the polymer. High energy radiation is used to amplify the doping of polymers by neutral dopants.

Conclusions

The synthesis of PANI is usually carried out by oxidative chemical polymerization method in both aqueous and non-aqueous medium; however, the better yield and successful synthesis is usually achieved in aqueous medium. The different ways of doping in polyaniline can be achieved by chemical method, charge injection doping, photo doping and by metal insulator sandwich (MIS) type of doping. Among all types of doping, redox chemical doping is the prioritized type of doping from both qualitative as well as quantitative aspect. Conductivity in polyaniline is due to the formation of polarons, bipolarons and solitons. It is believed that the poly (semiquinone radical cation) is the charge carrier in the emeraldine salt of polyaniline.

References

1. Kumar R, Singh S, Yadav BC. Conducting polymers: synthesis, properties and applications. International Advanced Research Journaling Science, Engineering and Technology. 2015; 2:110-124.

2. Karunakaran C, Santharaman P, Das M. Nanocomposite Matrix Functionalization for Biosensors (Chapter 2), Biosensors and Bioelectronics, 2015, 69-132.
3. Mac Diarmid G. A novel role for organic polymers Angewandte Chemie International Edition. 2001; 40:2581-2590.
4. Shirakawa H. The discovery of polyacetylene film: the dawning of an era of conducting polymers (Nobel Lecture), Angewandte Chemie International Edition. 2001; 40:2574-2580.
5. Heeger J. Semiconducting and metallic polymers: the fourth generation of polymeric materials (Nobel Lecture), Angewandte Chemie International Edition. 2001; 40:2591-2611.
6. Letheby H. On the production of a blue substance by the electrolysis of sulphate of aniline. Journal of the Chemical Society. 1862; 15:161-163.
7. Li J, Claude J, Norena Franco LE, Seok SI, Wang Q. Electrical energy storage in ferroelectric polymer nanocomposites containing surface-functionalized $BaTiO_3$ nanoparticles. Chemistry of Materials. 2008; 20:6304-6306.
8. Sultana S, Khan MZ, Umar K. Synthesis and characterization of copper ferrite nanoparticles doped polyaniline. Journal of Alloys and Compounds. 2012; 535:44-49.
9. Phang SW, Tadokoro M, Watanabe J, Kuramoto N. Synthetic Metals. 2008; 158:251-258.
10. Inzelt G. Chemical and electrochemical syntheses of conducting polymers. Conducting Polymers. Springer, Berlin, Heidelberg, 2012, 149-171.
11. Ghosh P, Samir K, Siddhanta S, Rejaul Haque, Amit Chakrabarti. Stable Polyaniline dispersions prepared in non-aqueous medium: synthesis and characterization, Synthetic Metals. 2001; 123:83-89.
12. Melad O, Alhendawi H, Fayyad M. The influence of organic solvents on the polymerization of polyaniline, Research and Reviews: Journal of Chemistry. 2014; 3:40-47.
13. Rafiqi FA, Majid K. Synthetic Metals. 2015; 202:147-156.
14. Mondal SK, Prasad KR, Munichandraiah N. Synthetic Metals. 2005; 148:275-286.
15. Sandi G, Vanysek P. Synthetic Metals. 1994; 64:1-8.

16. Blomquist M, Bobacka J, Ivaska A, Levon K. Journal of Solid State Electrochemistry. 2012; 16:2783-2789.

17. Zotti G, Cattarin S, Comisso N. Journal of electroanalytical chemistry and interfacial electrochemistry. 1988; 239:387-396.

18. Camalet JL, Lacroix JC, Aeiyach S, Lacaze PC. Journal of Electroanalytical Chemistry. 1998; 445:117-124.

19. Lyutov VV, Georgiev G, Tsakova V. Thin Solid Films, 517(24):6681-6688.

20. Pandey PC, Singh G. Journal of the Electrochemical Society. 2002; 149:51-56.

21. PhD Thesis Design, synthesis and use of conjugated copolymers for organic cells and optoelectronic devices-author Anna Calabrese, Scuola Superioredi Catania, University of Catania, 2011.

22. D Bloor, Movagher B. Conducting Polymers. IEEE Proceedings. 1983; 130:225-232.

23. Shirakawa H, Ito T, Ikeda S. Raman scattering and electronic spectra of poly (acetylene). Polymer Journal. 1973; 4:460-462.

24. Bredas JL, Street GB. Polarons, bipolarons, and solitons in conducting polymers. Accounts of Chemical Research. 1985; 18:309-315.

25. Mort J, Pfister G, Grammatica S. Charge transport and photogeneration in molecularly doped polymers. Solid State Communications. 1976; 18:693-696.

26. Santos-Lémus SJ, Yartsev VM. Zero electric field activation energy in molecularly doped polymer systems. Physica B: Condensed Matter. 1995; 205:4-8.

27. Lewis TJ. A simple general model for charge transfer in polymers. Faraday Discussions of the Chemical Society. 1989; 88:189-201.

28. Chien JCW. Polyacetylene-Chemistry, Physics and Materials Science, chapter 2, 1984.

29. Dai L. Intelligent macromolecules for smart devices: from materials synthesis to device applications. Springer Science & Business Media, 2004.

30. Heeger J, Kivelson S, Schrieffer JR, Su WP. Solitons in conducting polymers. Reviews of Modern Physics. 1988; 60:781-850.